공학박사학위논문

Modeling, Simulation, and Design Procedure Development of Micro-channel FT Reactor using Computational Fluid Dynamics

모델링, 시뮬레이션 및 설계 절차 전산 유체 역학을 이용한 마이크로 채널 FT 원자로 개발

2017년 8월

서울대학교 대학원

화학생물공학부

크리스나다스

Abstract

Modeling, Simulation, and Design Procedure Development of Micro-channel FT Reactor using Computational Fluid Dynamics

Krishnadash S. Kshetrimayum

School of Chemical & Biological Engineering

The Graduate School of Seoul National University

Fischer−Tropsch (FT) synthesis is the main step in Gas-to-Liquid (GTL), coal-to-liquid (CTL) and biomass-to-liquid (BTL) processes. In GTL, natural gas is used as feedstock to produce syn-gas (a mixture of carbon-monoxide-CO and hydrogen-H_2) needed for FT reaction where the reaction then produce hydrocarbon fuels (Fischer and Tropsch). In CTL and BTL, syngas is produced from coal and biomass through coal and biomass gasification. GTL is particularly of interest to oil and gas industry today, partly due to volatile fuel price, and partly due to environmental restrictions on flaring offshore stranded and associated gas, and the quest for monetizing these unusual resources. Commercial reactors in GTL are generally classified as high-temperature FT (593 − 623 K) and low-temperature FT (493 − 523 K) reactors depending on the product specifications and operating requirements. The reaction is

characterized by high exothermicity (heat of reaction = 165 kJ/mol CO reacted) with both product selectivity and catalyst deactivation showing high sensitivity to temperature. This demands adequate heat removal and temperature control of the FT reactors for high reactor yield

Low-Temperature FT synthesis in commercial GTL plants use conventional fixed bed and slurry bubble column reactors. However, fixed bed reactor has associated problem of high pressure drop and diffusion limitations, in addition to insufficient heat removal capacity. And, slurry bubble column has a major issue regarding liquid products-catalyst separation. In the recent years, microchannel reactors have attracted attention among researchers, as they are said to shorten the diffusion distance, and lower heat and mass transfer resistance, thus making it as an emerging technology for FT synthesis applications. Reduced mass and heat transfer distances provides enhanced process intensification, making it suitable for highly active FT catalyst. Moreover, many applications such as offshore and remote production facilities require compact and modular conversion technology. And, microchannel reactor blocks are considered to be highly integrated, compact, portable and safe technology making it ideal for those applications. Additionally, small-scale sources for syngas like municipal waste and biomass waste can utilize microchannel technology to produce liquid fuels. However, the high exothermic nature of FT reaction and short residence time of microchannel reactor demands an active coolant having high heat removal capacity, for instance, saturated water.

A microchannel reactor block, with reaction and coolant channel planes arranged in alternate manner and cross flow configuration was considered for Fischer–Tropsch (FT) synthesis. Since past few years, using Computational Fluid Dynamics (CFD) tool to study microreactor or microchannel reactor simulation to either supplement

or even replace expensive and difficult experiments have become a common trend. CFD simulation of heat transfer in the microchannel block was carried out to see the effect of wall boiling condition in coolant channel on reactor temperature. First, reaction inside a catalyst packed representative single channel was simulated to obtain typical heat generation profile along the channel length considering different operating conditions (GHSV 5000 hr^{-1}; 30,000 hr^{-1}; catalyst loading or activity 60 % - 300 %, where 100 % loading equals 1060 kg/m^3 of Cobalt based catalyst from Oxford Catalyst Ltd. and corresponding catalyst activity as 100%). Validity of single channel reaction model was checked by simulating an experimental single channel reactor model and comparing model prediction with the experimental data. Heat generation profiles of practical interest were then imported into multichannel block as time constant heat source input to carry out heat transfer simulation. Cooling oil (Merlotherm SH^{TM}), subcooled water and saturated water (saturated at the reactor operating condition) were chosen as coolants. In one simulated case, temperature difference between hottest spot and coldest spot was found to be 32 K, 17 K and 12 K for cooling oil, subcooled water and saturated water, respectively, indicating highest heat transfer across channel wall for saturated water. Saturated water flow rate of 3 - 6 g/min per channel predicted high wall heat flux above 8900 W/m^2-K. At intensified process condition (GHSV 30,000 hr^{-1}; catalyst loading 300 %), mean FT temperature obtained was 510 K for saturated water and 519 K for subcooled water.

Different candidate design of coolant and process channels geometry are evaluated to get insight into the effect of channel geometry on reactor heat transfer performance. A modified reactor block with an additional coolant layer gave improved thermal performance predicting noticeable heat transfer enhancement under wall boiling condition even at very low exit vapor fraction. Accordingly

modified reactor block is tested for intensified process condition (GHSV = 30,000 hr-1 and super active catalyst condition).

Strong correlation exists between temperature, reaction conversion and product selectivity. For low temperature FT synthesis, it is preferred to maintain reaction channel temperature below 523K. Based on the predicted result, temperature of 517 K could be an optimum value. However, in general, as the intrinsic activity of the catalyst declines, reactor is operated at slightly higher temperature to achieve the same level of CO conversion. From studying effect of syngas ratio and reactor operating pressure, syngas ratio of 2 and operating pressure of 20 – 22 bar predicts more desired product selectivity compared to other set of values.

Method of catalyst bed zone division and loading different % of catalyst in different zone is evaluated. Study indicates noticeable advantage of the method. Also, the method can be optimized to obtain optimum number of zone division, zone length and strategic loading % in each zone. Further, on evaluating heat transfer performance of cross-current flow and co-current flow configuration of syngas and coolant flows, there is clear indication that co-current configuration gives better heat transfer performance compared to cross-current flow configuration in microchannel reactor block operation. A systematic microchannel FT reactor design procedure is also formulated for future microchannel reactor simulation and design process.

Keywords: Computational Fluid Dynamics, Gas-to-Liquid, Microchannel modeling, Reactor block, Fischer-Tropsch synthesis, Wall boiling, Heat transfer coolants, Reactor configuration, Catalyst zone division, Design procedure

Student ID: 2011-30282

Contents

List of Figures

List of Tables

CHAPTER 1 : Introduction

1.1. Research motivation

Fischer−Tropsch (FT) synthesis is the main step in Gas-to-Liquid (GTL), coal-to-liquid (CTL) and biomass-to-liquid (BTL) processes[1]. In GTL, natural gas is used as feedstock to produce syn-gas (a mixture of carbon-monoxide-CO and hydrogen-H_2) needed for FT reaction where the reaction then produce hydrocarbon fuels[2]. In CTL and BTL, syn-gas is produced from coal and biomass through coal and biomass gasification Traditionally, GTL process was of interest to oil and gas industry, due to rising fuel price and diminishing crude oil reserve while natural gas resource was available in abundant, proved reserves over 150 trillion cubic meter as of 2005[3]. But with the decline in crude oil price, the interest on GTL process is mainly due to environmental restrictions on flaring associated gas and offshore stranded gas, and the quest for monetizing small-to-mid size gas resources which otherwise would be lost to flaring or lost unrecovered.

PetroSA in South Africa has a GTL plant that used Sasol's technology and under operation since 1991 with a capacity around 45,000 BPD. Commissioned in 1993, Shell has their first commercial GTL plant in Bintulu, Malaysia, and their world's largest GTL plant, Pearl GTL (capacity over 140,000 BPD), opened at Qatar in 2011. Another commercial GTL under operation since 2007 at Qatar is Oryx GTL plant which is jointly owned by Qatar Petroleum and Sasol[4].

Commercial reactors in GTL are generally classified as high-temperature FT (593 − 623 K) and low-temperature FT (493−523 K) reactors[5] depending on the product specifications and operating requirements. The reaction is sometimes represented by

a general model as the following: nCO + $(2n+1)H_2$ −> C_nH_{2n+2} + nH_2O and is characterized by high exothermicity (heat of reaction = 165 kJ/mol CO reacted) with both product selectivity and catalyst deactivation showing high sensitivity to temperature. This demands adequate heat removal and temperature control of the FT reactors for high reactor yield[6].

Low-Temperature FT synthesis in commercial GTL plants use conventional fixed bed and slurry bubble column reactors[7]. However, fixed bed reactor has associated problem of high pressure drop and diffusion limitations, in addition to insufficient heat removal capacity. And, slurry bubble column has a major issue regarding liquid products-catalyst separation. In the recent years, microchannel reactors have attracted attention among researchers, as they are said to shorten the diffusion distance, and lower heat and mass transfer resistance, thus making it as an emerging technology for FT synthesis applications [8-10]. Reduced mass and heat transfer distances provides enhanced process intensification, making it suitable for highly active FT catalyst. Moreover, many applications such as offshore and remote production facilities require compact and modular conversion technology. Conventional reactors are usually designed for high production capacity (over 30,000 BPD) to achieve the economics of scale[11] and scaling down the process to small or mid-scale capacity is considered impractical. Accordingly, a new type of reactor that is compact and which can be easily integrated to compact GTL process with small production capacity (1 to 1,000 BPD range) and which can stably operate under effect of sea waves have to be developed for FT synthesis application in offshore facilities and stranded gas resources. In the recent years, microchannel reactors have attracted attention among researchers of small scale GTL process as

they can provide methods for process intensification (enabling them to increase the reaction rates 10 to 1,000 times faster compared to conventional reactors) with their short diffusional distance, and lower heat and mass transfer resistance[6,9,10,12,13]. And microchannel reactor blocks are considered highly integrated, compact and modular in nature, allowing them to be portable and safe for applications in offshore and remote production facilities. The overall capital costs associated with FT microchannel reactors are said to be relatively low compared to conventional reactor systems[11]. Additionally, the small-scale sources for syn-gas like municipal waste and biomass waste can utilize microchannel technology to produce liquid fuels[6]. Few companies like compact GTL, Velocys Inc have developed small scale GTL technology that use microchannel reactor for FT synthesis unit. ENVIA Energy has a GTL plant built at Oklahoma City that use Velocys' novel modular microchannel reactor[14]. In this thesis, detail study of microchannel reactor for FT synthesis is conducted with the aim to develop an in-house small scale compact GTL technology and mainly targeting for remote stranded gas resources and offshore applications.

Heat removal is a typical challenge for all FT reactors. In microchannel reactor, the short residence time together with highly exothermic reaction in presence of active catalyst demands an active coolant having high heat removal capacity, for instance, saturated water. Saturated water, when used as a coolant, will undergo wall boiling due to the superheated channel walls of microchannel reactor, whereby the saturated water gets converted to steam. In industrial applications like thermal hydraulic flow in nuclear reactors where high heat transfer co-efficient is needed, wall boiling or pool boiling condition is often exploited to meet high heat transfer requirement [15]. Such evaporative cooling, despite having high potential for heat

removal, reported cases of applications as coolant in Fishcer-Tropsch synthesis experiments are rare. This may be, partly due to lack of understanding of wall boiling condition in small size channels as those of microchannels, and partly due to difficulty in getting saturated water suply at the operation facilities. Deshmukh et al.[6] in their scale up study of a pilot scale microchannel reactor with 276 process channels and 132 coolant channels arranged in cross-flow configuration, used saturated water as coolant to exploit wall boiling condition to meet enhanced level of heat removal. Tonkovich et al.[16] demonstrated the suitability of employing partial boiling coolant to control temperature of their inventive all welded FT reactor.

Several works exit in literature that used Computational Fluid Dynamics (CFD) tool to study microreactor or microchannel reactor to either supplement or even replace expensive and difficult experiments have become a common trend. Arzamendi et al.[1] studied the buoyancy effect on the thermal behavior of a microchannel reactor block through CFD simulation considering partial boiling of coolant and wall coated catalytic reaction zone. Gumuslu and Avci[17] considered 2D simulation model to represent a unit cell of a parrallely arranged microchannels with wall coated catalytic channels and coolant channels arranged in alternate fashion. They carried out CFD simulation to study effect of various geometrical and operating parameters on reaction temperature, and used steam as coolant indicating that the reactor in concern was for high-temperature FT synthesis. An et. al.[18] used CFD tool to study effect of various configurations of micro-reactor in their square cross-section micro-reactor performance study. Shin et al.[19, 20] presented experimental and CFD simulation study of catalytic bed modular microchannel reactor. But they considered much larger channels (40 mm wide and 140 mm long) stacked up to form plate heat exchanger configuration and using silicon oil as coolant. Channels of

lower width and height are preferred for high level of process intensification. Na et al.[21] studied the geometric effect of coolant channels on thermal performance of microchannel reactor using CFD simulation. Recently, Shin et al.[22] showed the effectiveness of micro-scale cross current cooling channel in thermal control of their modular reactor for FT synthesis through CFD simulation. Giovanni et al.[23] presented through their CFD simulation study influence of tube diameter on Fischer-Tropsch selectivity and thermal behavior, considering catalytic milli-fixed bed reactor. Park et al.[24] proposed cell decomposition model to simulate large scale microchannel reactor to avoid intensive CFD computation. However, in the light of numerous works available in literature on detail study of FT synthesis in microchannel, effect of coolant type and wall boiling condition in coolant channels on reactor temperature have not been evaluated quantitatively. In wall boiling condition, part of the heat from exothermic FT reaction is used to generate vapour, thereby enabling heat removal without changing much the coolant temperature. This is essential to maintain near isothermal condition throughout the block reactor. Additionally, it is of interest to evaluate different reactor flow configurations and investigate possible methods for heat removal and better control of reactor temperature.

1.2. Research objectives

This thesis attempts to address the challenges on microchannel reactor modeling, simulation, and design procedure development for FT synthesis mainly using CFD technique. A number of single channel and multichannel reactor models are considered for this purpose. Reaction conversion, selectivity, heat generation and temperature profiles in a reaction channel are analyzed. Different coolant types and

effect of wall boiling condition are evaluated. First, FT reaction inside a catalyst packed single channel was simulated and heat generation profile was obtained which is then imported into a multichannel reactor block model to carry out heat transfer simulation. Further, we explore the effect of flow rate of wall boiling coolant, saturated water in this case, on reactor thermal behaviour. Based on the simulation analysis, reactor design modifications are made. Heat removal under intensified process condition, different reactor flow configuration, effect of channel geometry and operating variables are examined in detail to get better insights on reaction characteristics and microchannel FT reactor. The work also aims to formulate a computer aided systematic design procedure development of microchannel FT reactor for future applications in similar design process.

1.3. Outline of the thesis

This thesis is organized as following; Chapter 1 introduces the thesis topic and also presents the research motivation, relevant literature and objectives of this study. Chapter 2 describes CFD modeling of microchannel reactor for FT synthesis. It includes model development of both single and multichannel types of microchannel reactors, model validation with experimental data from literature and different case simulations for further investigation on the reactor behavior. Chapter 3 presents the detail study on FT synthesis in microchannel reactor considering various aspects like channel geometry, reactor operating variables, wall boiling phenomena in coolant channels, different reactor configurations etc. In Chapter 4, we formulate design procedure for microchannel FT reactor providing a design flow chart consisting various stages of the design process. Finally, Chapter 5 concludes the thesis based on the finding of the present research and briefly presents the way forward.

CHAPTER 2 : CFD Modeling of Microchannel FT Reactor

2.1. Introduction

Modeling of Fischer-Tropsch synthesis in microchannel reactor has been a great challenge as the reaction system involves interaction of three phases—reactants syngas (mixture of CO and H2) in gas phase, wax product in thick liquid and catalyst in solid phase. Since past few years, Computational Fluid Dynamics (CFD) has become a common tool to model and carry out simulations to either supplement or even replace expensive and difficult experiments have become a common trend. Several works exist in literature on single and multichannel FT reactor experiments, simulation and optimization. For instance, Arzamendi et al [1] carried out heat transfer simulation using CFD model of microchannel reactor block to study the effect of buoyancy on reactor temperature considering partial boiling coolant in the coolant channels. Gumuslu and Avci [17] considered 2D model to simulate a unit cell of parallel arranged microchannels with catalyst coated on the channel walls and conducted parametric study to see effect of various geometrical and operating parameters on reactor temperature. Shin et al. [19,20] presented experimental and CFD simulation study of catalytic bed modular microchannel reactor with larger channel width (around 20 mm) and smaller channel height (around 1.6 mm) stacked up to form plate heat exchanger. They also showed the effectiveness of micro-scale cross current cooling channel for thermal control of their modular FT reactor through CFD simulation. Channels of lower width and height are expected to provide high level

of process intensification. Na et al. [21] studied the geometric effect of coolant channels on thermal performance of microchannel reactor using CFD simulation. Kshetrimayum et. al.[25-27] developed CFD models of both single channel and multichannel reactor block to conduct FT reaction and heat transfer analysis to investigate reaction runaway situations. They also evaluated effect of coolant type and wall boiling condition on the three-dimensional reactor temperature profile. Giovanni et al. [23] presented through their CFD simulation study influence of tube diameter on FT selectivity and thermal behavior, considering catalytic milli-fixed bed reactor. They showed that tube of inner diameter less than 2.75 mm can achieve high heat removal capacity for a wide range of syn-gas flow rate. Recently, Na et al [28] presented a multi-objective optimization of discrete catalyst loading method to obtain optimal catalyst loading that would maximize reactor performance using CFD and genetic algorithm.

This chapter mainly described the CFD modelling of microchannel reactors of various types considering the two dominating physical phenomena—reaction and heat transfer. First, we briefly discuss FT reaction kinetics, then modelling of catalyst packed bed reaction channel, coolant channel of both single phase and two phase flow, and heat transfer through the wall are described. Various models of both single channel and multichannel models developed to carry out simulations for specific purposes. Single channel model is used to mainly carry out reaction analysis while multichannel reactor in block form is used to study over all thermal performance of a typical multichannel reactor. Validations of both single channel model and multichannel model are also presented.

2.2. FT Reaction Kinetics

FT reaction involves complex interaction of reactants (CO and H2), catalyst surface and even intermediate radicals, and are sometimes represented by complex mechanistic reaction scheme describing each elementary steps involved[30,31]. In some cases[32-34], the reaction is modeled by one stop global reaction model. In yet other cases, a set of reaction is used to describe the reactant consumption and a range of product formation[16,35]. This study concerns low-temperature FT synthesis using active catalyst as that of Cobalt based catalyst. Accordingly, reaction scheme and kinetic data obtained by Tonkovich et al.[16] of Velocys using their cobalt based active catalyst as given in Table 2.1 is used for carrying out reaction analysis. For comparison of this Co- based kinetics used for low temperature FT synthesis to that of Fe-based catalyst mainly used for high temperature FT synthesis, reaction scheme and kinetic data of Marvast et al[35] that used Fe-based catalyst is considered, shown in Table 2.2.

Table 2.1. (a) Reaction Scheme and (b) Kinetic Parameters for Co-based Fischer–Tropsch Catalyst from Velocys Inc. Patent (US 2012/0132290)[16]

(a) Reactions and rate expressions

ID	Reaction	Reaction rate expression[a]
1	$3H_2 + CO \rightarrow H_2O + CH_4$	$r_{CH_4} = k_1 \exp(-E_1/RT)\, C_{H_2}$
2	$5H_2 + 2CO \rightarrow 2H_2O + C_2H_6$	$r_{C_2H_6} = k_2 \exp(-E_2/RT)\, C_{H_2}$
3	$7H_2 + 3CO \rightarrow 3H_2O + C_3H_8$	$r_{C_3H_8} = k_3 \exp(-E_3/RT)\, C_{H_2}$
4	$9H_2 + 4CO \rightarrow 4H_2O + C_4H_{10}$	$r_{C_4H_{10}} = k_4 \exp(-E_4/RT)\, C_{H_2}$
5	$H_2O + CO \rightarrow H_2 + CO_2$	$r_{CO_2} = k_5 \exp(-E_5/RT)\, C_{CO} C_{H_2O}$
6	$29H_2 + 14CO \rightarrow 14H_2O + C_{14}H_{30}$	$r_{C_{14}H_{30}} = \dfrac{k_6 \exp(-E_6/RT)\, C_{H_2} C_{CO}}{[1 + k_{ad} \exp(-E_{ad}/RT)\, C_{CO}]^2}$

[a]Concentrations in kmol/m^3.

(b) Kinetic parameters

ID	k_i [rate in kmol/(kg-cat s)]	E_i (J/kmol)
1	2.509×10^9	1.30×10^8
2	3.469×10^7	1.25×10^8
3	1.480×10^7	1.20×10^8
4	1.264×10^7	1.20×10^8
5	2.470×10^7	1.20×10^8
6	3.165×10^4 $k_{ad} = 63.5$	8.0×10^7 $E_{ad} = 8.0 \times 10^7$

Table 2.2. (a) Reaction Scheme and (b) Kinetic Parameters for Fe based Fischer–Tropsch Catalyst from Marvast et al[35].

(a) Reactions and rate expressions

ID	Reaction	Reaction rate expression[a]
1	$3H_2 + CO \rightarrow H_2O + CH_4$	$r_{CH_4} = k_1 \exp(-E_1/RT)\, P_{CO}^m \times P_{H_2}^n$
2	$4H_2 + 2CO \rightarrow 2H_2O + C_2H_4$	$r_{C_2H_4} = k_2 \exp(-E_2/RT)\, P_{CO}^m \times P_{H_2}^n$
3	$5H_2 + 2CO \rightarrow 2H_2O + C_2H_6$	$r_{C_2H_6} = k_3 \exp(-E_3/RT)\, P_{CO}^m \times P_{H_2}^n$
4	$7H_2 + 3CO \rightarrow 3H_2O + C_3H_8$	$r_{C_3H_8} = k_4 \exp(-E_4/RT)\, P_{CO}^m \times P_{H_2}^n$
5	$9H_2 + 4CO \rightarrow 4H_2O + n\_C_4H_{10}$	$r_{n\_C_4H_{10}} = k_5 \exp(-E_5/RT)\, P_{CO}^m \times P_{H_2}^n$
6	$9H_2 + 4CO \rightarrow 4H_2O + i\_C_4H_{10}$	$r_{i\_C_4H_{10}} = k_6 \exp(-E_6/RT)\, P_{CO}^m \times P_{H_2}^n$
7	$18.05H_2 + 8.96CO \rightarrow 8.96H_2O + C_{8.96}H_{18.18}$	$r_{C_{8.96}H_{18.18}} = k_7 \exp(-E_7/RT)\, P_{CO}^m \times P_{H_2}^n$
8	$H_2O + CO \rightarrow H_2 + CO_2$	$r_{CO_2} = k_8 \exp(-E_8/RT)\, P_{CO}^m \times P_{H_2}^n$

[a]Rate in mol / hr g-cat.

(b) Kinetic parameters

ID	k_i [mol/hr g-cat]	m	n	E_i (J/kmol)
1	142583.8	-1.0889	1.5662	83423.9
2	51.556	0.7622	0.0728	65018
3	24.717	-0.5645	1.3155	49782
4	0.4632	0.4051	0.6635	34885.5
5	0.00474	0.4728	1.1389	27728.9
6	0.00832	0.8204	0.5026	25730.1
7	0.02316	0.5850	0.5982	23564.3
8	410.667	0.5742	0.710	58826.3

2.3 Microchannel reactor modeling

2.3.1 FT reaction channel

Reaction channels are assumed to be filled with catalyst and inert support, and modeled as pack bed reactor with void fraction determined by the catalyst and inert material loading. The mass and momentum inside a reaction channel are described by Navier-Stoke equation with source term for porous media in the momentum equation, as given below.

Continuity equation: $$\frac{\partial \rho}{\partial t} + \nabla \cdot (\rho \vec{v}) = 0 \quad (2.1)$$

Momentum equation: $$\frac{\partial}{\partial t}(\rho \vec{v}) + \nabla \cdot (\rho \vec{v} \vec{v}) = -\nabla \cdot p + S_i \quad (2.2)$$

where ρ represents mixture density, $\vec{v}$ is velocity vector, p is the static pressure and S_i is the source term for porous media and modelled as sum of viscous loss term and inertial loss term as in eqn (2.3).

Source term for porous media: $$S_i = -\left(\sum_{j=1}^{3} D_{ij} \mu v_j + \sum_{j=1}^{3} C_{ij} \frac{1}{2} \rho |v| v_j \right)_i \quad (2.3)$$

μ is the viscosity of mixture and $|v|$ is the magnitude of the velocity. Inverse of D_{ij} is known by the term permeability and C_{ij} as inertial resistance factor[36] and are prescribed matrices. The source act as momentum sink and contributes to pressure drop inside porous reaction channel as a function of reaction species

superficial velocity. And, species transport equation is described as below:

Species transport: $$\frac{\partial}{\partial t}(\rho Y_i) + \nabla \cdot (\rho \vec{v} Y_i) = -\nabla \cdot \vec{J}_i + R_i \quad (2.4)$$

where, R_i is the source term from FT reaction, Y_i, the mass fraction of specie "*i*" and $\vec{J}_i$, the diffusive mass flux for specie "*i*" from Maxwell-Stefan equations[37] for multicomponent diffusion. Heat is continuously generated in the reaction channels as the syn-gas (CO + H2) undergoes catalytic conversion to various hydrocarbon products. The energy equation inside the reaction channel is described by that of porous media, as in eqn (2.5).

Energy equation:

$$\frac{\partial}{\partial t}\left(\varepsilon \rho_f E_f + (1-\varepsilon)\rho_s E_s\right) + \nabla \cdot \left(\vec{v}(\rho_f E_f + p)\right) = \nabla \cdot \left[k_{eff} \nabla T - \left(\sum_i h_i \vec{J}_i\right) + (\bar{\bar{\tau}} \cdot \vec{v})\right] + S_f^h \quad (2.5)$$

Where E_f and E_s are the energy for fluid and solid parts; ε and k_{eff} are the porosity and effective thermal conductivity inside the reaction channel; h_i is the enthalpy of specie '*i*'; and S_f^h is heat source term which in present study is the heat generation due to exothermic FT reaction. Second term of right hand side comes from enthalpy transport of multicomponent species diffusion. Presence of FT product liquid may change the value of k_{eff}. However, in the present study, to avoid over estimation, all fluid species are assumed to be in gas phase and k_{eff} is calculated as volume average of thermal conductivities of materials inside reaction channel, as $k_{eff} = \varepsilon k_f + (1-\varepsilon)k_s$ where k_f is the thermal conductivity of fluid phase, and k_s

the thermal conductivity of solid phase catalyst and inert support material. Due to millimeter scale of microchannel reactor, fluid phase is considered to be in laminar regime and turbulence contribution inside reaction channel is ignored. The assumption is that as the channel size decrease, the catalyst loading will approach uniformity and that heat transfer limit between catalyst surfaces to support material will not limit the heat transfer to wall.

2.3.2 Coolant channel

In coolant channels, flow can be single phase liquid, in case of cooling oil and subcooled water. Whereas, it is two-phase due to wall boiling condition in case of saturated water. Consequently, laminar flow is assumed for cooling oil and subcooled water, and turbulence flow for saturated water under wall boiling condition. Heat is transported from the heated wall to coolant fluid. Coolant fluid in case of wall boiling, comprises of two phases: subcooled liquid and vapour. Flow can be modelled by Eulerain-Eulerian multiphase framework with interpenetrating continua with liquid as continuous phase and vapor as discrete phase, as reviewed in detail by Ishii[38], Drew and Passman[39], and Yeoh and Tu[40] and not presented here for brevity.

Heat flux from the heated wall to the coolant is described by mechanistic model of Kurul and Podowski[41,42] which is a summation of heat flux due to different mechanisms. In the region where liquid is contact with heated wall, heat transfer is same as that of single phase flow, called convective heat transfer. In the region where bubbles suddenly form and grow, heat is taken up by vapour generation, called evaporative heat transfer. And heat transfer due to the liquid replacing the bubble sites due to recirculation is called quenching heat transfer. Accordingly, the total

wall heat flux is defined as sum of three parts:

Mechanistic wall heat flux: $$Q_{tot} = Q_C + Q_Q + Q_E \quad (2.6)$$

Where Q_C , Q_Q and Q_E represent the heat flux component due to convection, quenching and evaporation, respectively.

Detail models of the component heat flux, corresponding heat transfer co-efficient correlations including closing parameters: bubble diameter at detachment, nucleation site density, bubble influence area and bubble detachment frequency are reviewed in Krepper and Rzehak10. Mass transfer from the liquid phase to vapour is accounted by the rate of evaporation which is a function of bubble diameter at detachment, nucleation site density and bubble detachment frequency. Since temperature difference between liquid phase and vapour phase are expected to be small, heat transfer between the two phases is assumed to be negligible as compared to the heat transfer from the channel wall.

For single-phase coolant flow as is the case with subcooled oil and subcooled water, convective heat transfer is assumed to be the only means of heat removal and only the first term in eqn (2.6) will remain. The validity of continuum model and Navier -Stokes equations at such small scale was shown by Arzamendi et al.[1], through Knudsen number which says that if Knudsen number, $k_n=\sqrt{((\pi \times \gamma)/2)}\times Ma/Re$ where M_a is the Mach number, Re the Reynolds number and γ, the specific heat ratio (C_p/C_v) , is much lesser than characteristic length of the system, the assumption is valid. In the present study, Knudsen number was calculated to be order of 1×10^{-6} which is much less than characteristic length scale of millimetre used in our microchannel reactors.

2.3.3 Reactor solid walls

In the solid zone, the conduction heat flux through solid is defined as in eqn (2.7) with local temperature in reaction and coolant channels as the thermal boundary conditions. It is assumed that no heat is lost from reactor walls to the ambient air.

Heat conduction in solid wall zone: $q = -k_{w\ a} \nabla T$ (2.7)

where k_{wall} is the material conductivity of solid wall zone.

2.4 Reactor geometry, simulation conditions and settings

Both single channel reactor and multichannel reactor geometry models are considered in the present study. Single channel model is used to simulate FT reaction in catalytic packed channel and to obtain resulting reactant conversion, product selectivity, heat generation and temperature profile inside the channel. In multichannel model, heat transfer simulation is carried out with FT reaction heat generation implemented as time constant heat source in reaction channels and coolants flowing in coolant channels in cross flow configuration. Detail geometry of the reactor models considered are described in the following subsections.

2.4.1 Single channel model

Two single channel reactor models (single channel-A and single channel-B), see figure 1(a) & (b), were considered for two purposes; single channel-A to validate simulation model predictions with Velocys' experiment[6], and single channel-B for carrying out FT reaction simulation in a representative reaction channel of multichannel reactor block. Single channel model-A has reaction channel width 8 mm, height 1 mm and channel length 70 mm, and two coolant channels of same

dimensions on either sides. This single channel reactor has 38 mm long catalyst bed situated at the center with the region upstream and downstream of the catalyst bed filled with SiC as inert beds. Single channel model-B has channel width 1 mm, height 1 mm and channel length 21 mm and with no coolant channels. Heat removal in this case is faciliated by temperature as thermal boundary condition at the wall. Both the single channel geometries were meshed with fine grids of 0.0001 m and below, resulting to 0.86 million cells for single channel-A and 0.21 million cells for single-channel-B.

2.4.2 Multichannel model

Deshmukh et al.[6] and Almeida et al.[12] demonstrated the feasibility of using microchannel block in cross-flow configuration for commercial FT synthesis. In our present simulation study too, we considered a multichannel block reactor, adapted from Arzamendi et al.[1], as shown in Figure 2.1(c). It has dimensions: 21 mm x 21 mm x 17 mm, with four process channel planes and four coolant channel planes stacked up in alternate manner. Each channel planes has 10 parallel channels of 1 mm x 1 mm x 17 mm with gap between adjacent channels as 1 mm along lateral sides, and 1mm along stack height. This gives altogether 80 microchannels in the block with 40 each for FT reaction and coolant flow and arranged in cross flow configuration. Reactor material is assumed to be of stainless steel, SS304. Since heat transfer study is the focus here, reaction channels are considered as solid zone but with time constant heat source as obtained from FT reaction simulation in single channel. Hence, CFD model for reactor block consist of two types of solid zones-one for reaction channels and other for reactor body; and one fluid zone for coolant flow. It is assumed that in all reaction channels of the block reactor, reaction rates

are identical and accordingly heat generation rates are identical too. Therefore, reaction channels in this block reactor model are zones for time constant heat source. Coolant channels are zones for heat sink. Zones are meshed with tetrahedral and hexagonal elements with cell count of 2.2 million to ensure fine mesh quality and denser grid in fluid zones.

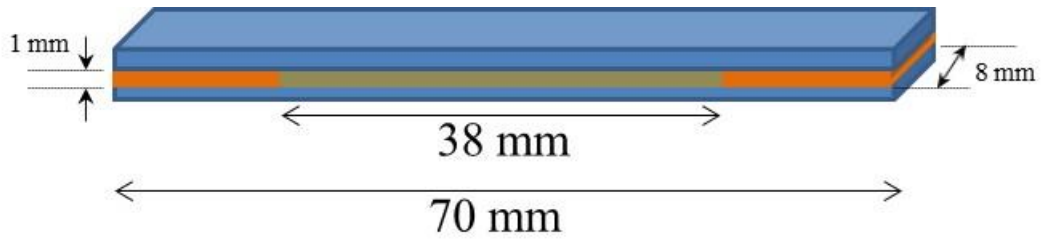

Reaction channel (cross section: 8 mm x 1mm)

Coolant channel (cross section: 8 mm x 1 mm)

Catalyst packed bed

(a) Single Channel-A

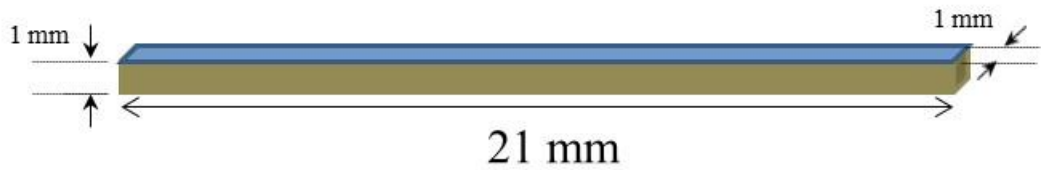

Catalyst packed bed (cross section: 1mm x 1mm)

Wall cooled at top and bottom

(b) Single Channel - B

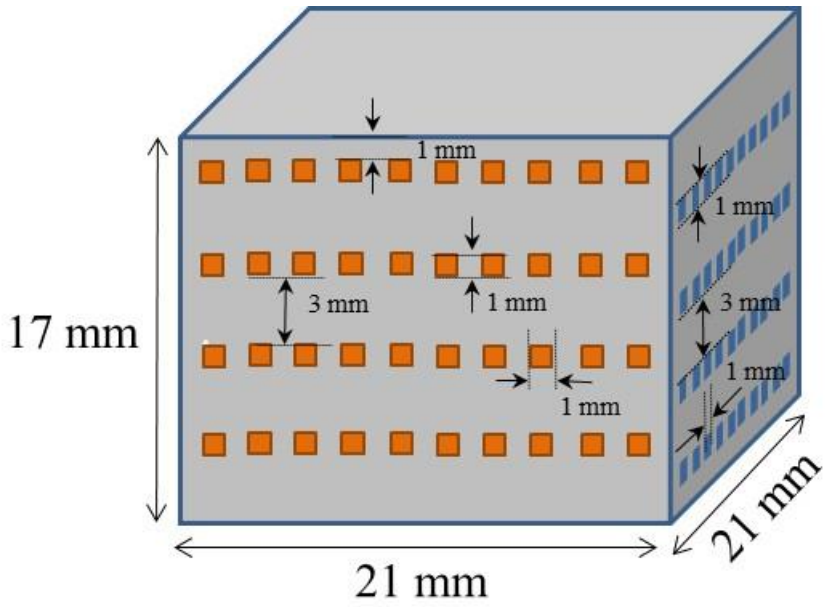

Reaction channel (cross section: 1 mm x 1mm)

Coolant channel (cross section: 1mm x 1 mm)

Reactor body

(c) Microchannel reactor block with 40 reaction channels and 40 coolant channels

(Adapted from Arzamendi et al., 2010)

Figure 2.1. Schematic of the single channel and multichannel reactor models considered. Single Channel-A model has one reaction channel sandwiched between two coolant channels. Single Channel-B model has one reaction channel with wall cooled at top and bottom. Microchannel reactor block model has 40 reaction channels and 40 coolant channels in cross-flow configuration.

2.4.3 Simulation conditions and settings

Simulation was carried out using commercial CFD software ANSYS FLUENT 14.5 An et al.[18] satisfactorily simulated micro-reactor for various configurations using the software tool to demonstrate the applicability. For Single Channel-A, conditions similar to that of Velocys's experiment (Deshmukh et al.[6], Tonkovich et al.[16]) was used; syngas flow rate of 12400 h^{-1} GHSV (Gas Hourly Space Velocity) at inlet temperature of 503 K and operating pressure of 25 bar with catalyst loading, 1060 kg/m^3 (Cobalt based catalyst from Oxford Catalyst Ltd.). Since the main interest with single channel model was to obtain heat generation profile under different operating conditions, syngas flow rate of 5000 h^{-1} GHSV with catalyst loading varying from 60 to 120 % were considered, as given in Table 2.3. Syngas ratio (H_2/CO) was kept constant at 2 for all reaction simulations. Reaction scheme containing 6 equations and corresponding kinetic parameters for low temperature FT synthesis given in Tonkovich et al.[16] was used. Bed parameters for the porous media are given in table 2(a). Thermo-physical properties of species: CO, H_2, CH_4, C_2H_6, C_3H_8, C_4H_{10}, H_2O, CO_2, and inert N_2 were used as they are in FLUENT 14.5 inbuilt library after verification with Perry's Handbook[43]. Properties of $C_{14}H_{30}$ which is not present in the library was taken from same source in Perry's Hanbook[43].

Table 2.3. Simulation conditions for single channel and multichannel FT reactors.

Reactor model	GHSV(hr^{-1})	Catalyst loading (%)	Coolant type
Single channel - A	12,400	100	Subcooled water
Single channel - B	5000	60 - 120	Subcooled water
	30,000	220 - 300	Subcooled water
Multichannel	5000	120	Subcooledwater, Cooling oil (Merlotherm SH), Saturated water
	30,000	300	Subcooledwater, Saturated water

100 % Catalyst loading = 1060 kg/m^3

Table 2.4. Simulation parameters of single channel and multichannel models.

(a) Bed parameters	*Values*
Gas mixture viscosity (kg/m-s)	0.001
Gas mixture conductivity (J/s-m-K)	0.104
Porosity	0.4
Catalyst density @ 100% loading	1060
Permiability ($1/m^2$)	$1.46x10^8$
Intertial resistance (1/m)	$1.37x10^4$

(b) Properties	Density	Heat capacity	Conductivity	Viscosities
	kg/m^3	J/Kg-K	J/s-m-K	kg/m-s
Catalyst support material	3210	473	20.4	-
Cooling oil(Marlotherm SH)	936	1967	0.0974	$1x10^{-3}$
Subcooled water	998.2	4182	0.6	$1x10^{-3}$
Water vapor	1.55	2014	0.0261	$1x10^{-5}$
Solid Wall(SS304)	8000	500	20.1	-

Heat generation profile obtained from FT reaction simulation in single channel model was implemented as time constant heat source into multichannel reactor block CFD model using User Defined Function (UDF). Simulation settings for heat transfer simulation in multichannel reactor block are as follows: Laminar for single phase coolant; SST-k Omega turbulent model for turbulence in multiphase; SIMPLE algorithm for pressure velocity coupling; second order discretization for momentum

and energy equation; RPI boiling model (Kurul and Podowski[41, 42]) for wall boiling. Fincher[44] tested the capability of RPI boiling model implemented in commercial CFD software ANSYS FLUENT 14.5 in predicting experimental results and the predictions were found to be well in agreement. Reactor body is assumed to be made of stainless steel, SS304. Thermo-physical properties of different coolant materials, catalyst support material and solid reactor materials are given in table 2(b). Saturation temperature for wall boiling model was set as 500 K, which is the saturation temperature of water at operating pressure of 25 bar. Simulations were carried out on a workstation with 24 core Intel Xeon CPU and 16 GB RAM as unsteady state simulation and results were collected when reactor temperature has become static over several 100 time steps for all cases.

2.5 Simulation of Velocys' single channel experiment

Velocys' experiment (Deshmukh et al.[6],Tonkovich et al.[16]) with a short single channel, modelled as Single Channel-A in our study, was simulated to validate single channel FT reaction model. Figure 2.2 shows mole fraction of CO and CH_4, heat generation due to exothermic reaction in the catalyst packed region, and temperature contour for the reaction channel obtained from simulation. As expected, reaction is higher near the inlet and gradually decreases along the channel length as can be understood from CO conversion profile and selectivity to CH_4 along channel length, see inset plot in Figure 2.2(a) and (b). Accordingly, heat generation and temperature profile are higher near the inlet and decreases along the channel length, as can be seen from Figure 2.2(c) and (d). As expected, reaction and hence heat generation occurs only in the catalyst packed region. To minimize temperature change along channel length, subcooled water flow rate of 89.85 g/min was set in each of the two coolant channels.

Changing kinetic parameters in proportion to change in catalyst loading results in different conversion and selectivity. At catalyst loading of 1060 kg/m^3 CO conversion of 60.02% was achieved with selectivity for CH_4 and C_{5+} (modeled as $C_{14}H_{30}$ here) as 8.38% and 87.41% respectively. Other products: C_2H_6, C_3H_8, C_4H_{10}, and CO_2, altogether have selectivity below 5%. When the catalyst loading was increased 1.2 times, CO conversion increased to 74.60 % while the selectivity for CH_4 and $C_{14}H_{30}$ increased to 11.18% and 85.26% respectively. These values are in reasonable agreement with the experimental results of Deshmukh et al.[6] where CO conversion of 73.6 % with selectivity for CH_4, C_2-$C_4$and C_{5+} as 8.0 %, 3.6% and 88.2 % respectively, were obtained. Small difference in the results can be attributed to lower reactor temperature in experiment, as it loses heat to ambient air. In fact, when 0.1 W/m^2-K ambient heat transfer coefficient, a value from literature[14]considered reasonable for such applications, was applied to the reactor walls, reactor temperature lowers by 1.5 ^oC. Correspondingly, CO conversion decreases by 2.2%, and selectivity for CH_4 and $C_{14}H_{30}$ decreases by 1.0% and increases by 1.1% respectively.

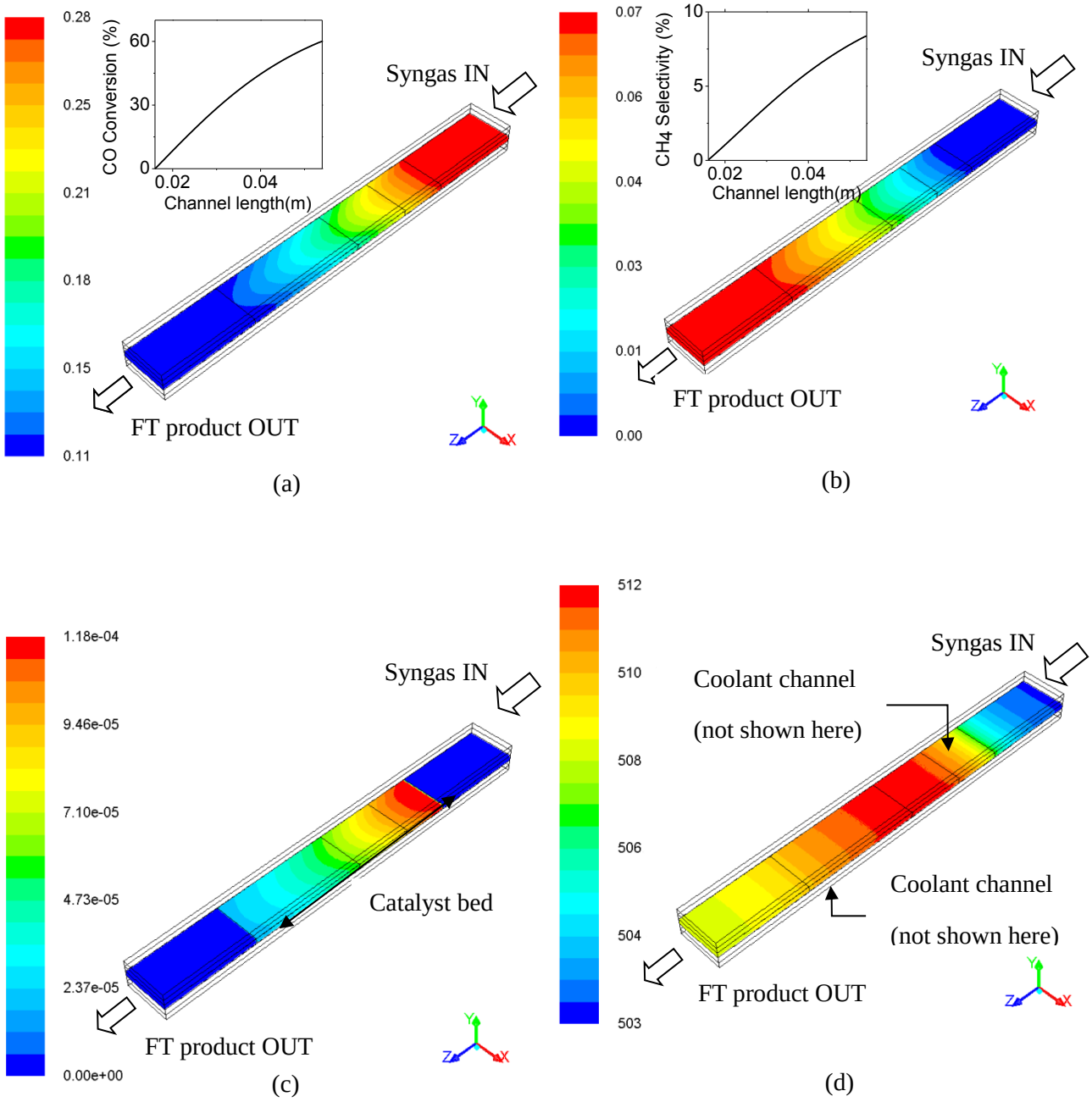

Figure 2.2. Mole fraction of *CO* (a), mole fraction of CH_4 (b) heat generation [J/s] (c) Temperature contour [K] (d) in reaction channel from FT reaction in Singel Channel-A (Velocys experiment-*short channel*. Channel thickness: 1 mm; channel width: 8 mm ; catalyst zone: 38 mm at the center).

2.5.1 Heat generation in single channel

Single Channel-B represents a unit reaction channel in multichannel block model. FT reaction simulation was carried out in Single Channel-B to obtain conversion, selectivity and corresponding heat generation profile. Same reaction model settings and parameters were applied as in simulation of Velocys' experiment[4,16]. Process conditions were, however, changed. First, syngas flow rate of 5000 h^{-1} GHSV with syngas ratio (H_2/CO) of 2 at 523K was checked for catalyst loading of 60 %, 80 %, 100 % and 120 %, where 100 % corresponds to 1060 kg/m^3 of Co-based active catalyst developed by Oxford Catalyst (Tonkovich et al.[11]).

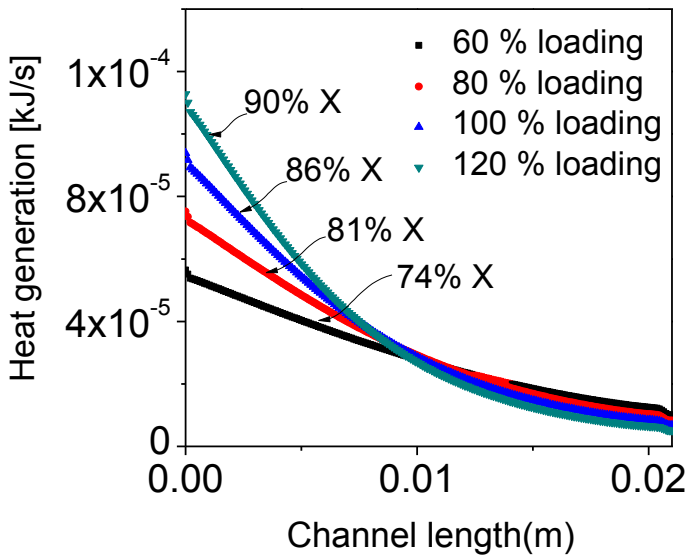

Figure 2.3. Heat generation profile from FT reaction simulation in Single Channel-B for different catalyst loading [GHSV = 5000 hr^{-1}; H_2/CO = 2]. 120 % loading corresponds to catalyst activity 1.2 times of the present catalyst.

Alternatively, we can assume these loading percentages as the level of activity of catalyst and hence can be understand as 0.6, 0.8, 1 and 1.2 times the activity of reference catalyst. Since Single Channel-B does not have adjacent coolant channels, a pair of opposite walls are maintained at syngas inlet temperature, 523K in this case. The other pair of opposite walls have zero heat flux as thermal boundary condition. Reactor operating pressure was set as 25 bar. As expected, CO conversion and heat generation are higher for higher catalyst loading, as can be understood from heat generation profiles in Figure 2.3. However, towards the end of catalyst bed, heat generation for higher catalyst loading is slightly lower than that of lesser catalyst loading as the reactant concentration has depleted more and reaction rate decreased slightly more in the former compared to the latter. On comparing heat generation rates between 60 % loading and 120 % loading (0.6 and 1.2 times activity), heat generation rate increases almost in proportion to the catalyst loading or catalyst activity, indicating that active cooling method is required for FT synthesis that uses high active catalyst.

2.6 Heat transfer simulation of multichannel model

To reduce computational load with 3D simulation of FT reaction and heat transfer in multichannel, reaction and heat transfer phenomena were decoupled and simulations were carried out separately, as shown by the schematic in Figure 2.4. To examine the validity of decoupling approach, three single channel model were considered: FT reaction and heat transfer coupled (Model 1), FT reaction and heat transfer decoupled with syngas flow (Model 2), and FT reaction and heat transfer decoupled with no syngas flow (Model 3). In Model 2 and Model 3, heat generation rate obtained from Model 1 was implemented as heat source in reaction

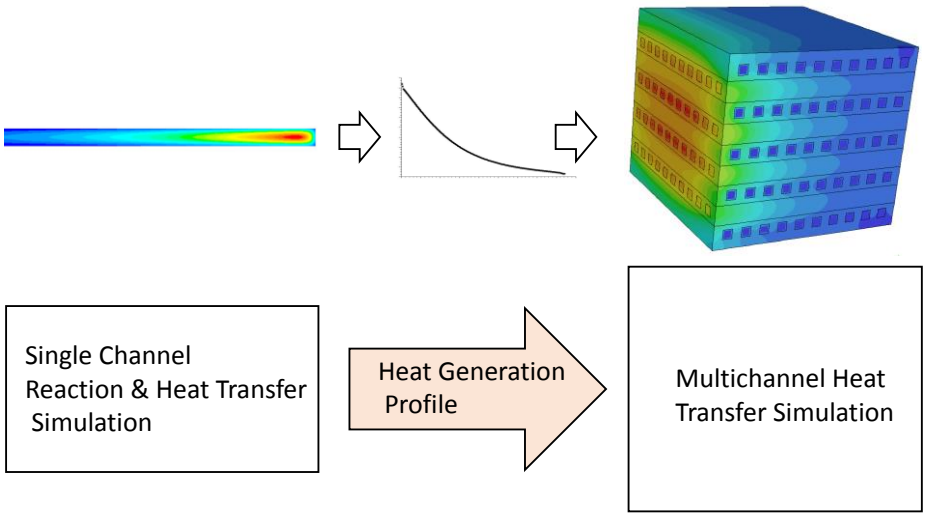

Figure 2.4. Schematic showing strategy for heat transfer simulation in multichannel reactor model.

channel using UDF. Heat transfer simulation on Model 2 and Model 3 gave temperature profiles comparable to that of Model 1, although with small difference along the channel length, less than 1 K, see Figure 2.5. Advection heat transfer along channel length and its effect on reaction rate in Model 1 may have attributed to the small difference in temperature profile along channel length. Nevertheless, the reasonable agreement in temperature profiles between the three models considered, makes the decoupling approach attractive for heat transfer simulation with a large multichannel reactor where problem simplification is generally demanded. We therefore, applied similar approach to simulate heat transfer in our microchannel reactor block for FT synthesis. The approach is particularly useful when a more complex physics is to be accounted on the coolant side, as is the case with wall boiling condition in present study.

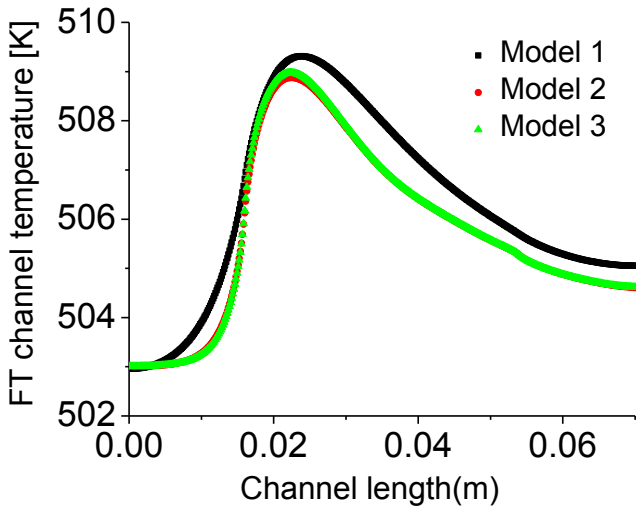

Figure 2.5. Temperature [K] profile inside FT reaction channel: Comparison between model prediction between model with reaction and heat transfer coupled (Model 1), model with reaction and heat transfer decoupled and considering syngas flow (Model 2), and decoupled model considering no syngas flow (Model 3).

Heat generation profile corresponding to process condition of 5000 hr^{-1} GHSV and 120 % catalyst loading was considered for microchannel reactor block. Cooling oil (Merlotherm SH™), subcooled water and saturated water at inlet temperature of 498 K was considered as coolant medium. Both cooling oil and subcooled water behaves as single phase coolants, whereas, saturated water undergoes phase change due to wall boiling once channel wall temperature rises above saturation temperature, 500 K in this case. Please note that we assumed coolant stream in case of subcooled water to be slightly over pressurized to kept it from becoming saturated. In case of saturated water as coolant, latent heat of vaporization due to wall boiling condition is expected to provide additional higher heat removal as compared to that of single phase coolants.

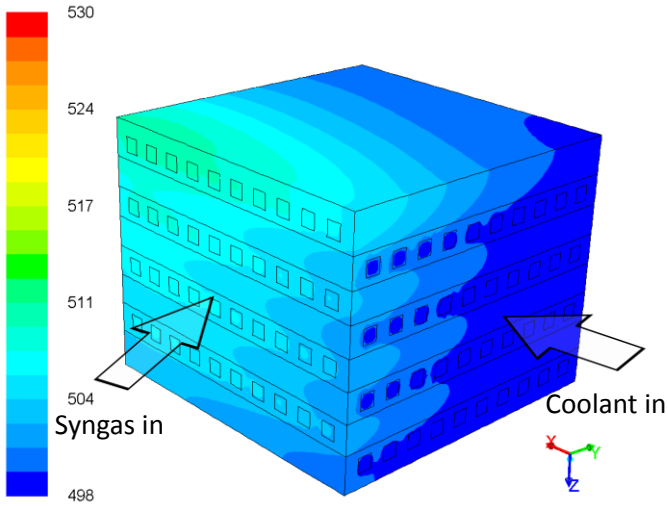

(a)

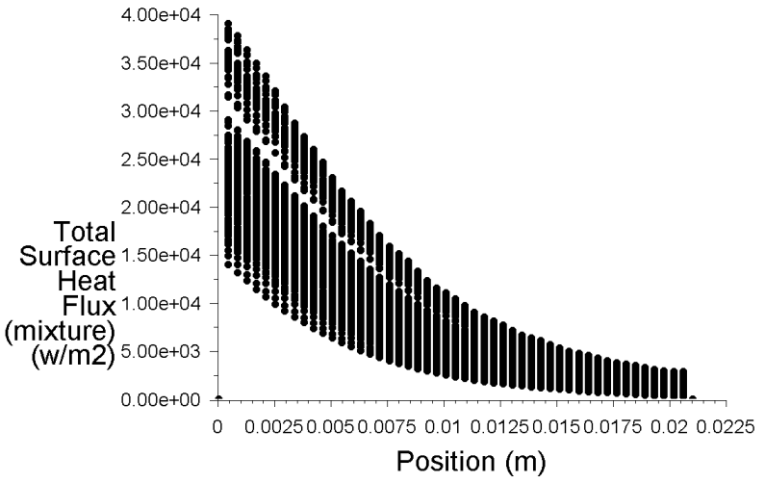

48

(b)

Figure 2.6. (a) 3D Temperature [K] contour on microchannel reactor block with saturated water as coolant (flow rate = 5.4 g/min), and (b) Heat flux distribution over reaction channel (GHSV = 5000 hr^{-1}; catalyst loading 120 %)

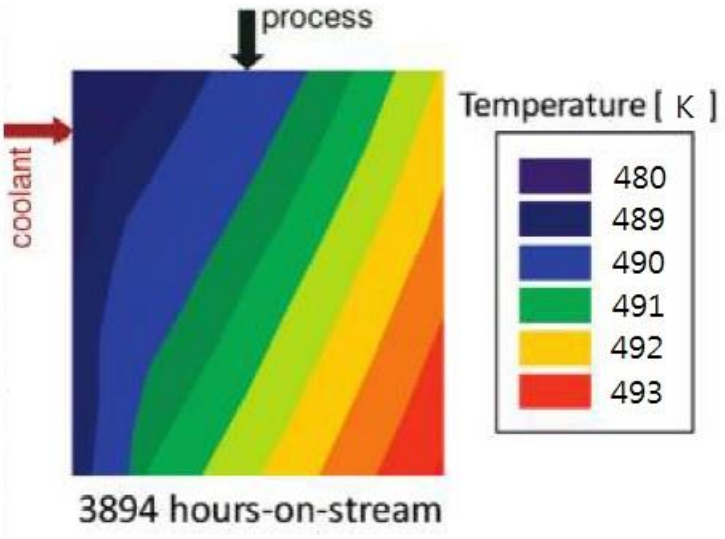

(a)

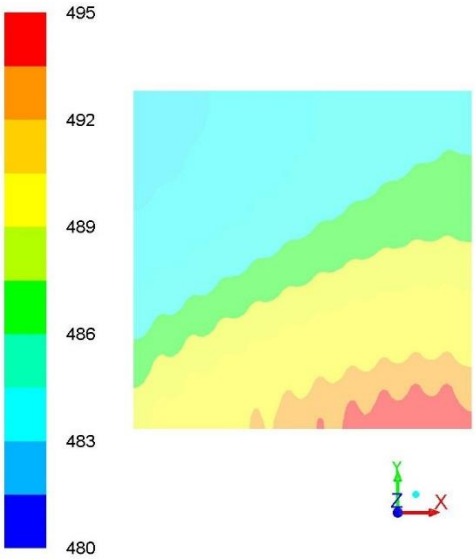

(b)

Figure 2.7. Qualitative comparison of temperature contour from (a)Velocys's pilot scale operation data with (b) simulation result. Temperature values slightly differ due to different operating and coolant conditions.

Figure 2.6 (a) shows the 3D temperature profile of the simulated microchannel reactor block. As expected temperature is higher near the syngas inlet region and decreases along the channel length. Maximum temperature is seen at the corner furthest away from coolant inlet and region above the process channel layer not flanked by coolant channel layers on both side. For the coolant channel layer, the channels near the syngas inlet region has higher temperature compared to the channels at exit region of FT product. Over all, the maximum temperature difference between the hottest region and the coldest region is below 15 ^{o}C, which is the desired ΔT_{max} for normal operation of low temperature FT synthesis. Figure 2.6 (b) shows heat flux distribution over the lateral surface and along one of the process channel. This profile indicates that most of the heat transfer occurs in the first half of the catalyst packed process channel. Figure 2.7 (a) and (b) shows the qualitative comparison of temperature contour for process channel plane of the simulated microchannel reactor block with that of thermocouple data obtained from pilot scale reactor of Velocys. Because of the difference in process and coolant conditions, both qualitative comparison is possible.

2.7 Conclusion

In this chapter, we presented our CFD modeling and simulation of FT synthesis in a catalyst packed microchannel reactor considering both single channel and multichannel reactor models. Simulation of Velocys' experiment ((Deshmukh et al.[6],Tonkovich et al.[16]) with short single channel reactor validated our single channel model. At catalyst loading of 1060 kg/m^3 CO conversion of 60.02% was achieved

with selectivity for CH_4 and C_{5+} (modeled as $C_{14}H_{30}$ here) as 8.38% and 87.41% respectively. When the catalyst loading was increased 1.2 times, CO conversion increased to 74.60 % while the selectivity for CH_4 and $C_{14}H_{30}$ increased to 11.18% and 85.26% respectively. Temperature effect on CO conversion and selectivity for CH_4 and C_{5+} revealed necessity for maintaining reaction channel temperature below 523 K, for low-temperature FT synthesis.

On comparing heat generation rates between 60 % loading and 120 % loading (0.6 and 1.2 times activity), heat generation rate increases almost in proportion to the catalyst loading or catalyst activity, indicating that active cooling method is required for FT synthesis that uses high active catalyst.

Heat transfer simulation in a complex microchannel reactor block can be conducted by decoupling reaction and heat transfer. Comparing a decoupled model with that of reaction and heat transfer coupled model shows less than 1^oC difference in temperature profile along the channel length. Thermal profile for the simulated microchannel reactor block is also qualitatively compared with temperature data of Velocys' pilot plant operation. Overall, based on the validation of the single channel reactor with Velocys single channel operation data and qualitative comparison with multichannel reactor operation data, it can be understood that the various microchannel reactor models developed using CFD tools can be used to conduct detail study of FT synthesis.

CHAPTER 3 : Detail Study of FT Synthesis in Microchannel Reactor

3.1 Introduction

In the recent years, microchannel reactors have attracted attention among researchers of small scale GTL process as they can provide methods for process intensification (enabling them to increase the reaction rates 10 to 1,000 times faster compared to conventional reactors) with their short diffusional distance, and lower heat and mass transfer resistance[6,9,10,12,13]. And microchannel reactor blocks are considered highly integrated, compact and modular in nature, allowing them to be portable and safe for applications in offshore and remote production facilities. The overall capital costs associated with FT microchannel reactors are said to be relatively low compared to conventional reactor systems[12]. Additionally, the small-scale sources for syn-gas like municipal waste and biomass waste can utilize microchannel technology to produce liquid fuels[6]. Few companies like compact GTL, Velocys Inc have developed small scale GTL technology that use microchannel reactor for FT synthesis unit. ENVIA Energy has a GTL plant built at Oklahoma City that use Velocys' novel modular microchannel reactor [14]. Detail study of FT synthesis in microchannel reactor was conducted with the aim to develop an in-house small scale compact GTL technology and mainly targeting for remote stranded gas resources and offshore applications.

Design of microchannel reactor for a highly exothermic reaction like FT synthesis has remained as a big challenge. A number of design decisions are to be made before coming up with a final design. Additionally, various kind of issues may

arise at the time of reactor operation. To address all the possible issues during a design process and later during reaction operation, a detail study of FT synthesis in microchannel reactor is conducted through various simulation experiments. First, characteristics of FT reaction in microchannel reactor is discussed followed by strategies for exothermic heat removal, discussion on process intensification, modified reactor block, comparison of reactor flow configuration and comments on FT product distribution.

3.2 Microchannel FT reaction characteristics

FT reaction is characterized by high exothermicity (heat of reaction = 165 kJ/mol CO reacted) with both product selectivity and catalyst deactivation showing high sensitivity to temperature. Accordingly, it is necessary to understand the effect of operating conditions likes temperature, pressure and syn-gas ratio (H2/CO) on CO conversion, CH4 selectivity and C5+ selectivity (the desired product in low temperature FT synthesis). In high-temperature FT synthesis, reactor is operated well above low-temperature FT synthesis, between 593−623 K and Iron-based catalyst are generally used and product distribution is mainly oriented to gasoline. Of three main operating variables (temperature, pressure and H2/CO), temperature control possess the biggest challenge as both operating pressure and H2/CO can be set to a desired value and maintained for the entire duration of reactor operation without much fluctuation. On the other hand, reactor temperature is a function of the instantaneous rate of reaction and subsequent heat generation inside the reaction channel. Therefore adequate heat removal and temperature control of the FT reactors is demanded for high reactor yield and operational safety. If the reactor does not have

sufficient cooling system, just within 1 hour after the start of reactor operation, temperature can shot up to a high value and reaction runaway can happen. In general, understanding of the reaction kinetics, effect of reactor geometry design variables and operating conditions on reactor performance are necessary in most reactor design problem. Therefore, in this section, we present study on FT reaction characteristics considering two type of reaction kinetics (kinetics-I and kinetics –II), effect of channel geometry and effect of operating variables on reactor performance.

3.2.1 FT kinetics

In FT reaction, CO and H2 are the reactants and hydrocarbon with wide range of carbon content are the products. Therefore, depending on the desired product distribution, reactor can be operated at high temperature FT synthesis mode or at low temperature FT synthesis mode. Two reaction kinetics are considered to understand the characteristics of FT reaction in this study: kinetics-I (Fe-based catalyst of Marvast et al[35] and kinetics –II (Co-based catalyst of Velocys US Patent 2012/0132290 A1)[16]. Reaction scheme and corresponding kinetic data are given in section 2.2 of previous chapter. Both kinetics –I and II were implemented in the single channel CFD model of catalyst packed channel of 1 mm × 1 mm × 21 mm dimension.

Figure 3.1 (a) and (b) shows mole fraction from Fe-based catalyst and Co-based catalyst. It can be understood that product is well distributed over CH4 to C5+ with highest mole fraction for CH4 and least for the C5+. Generally, according to experimental data for almost every mole of CO converted, a mole of H2O is

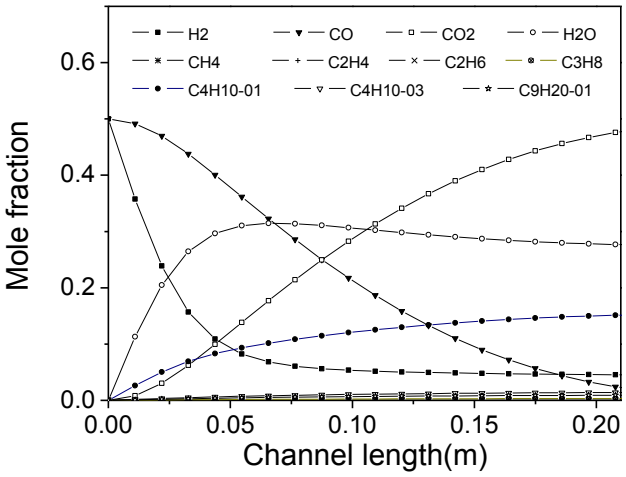

(a)

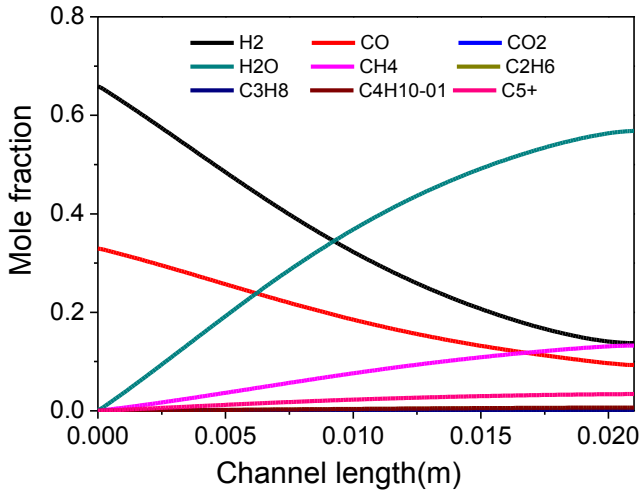

(b)

Figure 3.1 Mole fraction from (a) Kinetics-I (Fe-based catalyst of Marvast et al[35] and (b) Kinetics –II (Co-based catalyst of Velocys US Patent 2012/0132290 A1)[16]

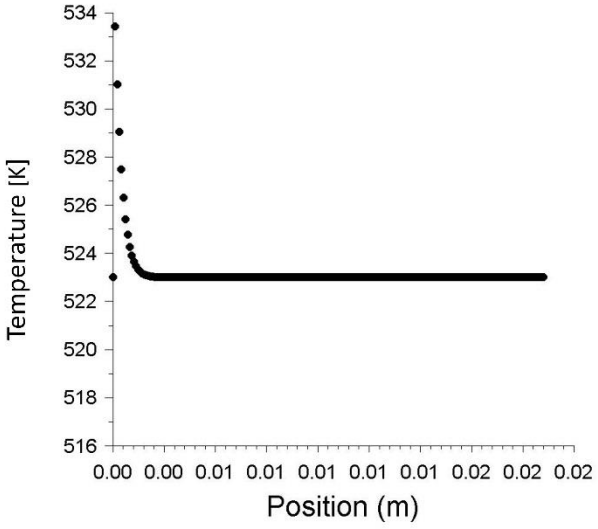

(a)

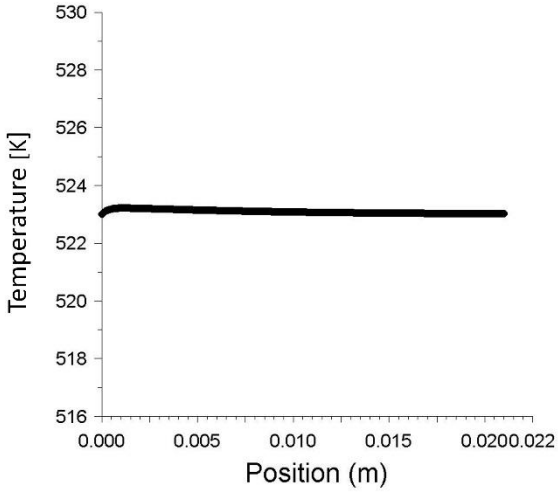

(b)

Figure 3.2 Temperature profile from a single channel model using (a) kinetics –I and (b) kinetics-II

produced. This is predicted from both the reaction kinetics. However, in comparing the two kinetics, kinetics-I predict much higher mole fraction of CH4. This outcome is not preferred in FT synthesis as CH4 itself (in case of natural gas to liquid process) is the feed material for syngas (CO & H2) production. Also, from Figure 3.2 (a) and (b), it can be seen that kinetics-I predicts excessively high temperature at the inlet region as against the uniform temperature profile predicted by kinetics –II for the same reactor model and with similar operating conditions. This indicates that kinetics-I is not completely reliable or not robust and hence not applicable in case of microchannel reactor model. Nevertheless, since the demand for gasoline is beginning to shrink, clean liquid syn-crude or wax is the desired product, low-temperature FT synthesis (493− 523 K) using cobalt based catalyst is desired operation type. Accordingly, reaction kinetic data of Velocys cobalt catalyst[16] is used in the rest of the simulation study.

3.2.2 Effect of channel geometry

This section is divided into two parts – Part A for effect of coolant channel dimensions and Part B for effect of process channel dimensions. This section summarizes the CFD simulation study to evaluate heat transfer performance of few (3 to 4) microchannel design candidates. The candidates vary in terms of the channel geometrical parameters like channel height, width, channel cross sectional aspect ratio, wall thickness between channels, etc. Separate studies were carried out to determine the best candidate out of the chosen candidates for (Part A) coolant channel and (Part B) process channel.

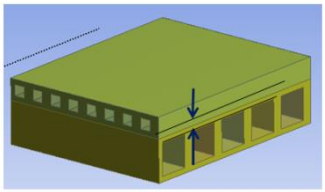

(a) 0.5 mm thickness

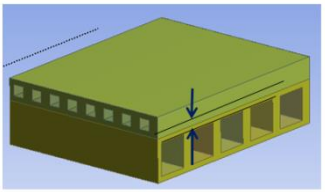

(b) 1 mm thickness

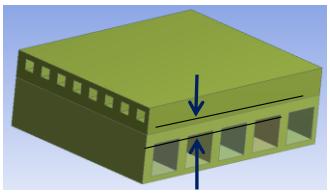

(c) 2 mm thickness

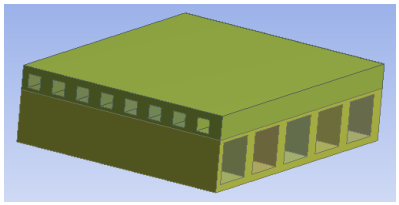

(d) 1 mm x 1 mm

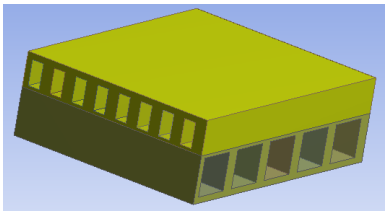

(e) 1 mm x 2 mm

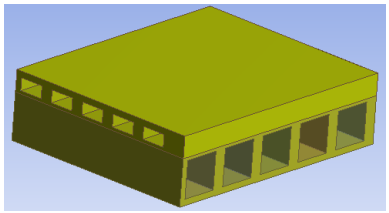

(f) 1 mm x 1 mm

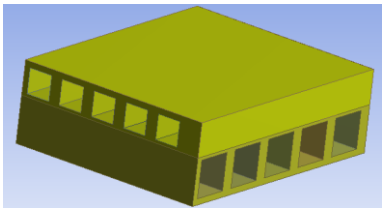

(g) 1 mm x 2 mm

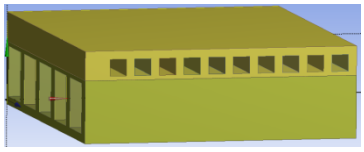

(h) 0.5 mm thickness

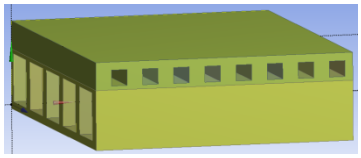

(i) 1 mm thickness

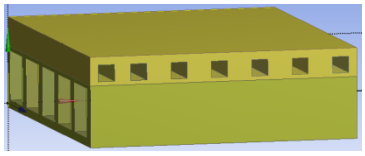

(j) 1.5 mm thickness

Figure 3.3. Multichannel micro reactor design with different thickness between coolant and process channel plane (a – c), different coolant channel cross section (d – e) and different thickness between two coolant channels (h – j).

Part A: *Coolant channel design evaluation*

A compact microchannel reactor design with two layers of microchannels, each for a coolant channel layer and a process channel layer was considered for the present study. The same microchannel reactor is modified to create a number of reactor design that varies coolant channel width, height, thickness between coolant channel and process channel layer, thickness between two coolant channels etc, as shown in Figure 3.3.

Assumption:

Process channel:

Considered as heat generation region(a heat generation profile as calculated from ASPEN model with reaction kinetics considered) with heat flow only and no fluid flow

Coolant Channel:

Fluid flow with no phase change and only sensible heating

Channel Walls:

No heat loss from any exterior wall to the surrounding. Meaning, the generated heat is taken up only by the coolant by way of conduction through the contact walls.

Material considered for the simulation

Table 3.1. Materials considered for the simulation

Coolant	Liquid water
Process channel	Nickel (material property close to catalyst)
Wall	Steel

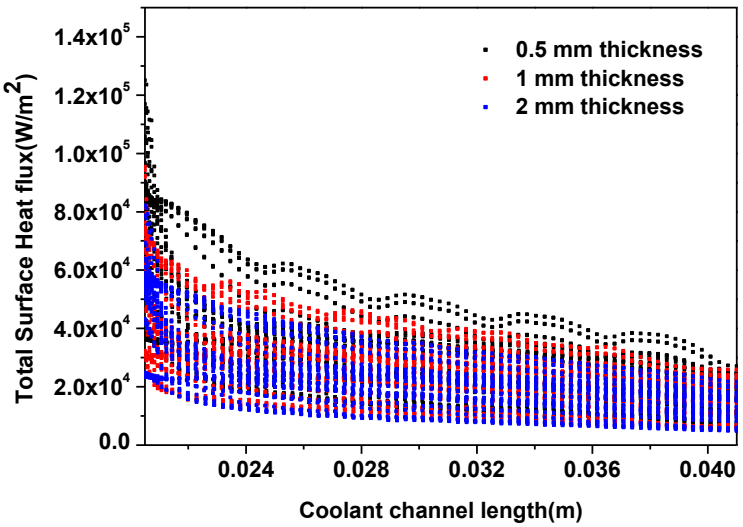

Figure 3.4. Total surface heat flux to the coolant channel along the channel length for different thickness between coolant channel layer and process channel layer after 5 sec simulation time.

Table 3.2. Effect of channel layer thickness

	Channel layer thickness		
	0.5 mm	1 mm	2 mm
Average surface heat flux	34579.72	27169.72	23359.90
% Effect on heat flux	48.03	16.31	0

Effect of thickness between process channel layer and coolant channel layer on heat transfer performance is first investigated. From heat transfer perspective, lesser thickness allows higher heat flux, as evident from the heat flux comparison between multi-channel design of different layer thickness. Therefore, 0.5 mm thickness

allows higher heat flux as compared to 1 mm and 2 mm thickness.

Four designs of coolant channel cross sections were considered as given in Figure 3.3 (d –g).

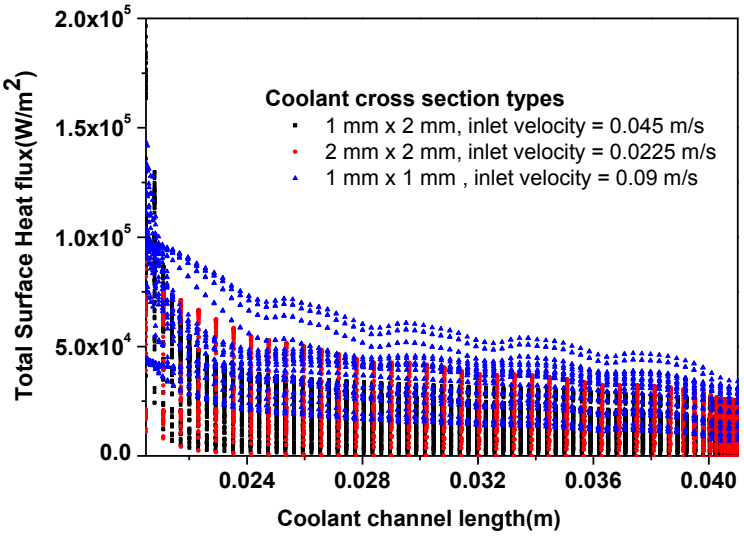

Figure 3.5. Total surface heat flux to the coolant channel along the channel length for different coolant channel cross section types at 7 sec simulation time [same mass flow rate differing inlet velocities]. Coolant inlet velocity differs in order to maintain same coolant mass flow rate.

Table 3.3. Effect of different coolant channel cross section types [same mass flow rates differing inlet velocities]

	Coolant Channel cross section type [same mass flow rates]		
	1 mm x 1mm	1 mm x 2mm	2 mm x 2mm
Inlet velocity [m/s]	0.09	0.045	0.0225
Average surface heat flux[W/ m^2]	40911.32	21891.43	21217.36
% Effect on heat flux	92.82	3.17	0

For coolant with same mass flow rates differing in velocities, 1 mm x 1 mm channel type allows higher heat flux as compared to that of 1 mm x 2 mm and 2 mm x 2 mm channel types.

Table 3.4. Effect of different coolant channel cross section types [different mass flow rates keeping same inlet velocities]

	Coolant Channel cross section type [same inlet velocities, 0. 09 m/s]			
	1 mm x 1mm	1 mm x 2mm	2 mm x 1mm	2 mm x 2 mm
Average surface heat flux[W/ m^2]	34579.72	20194.52	23880.62	21790.48
% Effect on heat flux	71.23	0	18.25	7.9

For same coolant velocities differing in mass flow rates also 1 mm x 1 mm channel type allows higher heat flux as compared to that of 1mm x 2 mm, 2 mm x 1 mm and 2 mm x 2 mm channel types.

Table 3.5. Effect of different coolant channel cross section types/orientation [same mass flow rates, same inlet velocities]

	Coolant Channel orientation	
	1 mm x 2mm	2 mm x 1mm
Average surface heat flux [W/ m^2]	21217.36	23572.40
% Effect on heat flux	0	11.10

Table 3.6. Effect of wall thickness between coolants [same mass flow rates, different inlet velocities] after 7 sec simulation.

	Coolant channel wall thickness (7 second simulation)		
	0.5 mm	1 mm	1.5 mm
Average surface heat flux[W/ m^2]	41919.08	40927.36	31305.35
% Effect of 1 mm over 2 mm on heat flux	33.90	30.73	0

Table 3.2 – 3.6 summarize the simulation analysis considering microchannel reactor geometry design. If the coolant channel is oriented in such a way that surface area of the wall facing the process channel layer is higher, it ensures higher heat flux. This

is evident from the heat flux comparison between coolant channel orientation of 1 mm x 2 mm and 2 mm x 1 mm. 2 mm x 1 mm orientation (more surface area in contact with the process channel layer) allows 11.1 % increase in the average heat flux.

On comparing the heat flux for design with 1.5 mm and 0.5 mm wall thickness, the later has 5.26 % increment over the former implying that effect of coolant velocity slightly dominates when the heat transfer surface areas are not significantly different. There are 8 coolant channels with 1 mm wall thickness and 7 coolant arrangement with 1.5 mm coolant thickness. And as the total coolant flow rate is fixed, the coolant velocities for 1 mm and 1.5 mm thickness are 0.09 m/s and 0.102 m/s respectively.

Simulation analysis on effect of wall thickness indicates that lesser thickness allows higher heat flux. 0.5 mm wall thickness allows higher heat flux as compared to 1 mm and 2 mm thickness. Therefore 0.5 mm wall thickness may be more suitable for the compact GTL reactor design. For same mass flow rates differing in velocities, 1 mm x 1 mm channel type allows higher heat flux as compared to that of 1mm x 2 mm and 2 mm x 2 mm channel types. Coolant channel oriented in such a way that surface area of the wall facing the process channel layer is higher, ensures higher heat flux. This is evident from the heat flux comparison between coolant channel orientation of 1 mm x 2 mm and 2 mm x 1 mm.2 mm x 1 mm orientation (more surface area in contact with the process channel layer) allows 11.1 % increase in the average heat flux as compared to 1 mm x 2 mm. Reducing the coolant channel height to 1 mm from 2 mm has an effect of 12.51 % increase in average heat flux (for coolant channel base width as 2 mm) and 71.23 % increase in average heat flux for (coolant channel base width as 1 mm).

Coolant wall thickness (from study of 0.5 mm, 1mm and 1.5 mm thickness) has an effect in a way that how many coolant channels can be lined up within a fixed length (constrained by process channel length), and hence the consequence on the heat flux rate. However, rate of heat flux is found to be dominated by the coolant velocities in the coolant channels. This is evident from the heat flux comparison for 0.5 mm, 1 mm and 1.5 mm wall thickness between the coolant channels. For the fixed mass flow rate of the coolant by varying velocities, 1 mm and 1.5 wall thickness showed higher heat flux as compared to 0.5 wall thickness. This is because the coolant velocities are higher in channels with wall thickness 1 mm and 1.5 mm than that of 0.5 mm thickness.

Part B: *Process channel design evaluation*

In this part of the report, simulation study to compare heat transfer quantities like heat flux, and lateral temperature profile of candidate channel heights of 2 mm, 3 mm and 5 mm is presented. It is generally expected that shorter channel height of process channel will be more efficient in term of heat removal. This aspect is investigated quantitatively in section part. Also as the channel size decrease, the catalyst loading will approach uniformity and lead to uniform rate of reaction any cross section area, thereby resulting to near uniform radial temperature.

Figure 3.6 shows Lateral (or radial) temperature profile for 2 mm, 3 mm and 5 mm channel height and considering same channel length of 200 mm. Although the temperature difference is very less (less than 1 ^{o}C), shorter channel height predicts much uniform radial temperature.

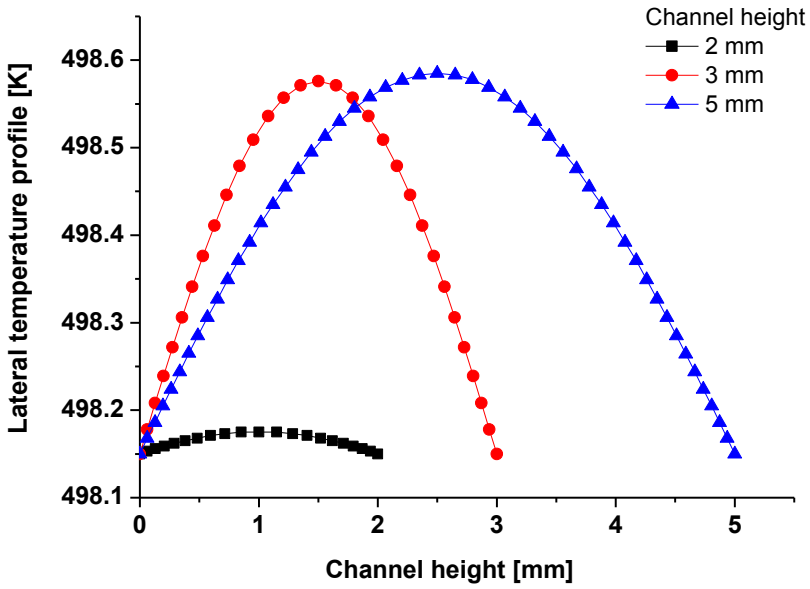

Figure 3.6. Lateral (or radial) temperature profile for 2 mm, 3mm and 5 mm channel height and channel length of 200 mm

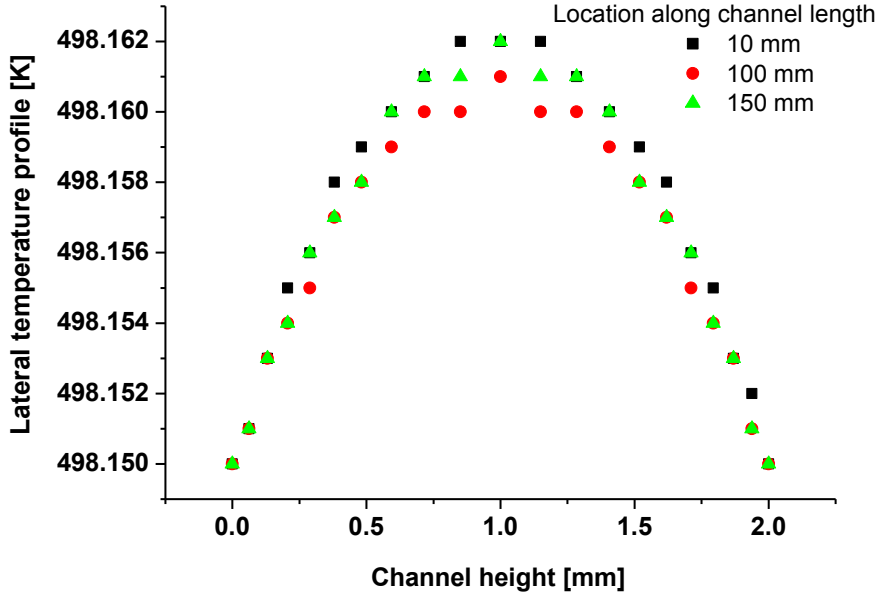

Figure 3.7 Lateral (or radial) temperature distribution along the channel length for 2 mm channel height and channel length of 200 mm

Figure 3.7 shows radial temperature distribution along the channel length for 2 mm channel height. Simulation predicts less than 1 ^{o}C temperature difference along the channel length for process channel height of 2 mm. This indicates that shorter channel height is preferred as against higher channel height for efficient heat removal from process channel in microchannel reactor.

3.2.3 Effect of operating conditions

To understand the importance of maintaining reactor temperature at particular value, effect of reactor temperature on CO conversion, CH_4 selectivity and C_{5+} selectivity

were re-examined. This was facilitated by setting different temperatures as the wall thermal boundary condition on a pair of the opposite walls of Single Channel-B shown in Figure 2.1 of Chapter 2. Due to the short heat transfer distance with 1 mm x 1 mm cross sectional channel, temperature at reactor internal was almost equivalent to that of wall temperature. Simulation results in Figure 3.8 shows that increase in channel temperature leads to increase in both CO conversion and undesired product - CH_4 selectivity, while selectivity for desired product - C_{5+} decreases. For example, when syngas flow rate was 5000 hr^{-1} GHSV and catalyst loading as 120 %, reactor temperature maintained at 523 K gives CO conversion of 86.6%, with selectivity for CH_4 and C_{5+} as 19.5 % and 74.9% respectively. But when the reactor temperature was reduced to 508K, CO conversion was reduced to 69.2% while selectivity for CH_4 decreases to around 12.6% and selectivity for C_{5+} increases to around 83.2%. Similar trend was observed by Myrstad et al.[9], Tonkovich et al.[16] and Ying et al.[45] in their experiments. This indicates that for a desired reaction conversion and product selectivity, it is necessary to maintain reaction channel temperature below a particular value, say 523K in this case. Generally, as the intrinsic activity of the catalyst decline, reactor is operated at slightly higher temperature to achieve the same level of CO conversion.

On simulating different syngas ratio with the same reactor model, result indicates higher CH4 selectivity and lower C5+ selectivity for syngas ratio of 1.5 compared to syngas ratio of 2, as shown in Figure 3.9. Also at higher syngas ratio of 2.5, CH4 selectivity is high (above 25 %). This is expected as higher syngas ratio promotes methanation reaction and lower syngas ratio promotes carbon formation through Boudouard reaction. In most microchannel FT synthesis, syngas ratio of 2 is considered optimum stoichiometric ratio. This is indicated from our simulation

analysis where syngas ratio of 2 gives optimum CH4 and C5+ selectivity.

On studying the effect of operating pressure on CO conversion, CH4 and C5+ selectivity, the result indicates CO conversion above 8)% for the range of simulated conditions (operating from 18 bar to 26 bar), but with undesired CH4 and C5+ selectivity for 18 bar and 26 bar. On the other hand, at operating pressure of 22 bar highest C5+ selectivity is predicted. This result indicates that operating pressure of 20 bar to 22 bar could be optimum operating range.

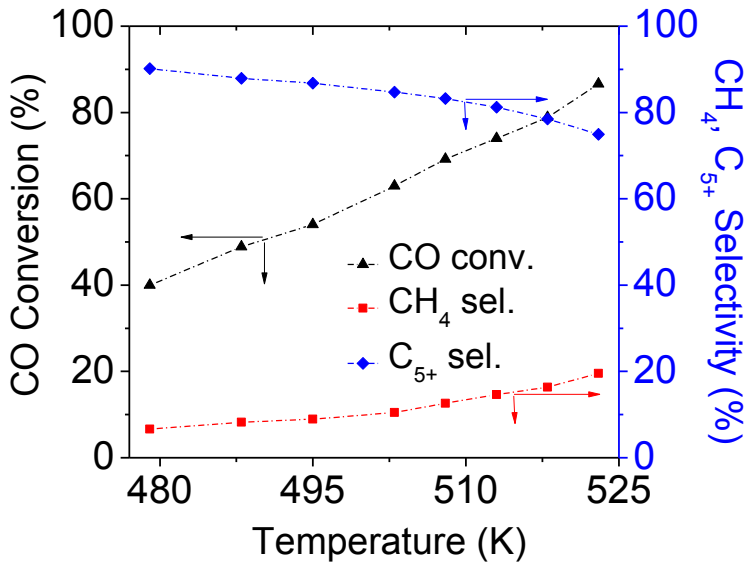

Figure 3.8. CO Conversion (conv.), CH4 and C_{5+} selectivity (sel.) from FT reaction simulation with Single-Channel-B at different channel temperature [Process condition: GHSV = 5000 hr^{-1}; catalyst loading =120 %]

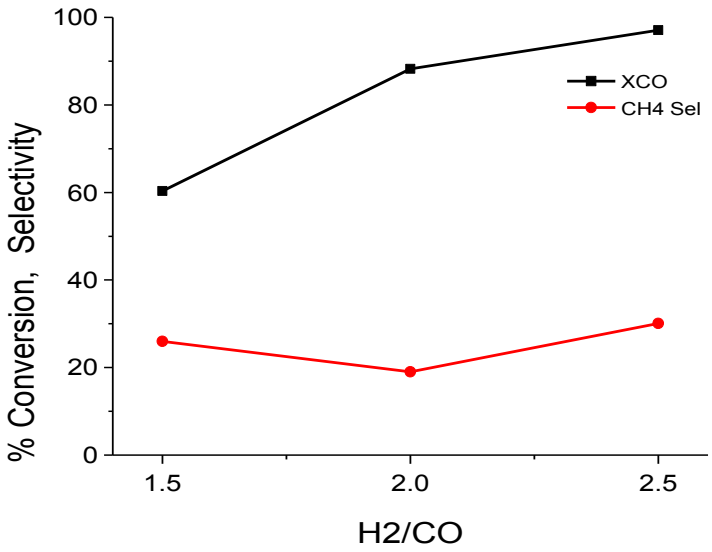

Figure 3.9. Effect of syngas ratio on CO conversion and CH4 selectivity.

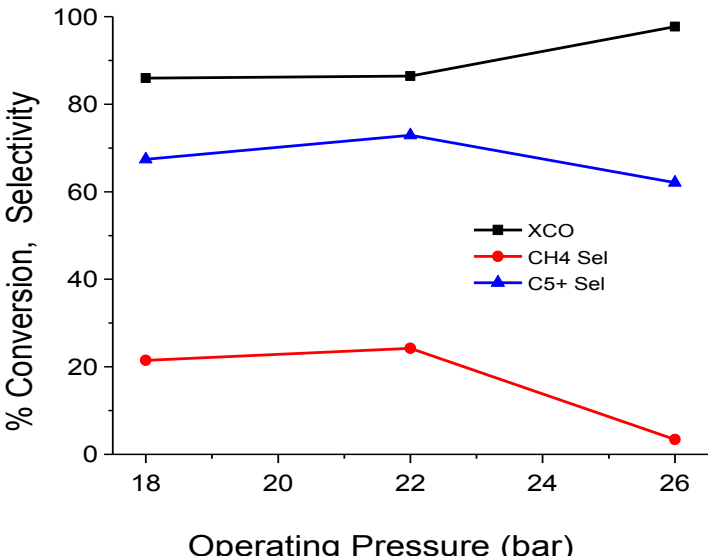

Figure 3.10. Effect of operating pressure on CO conversion and CH4 selectivity [Process condition: GHSV = 5000 hr^{-1}; catalyst loading =120 %].

3.3. Strategies for heat exothermic heat removal

In this section, we present our investigation on common strategy used at industrial and lab-scale to adequately remove exothermic heat from a typical microchannel reactor block. Multichannel reactor model developed using CFD tool and described in the previous chapter is coupled with wall boiling phenomena in coolant channels to quantify effect of wall boiling condition on heat transfer enhancement and comparison of wall boiling coolant to that of common single phase coolant – water and heating oil.

3.3.1 Wall boiling coolant and heat transfer enhancement

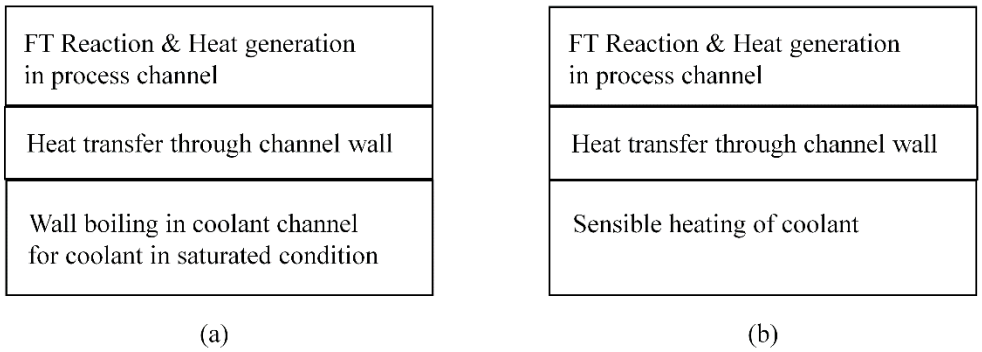

Figure 3.11. Schematic of heat transfer in microchannel reactor system (a) for wall boiling condition, (b) non-evaporative coolant.

In coolant channels, flow is single phase liquid, in case of cooling oil and subcooled water. Whereas, it is two-phase flow in case of saturated water due to wall boiling condition. Consequently, laminar flow is assumed for cooling oil and

subcooled water, and turbulence flow for saturated water under wall boiling condition. Relevant conservation equations for phase continuity, momentum and energy transfer are applied. Source term in continuity equation and buoyancy effect in momentum equation are also considered in case of two-phase wall boiling flow. Eulerain-Eulerian multiphase framework with interpenetrating continua, reviewed in detail by (Ishii[38]; Drew and Passman[39]; Yeoh and Tu[40]), was applied to model two-phase wall boiling flow with liquid as continuous phase and vapor as discrete phase.

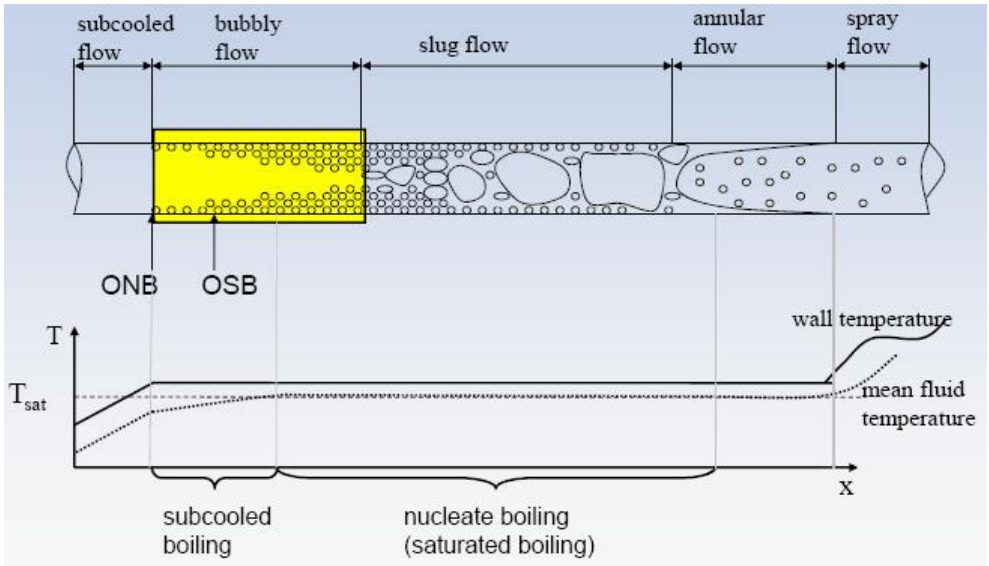

Figure 3.12. Schematic of mechanistic wall boiling model of saturated coolant (Kurual and Podowski, 1991)[41]

Heat flux from the heated wall to the coolant is described by mechanistic model of Kurul and Podowski[41,42] which is a summation of heat fluxes due to different mechanisms, as described in Figure 3.12. In the region where liquid is in contact

with heated wall, heat transfer is same as that of single phase flow, called convective heat transfer. In the region where bubbles suddenly form and grow, heat is taken up by vapor generation, called evaporative heat transfer. And heat transfer due to recirculation and the liquid replacing the bubble sites is called quenching heat transfer. Accordingly, the total wall heat flux is defined as sum of the three parts:

Mechanistic wall heat flux: $$Q_{tot} = Q_C + Q_Q + Q_E \quad (3.1)$$

Where Q_C, Q_Q and Q_E represent the heat flux component due to convection, quenching and evaporation, respectively. Detail models of the component heat fluxes, corresponding heat transfer co-efficient correlations including closing parameters: bubble diameter at detachment, nucleation site density, and bubble influence area and bubble detachment frequency are reviewed in Krepper and Rzehak[15]. Mass transfer from the liquid phase to vapor is accounted by the rate of evaporation which is a function of bubble diameter at detachment, nucleation site density and bubble detachment frequency. Since temperature difference between liquid phase and vapor phase are expected to be small, heat transfer between the two phases is assumed to be negligible as compared to the heat transfer from the channel wall.

For single-phase coolant flow as is the case with subcooled oil and subcooled water, convective heat transfer is assumed to be the only means of heat removal and only the first term in eq. (3.1) will remain.

Figure 3.13 shows the temperature contour of reactor block when same value of flow rates (5.4 g/min) was applied for all three coolant types. ΔT_{max}, defined as

temperature difference between hottest spot and coldest spot in the reactor (coldest spot is equal to coolant inlet temperature which is 498 K in the present case) is highest in case of cooling oil as coolant ($\Delta T_{max} = 32$ K) and least for saturated water as coolant ($\Delta T_{max} = 12$ K) with that of subcooled water lying in between($\Delta T_{max} = 17$ K). The result implies that subcooled water has higher cooling capacity than cooling oil. And saturated water has higher cooling capacity than subcooled water with relative difference varying over extend of wall boiling.

On comparing computed heat fluxes through coolant channels, see Figure 3.14(a) -(c), higher heat flux was obtained in case of saturated water compared to subcooled water and cooling oil. However, in all three cases, coolant channels adjacent to the reaction channel inlets have higher heat fluxes compared to other coolant channels on the same plane. This is expected as reaction rates and hence heat generation rate are much higher at the channel inlet region. Similar trend was reported by Tonkovich et al.[16]. Computed average heat transfer co-efficient (h) and heat flux ($\dot{Q}$) through the channels for three coolants cases are given in Table 3.7. Lower heat flux was achieved with cooling oil, 8783.4 W/m^2 as compared to subcooled water, 8850.1 W/m^2 and saturated water, 8952.9 W/m^2.

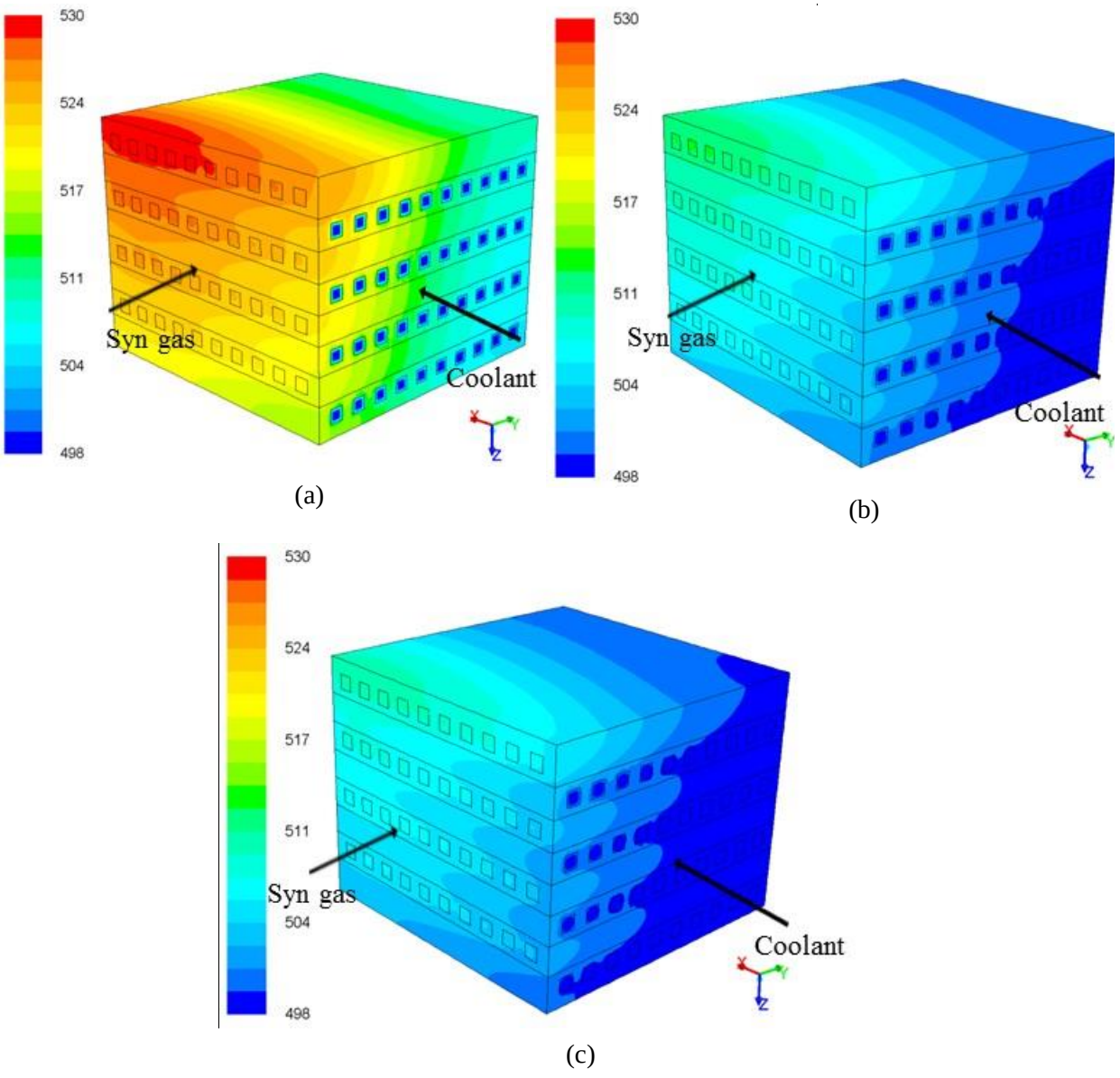

Figure 3.13. 3D Temperature [K] contour on microchannel reactor block for cooling oil (a), subcooled water (b) and saturated water (c) as coolants with flow rate = 5.4 g/min per channel (GHSV = 5000 hr^{-1}; catalyst loading 120 %). +ve X direction: coolant flow; +ve Y direction: syngas flow

Higher heat flux in subcooled water and saturated as compared to that of cooling oil is primarily due to higher thermal conductivity of the former two. However, between subcooled water and saturated water, wall boiling condition in case of saturated water provided additional heat removal capacity. Degree of additional heat removal capacity (or heat transfer enhancement) would however depend on extend of boiling along the coolant channels. With average exit vapor fraction of 0.13, enhancement in wall heat flux was nearly 3 W/m^2. By allowing slightly higher exit vapor fraction, more enhancement in heat transfer is expected as more fraction of coolant will get vaporized in coolant channels.

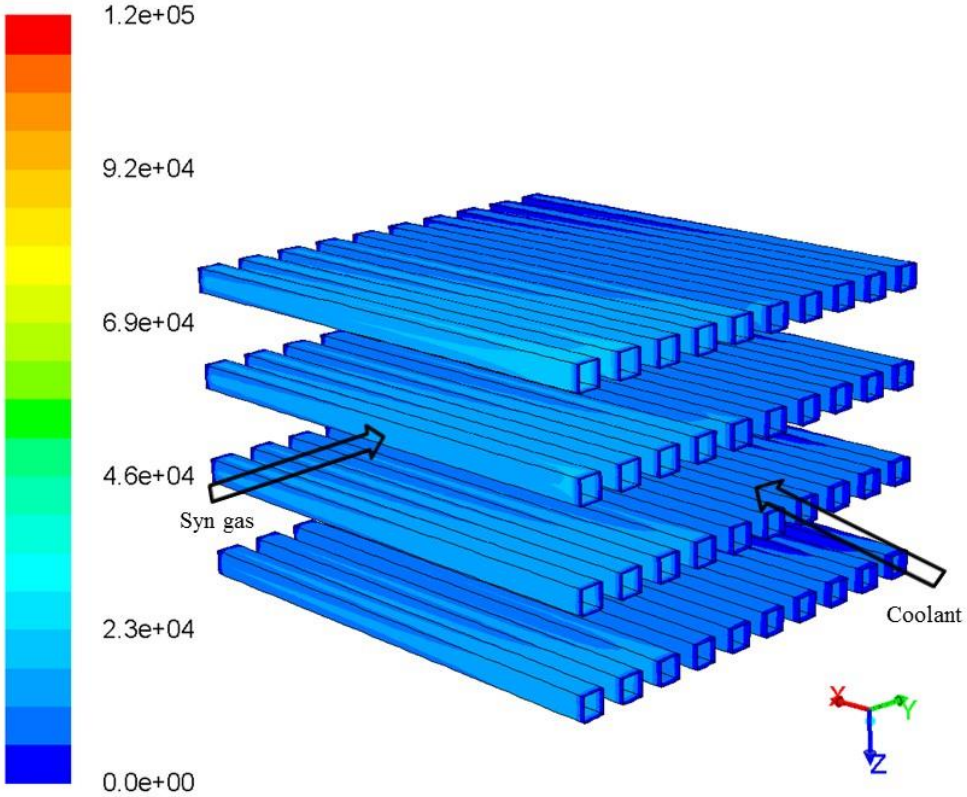

Figure 3.14(a). 3D Heat flux [W/m^2] contour on coolant channels for oil as coolant with flow rate = 5.4 g/min per channel (GHSV = 5000 hr^{-1}; catalyst loading 120 %). +ve X direction: coolant flow; +ve Y direction: syngas flow

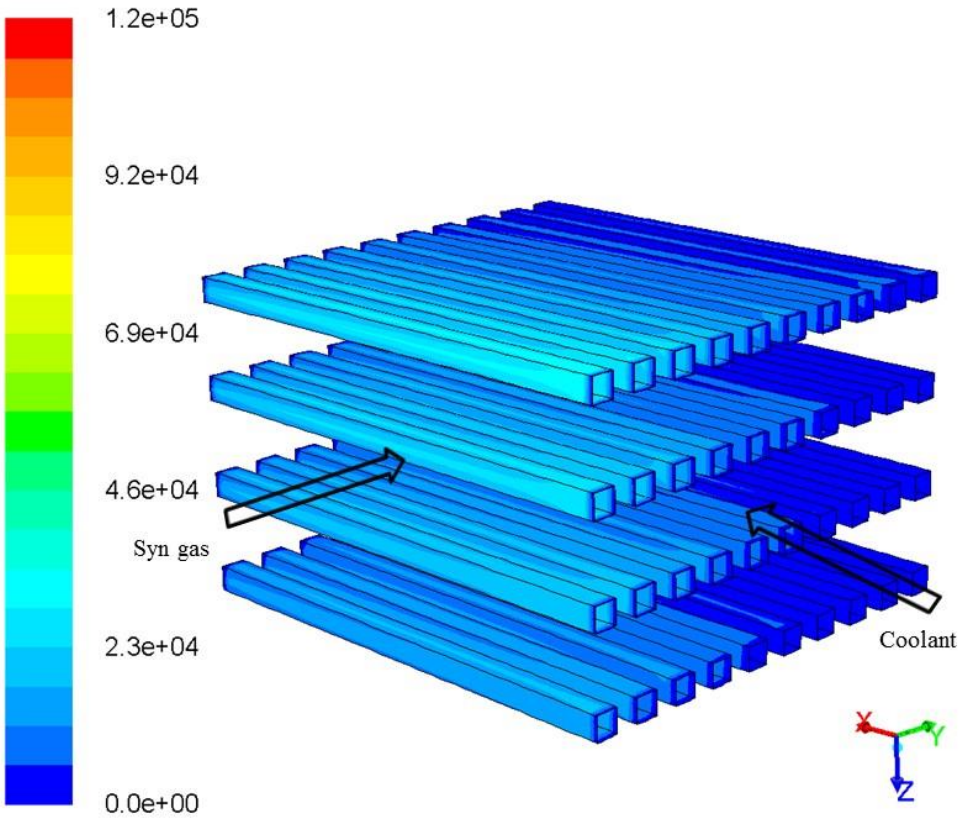

Figure 3.14(b). 3D Heat flux [W/m^2] contour on coolant channels for subcooled water as coolant with flow rate = 5.4 g/min per channel (GHSV = 5000 hr^{-1}; catalyst loading 120 %). +ve X direction: coolant flow; +ve Y direction: syngas flow

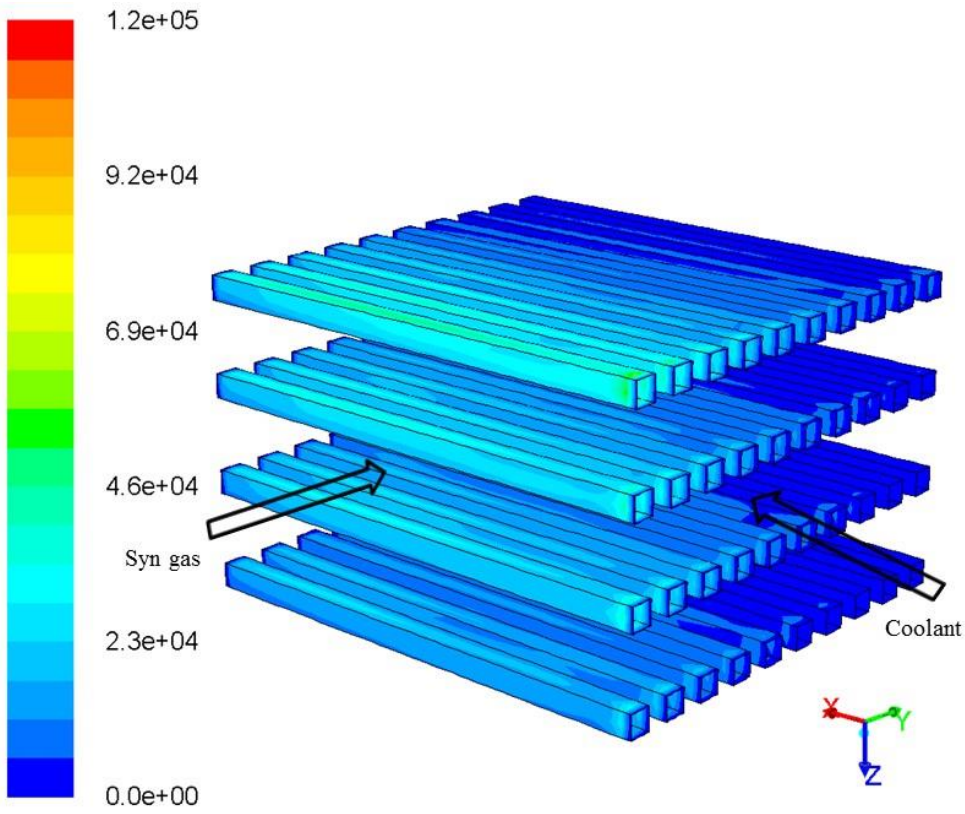

Figure 3.14(c). 3D Heat flux [W/m^2] contour on coolant channels for saturated water as coolant with flow rate = 5.4 g/min per channel (GHSV = 5000 hr^{-1}; catalyst loading 120 %). +ve X direction: coolant flow; +ve Y direction: syngas flow

Table 3.7. Heat flux & heat transfer coefficients for GHSV 5000 hr^{-1} & catalyst loading 120 % (100% catalyst loading = 1060 kg/m3).

Parameters	Cooling oil	Subcooled water	Saturated water
$h_{coolant}$ (W/m^2-K)	39.6	41.2	41.9
$\dot{Q}_{coolant}$ (W/m^2)	8783.4	8850.1	8952.9
$h_{process}$ (W/ m^2-K)	38.4	40.9	41.3
$\dot{Q}_{process}$ (W/m^2)	8881.6	8885.3	8887.7
ΔT (K)	32	17	12
Avg. exit vapour fraction	-	-	0.13

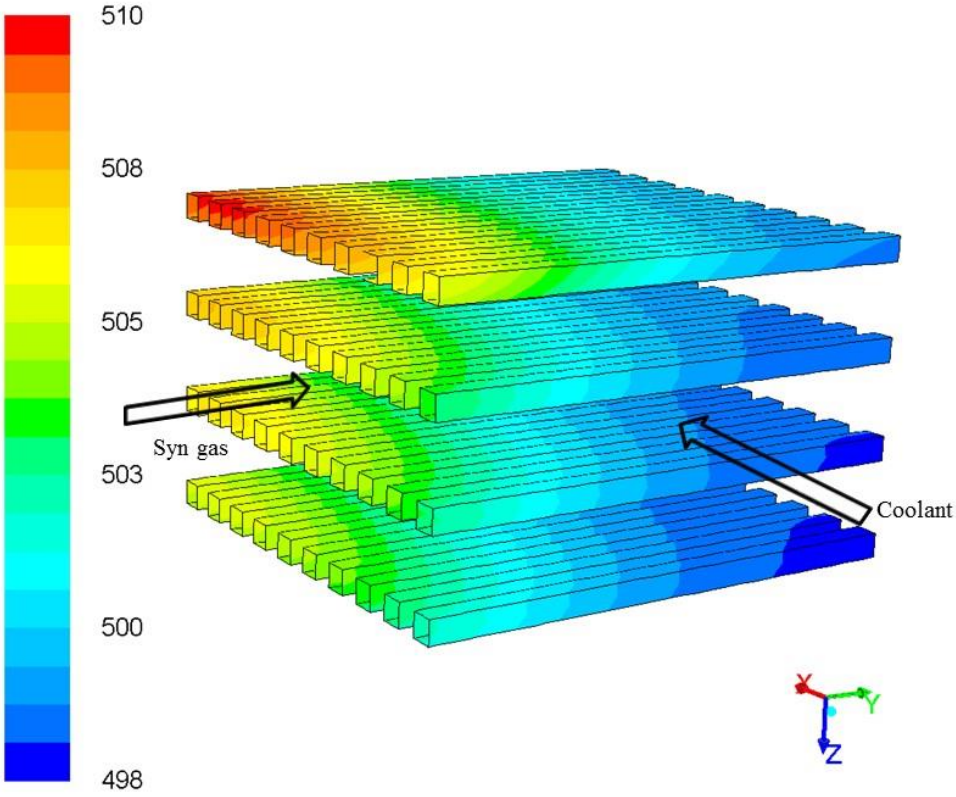

Figure 3.15(a). 3D Temperature [K] contour on reaction channels of microchannel reactor block for wall boiling coolant flow (GHSV = 5000 hr^{-1}; catalyst loading 120 %; saturated water flow rate = 5.4 g/min per channel). +ve X direction: coolant flow; +ve Y direction: syngas flow

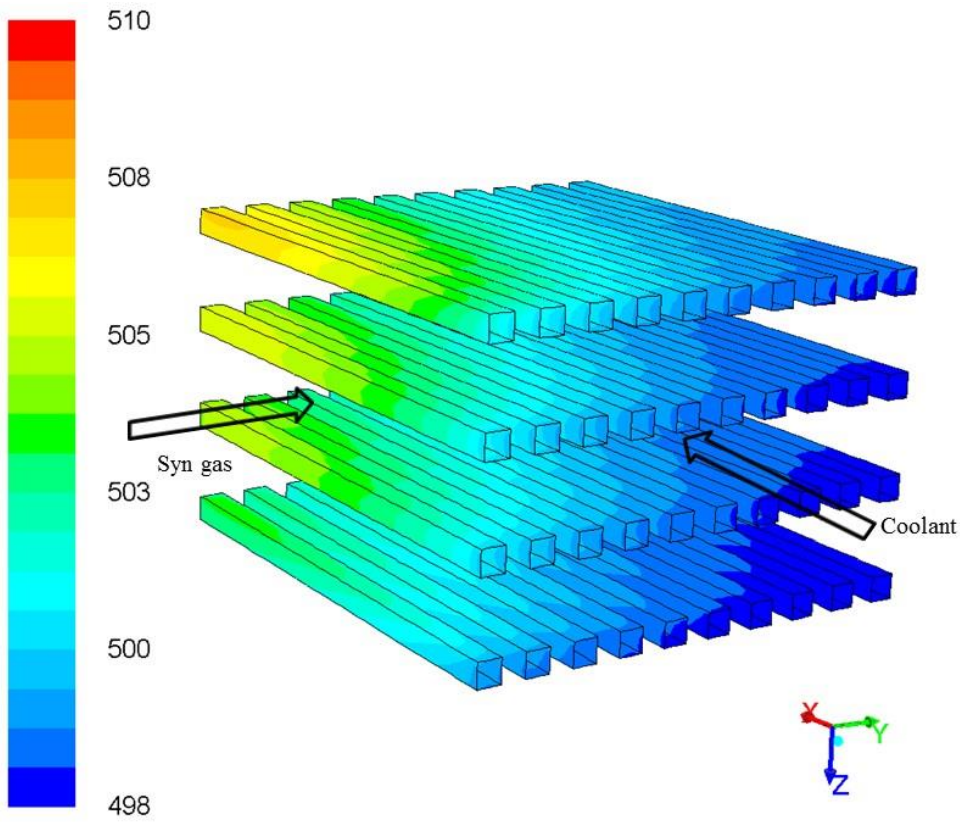

Figure 3.15(b). 3D Temperature [K] contour on coolant channels of microchannel reactor block for wall boiling coolant flow (GHSV = 5000 hr^{-1}; catalyst loading 120 %; saturated water flow rate = 5.4 g/min per channel). +ve X direction: coolant flow; +ve Y direction: syngas flow

Temperature range of 483 to 513 K is generally desired to maximize the middle distillate for low temperature FT synthesis (Arzamendi et al.[1]). In this present case of syngas flow rate of 5000 hr^{-1} GHSV, catalyst loading 120 % and H_2/CO as 2,

saturated water flow rate range of 3 g/min to 9 g/min can be considered an adjustable range. When saturated water flow rate was 5.4 g/min in each coolant channel, ΔT_{max} (defined as temperature difference between hottest spot and coldest spot in the reactor) was less than 15 K. Temperature in all three reaction channel planes were predicted between 498 K and 508 K, see Figure 3.15(a), expect for one reaction channel plane which has only one coolant channel plane at below to remove heat. Intuitively, it can be commented that if a coolant channel plane is added on the other side (at above), then this reaction channel plane will probably have its hottest spot (also called as peak temperature) not exceeding 508 K. As far as coolant channel planes are concern, temperature is nearly isothermal in most of the region, except for the regions near reaction channel inlet and hottest spot, as seen in Figure 3.15(b). This is expected with saturated water as coolant as some of the heat is removed through evaporative heat flux (Q_E) and quenching heat flux (Q_Q) in addition to convective heat flux (Q_C).

For a particular process condition, reactor temperature can be controlled at a value within a desired range by adjustable coolant flow rate, saturated water flow rate in this case. Simulations were carried out to see effect of saturated water flow rate on reactor temperature of the multichannel block model. Figure 3.16 and figure 3.17 illustrates the saturated water volume fraction profile along coolant channel length for two different coolant inlets, 0.02 m/s and 0.09 m/s. As expected, with higher coolant inlet, higher exit liquid volume or lower vapor fraction is obtained. From Figure 3.18, it is understood that both average exit vapor fraction and mean FT temperature can be strong function of saturated water flow rate. Average exit vapor

fraction is the average of vapor fraction by mass at the exit of all 40 coolant channels. Mean FT temperature is the mean temperature of all 40 reaction channels. For saturated water flow rate of 1 g/min, vapour fraction was around 0.4 and the value decreases to 0.2 when the saturated water flow rate was increased to 5.5 g/min. The values of coolant flow rate given here are per channel basis. At around saturated water flow rate of 3 g/min, mean FT temperature is around 510 K and the value decreases as we increase the coolant flow rate. But the decrease in temperature slows down for flow rates above 6 g/min, and eventually tends to settle down to the saturated temperature, 500 K in this case. On the other side, if the coolant flow rate is lower than a particular value, coolant flow under wall boiling condition will be predominantly vapor and local dry out can occur inside coolant channel, in addition to the insufficient cooling of reaction channels. Local dry out inside coolant channels is highly undesired as it can lead to drastic reduction in heat transfer and subsequent over heating of the spot resulting into possible thermal runaway. Therefore, a range of adjustable saturated water flow rate should be sought for a particular process condition to maintain reactor temperature to a desired value and still prevent risky condition of local dry out.

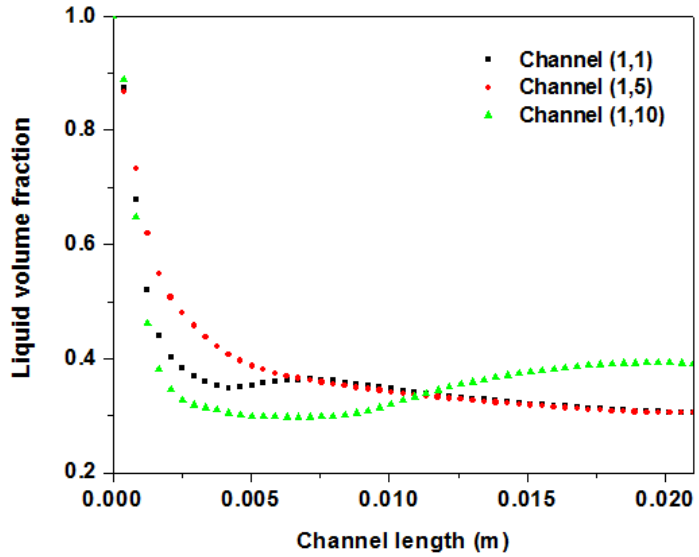

Figure 3.16. Liquid volume fraction in wall boiling coolant channel for 0.02 m/s inlet velocity

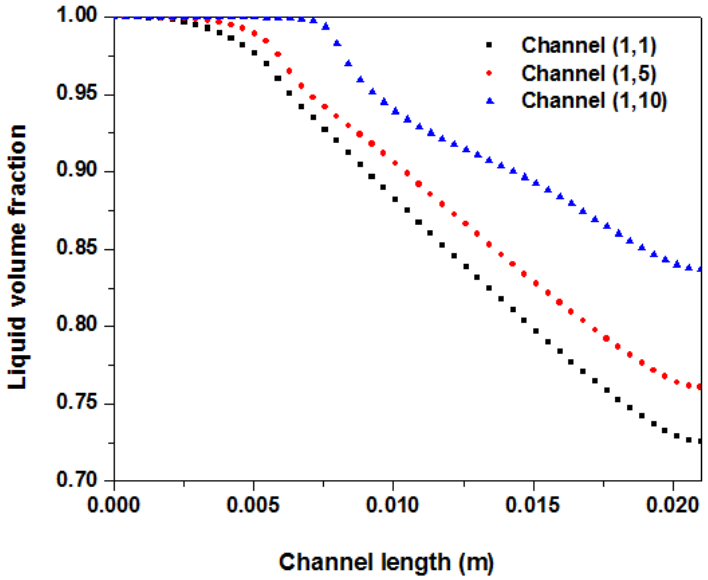

Figure 3.17. Liquid volume fraction in wall boiling coolant channel for 0.09 m/inlet velocity.

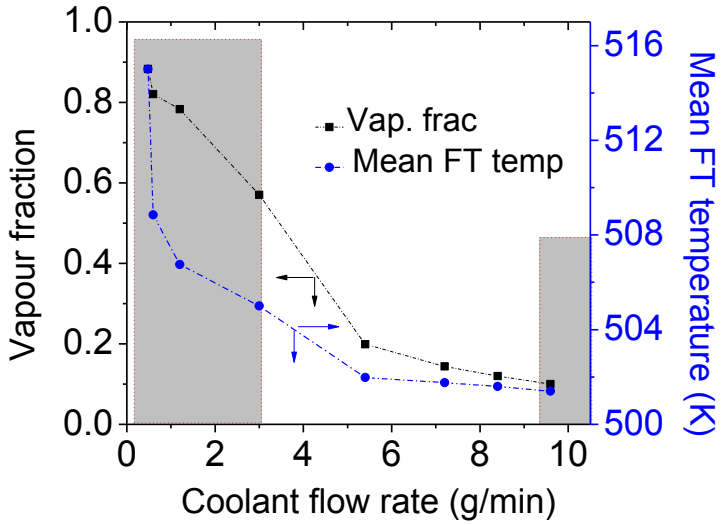

Figure 3.18. Effect of saturated water flow rate on vapor fraction and mean FT channel temperature (GHSV = 5000 hr^{-1}; catalyst loading 120 %)

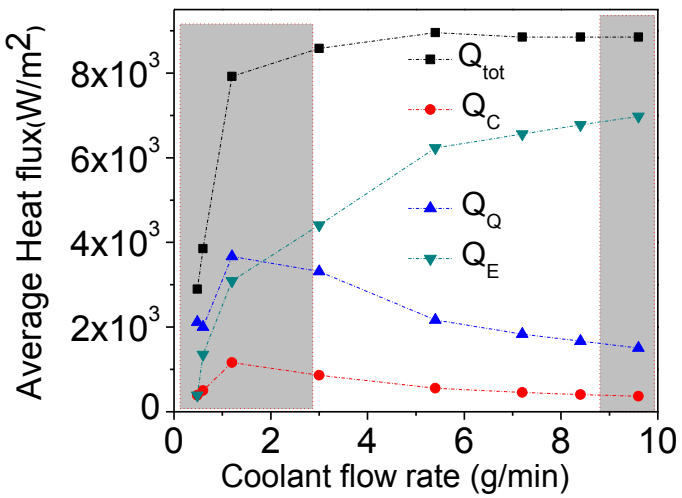

Figure 3.19. Effect of saturated water flow rate on average heat flux through coolant channels (GHSV = 5000 hr^{-1}; catalyst loading 120 %).

To explain the effect of saturated water flow rate on average vapor fraction and mean FT temperature, we need to look at the trends for component heat fluxes over saturated water flow rates considered. In Figure 3.19, it is seen that Q_E increases for saturated wate flow rates until around 1.2 g/min and then goes on to decrease slightly as the coolant flow rate is increased. This is because, at lower saturated water flow rates and up to a value, extend of boiling is higher, but decreases as flow rate increases beyond that value. While Q_Q also follows nearly the same trend, Q_C on other hand, increases as the coolant flow rate increases, which is expected. It is interesting to note that between a range of saturated water flow rate, 3 g/min to 9 g/min here, the total heat flux values are almost constant and at their highest limit. This gives an idea for adjustable range of saturated water flow rate.

It may be commented that for laboratory scale single channel Fischer-Tropsch reaction, higher cooling capacity coolants like saturated water may not be necessary and the generated heat can be removed by lower rank coolant like heating oil-Marlotherm SH (Deshmukh et al.[6]). For laboratory scale operation, getting saturated water supply may either be not economical or difficult to get. Also, high-temperature FT synthesis require less cooling load compared to low-temperature FT synthesis. This is evident from the work of Gumuslu and Avci[17] where they used steam to remove heat from their microchannel FT reaction channels. In low temperature FT, temperature between 493 and 523 K is preferred as the desired product is middle distillate and any increase in temperature beyond this range will not favor chain growth.

3.3.2 Catalyst zone division and discrete dilution

Use of highly active modern Iron and Cobalt based catalyst, coupled with high heat generation (165 kJ/ mol CO) of FT synthesis have resulted to the problem of high temperature gradient along the channel length. One method to address the problem is to use highly effective commercially available thermal fluids such as Melotherm™, and saturated water as coolants, as explored by Deshmuk et al[6] and Tonkovich et al[16] in their experimental study, and simulation study in the previous section. However, thermal fluids can be expensive, and saturated water can be difficult to handle in actual operations compared to those of cheaper and single phase coolant like subcooled water. Another method to avoid high thermal gradient and maintain a minimum thermal gradient along the channel is to divide the whole reactor length into a number of discrete zones and load different amount of catalyst in each zone, a method hereby called as method of discrete dilution. Figure 3.20 shows the schematic of catalyst zone division and application of different % catalyst loading to each zone.

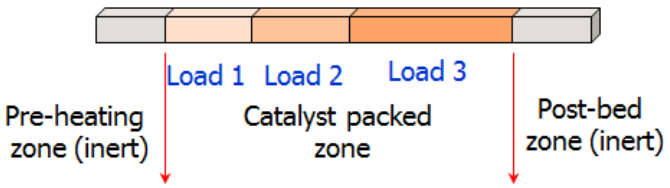

Figure 3.20. Schematic showing catalyst bed zone division

The method of catalyst dilution to control reaction rates and prevent excessively

high temperature peak inside reactors have been considered in existing works on catalyst packed tubular reactor[46-49] for other highly exothermic reactions. For instance, Hwang and Smith[50] employed combined effect of catalyst dilution and feed-stream distribution to achieve optimal control of temperature profile inside their multi-bed multi-tubular reactors for nitrobenzene hydrogenation and ethylene oxidation.

Simulation was conducted with different catalyst loading considering validated Velocys short single channel model (Single channel A described in Table 2.1 of chapter 2). In the first simulation case, catalyst bed zone was divided into three different zones and loaded with 30% for the zone closest to inlet region, 40% for the middle zone and 50% for the remaining zone. Figure 3.21 shows the comparison of heat generation profile for discrete catalyst loading with that of uniform catalyst loading. As expected, the simulation predicted lower heat generation in the zone closest to syngas inlet compared to that of uniform loading all throughout the channel length. Therefore the simulation indicates that discrete catalyst dilution is a feasible strategy for distributing the heat generation evenly along the channel length. This further will remove the challenge to maintain uniform temperature profile along the reaction channel. This strategic loading can also help in easer flow of the FT product down the channel, especially for C5+ product components like wax, if most of the C5+ products are formed in the second half of the catalyst packed region, as shown in Figure 3.22.

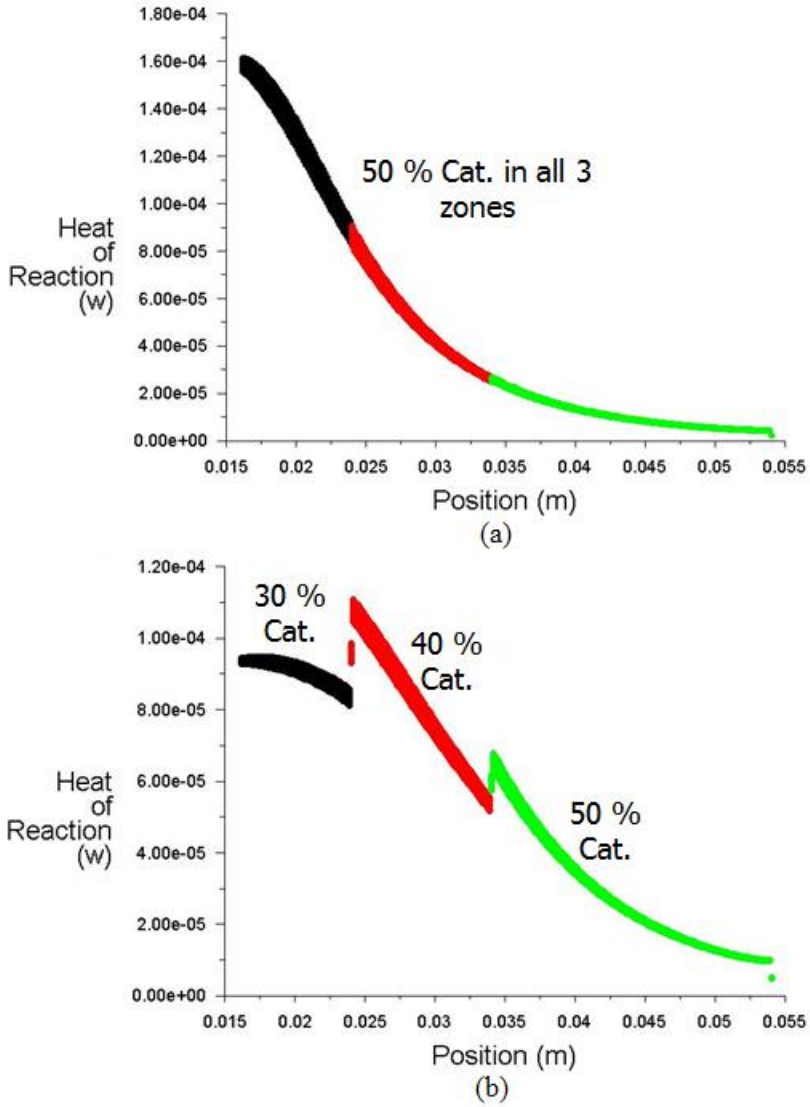

Figure 3.21. Heat generation profile for different catalyst loading method (a) uniform loading (50 % catalyst loading), (b) catalyst zone division and non-uniform loading (1st zone 30 %, 2nd zone 40% and 3rd 50 %)

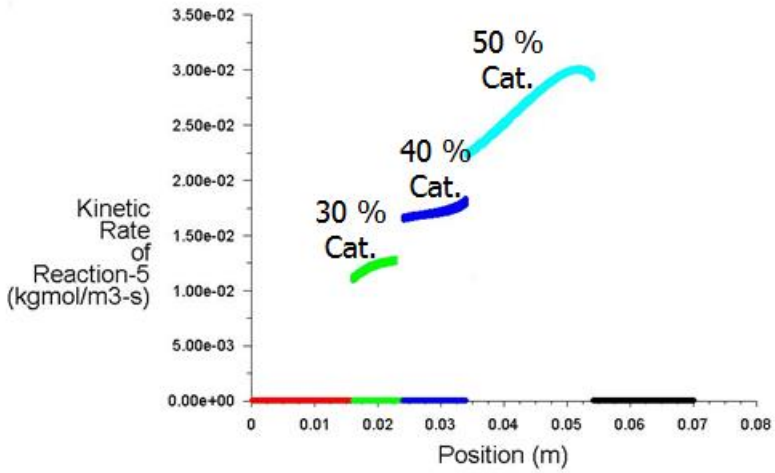

Figure 3.22. Reaction rates for C5+ product formation at different catalyst zones with 30%, 40 % and 50 % catalyst loading.

However, a non-optimized method of discrete dilution would not necessarily guarantee an optimal reactor performance. On the other hand, an optimal number of discrete zones, zone length and % loading is expected to prevent abnormally high FT reactions and consequently undesirably high heat generation at any region inside the reaction channel. On that regard, different cases with different number of catalyst zone division, different zone length and different % loadings are considered. Figure 3.23 shows the heat generation and temperature profile for strategy –I (1^{st} zone 30 %, 2^{nd} zone 40% and 3^{rd} 50 %) and strategy –II (1^{st} zone 30 %, 2^{nd} zone 50% and 3^{rd} 60 %).

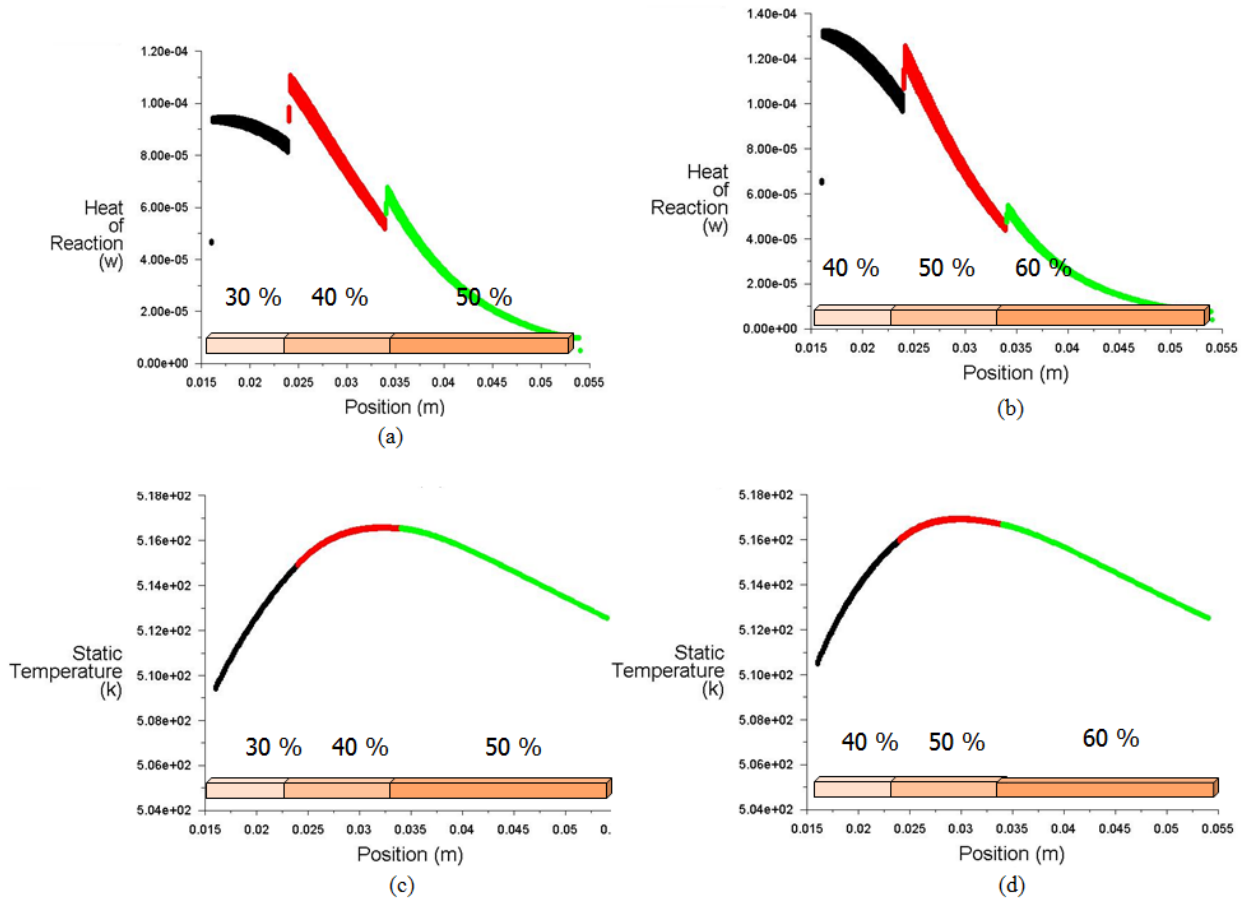

Figure 3.23. Heat generation and temperature profile showing effect of different catalyst loading strategy in divided zones. (a) Heat generation profile for strategy –I (1^{st} zone 30 %, 2^{nd} zone 40% and 3^{rd} 50 %). (b) Heat generation profile for strategy –II (1^{st} zone 30 %, 2^{nd} zone 50% and 3^{rd} 60 %). (c) Temperature profile for strategy-I and (d) temperature profile for strategy-II.

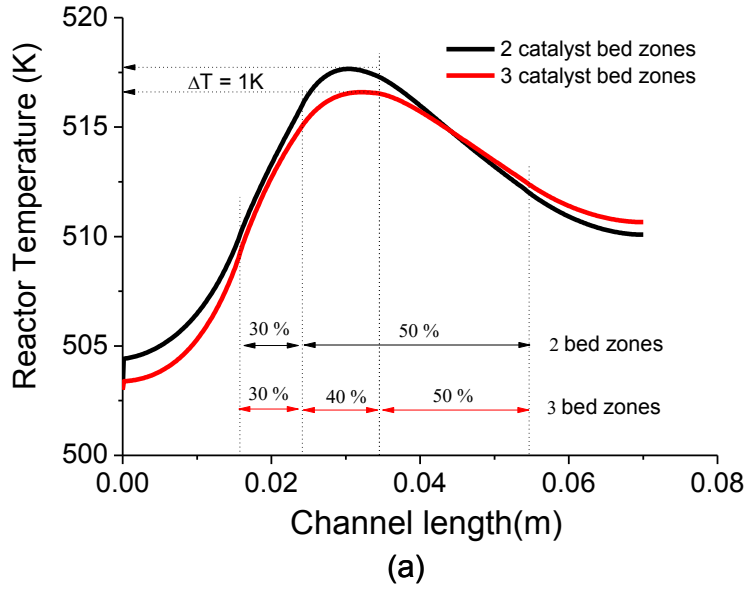

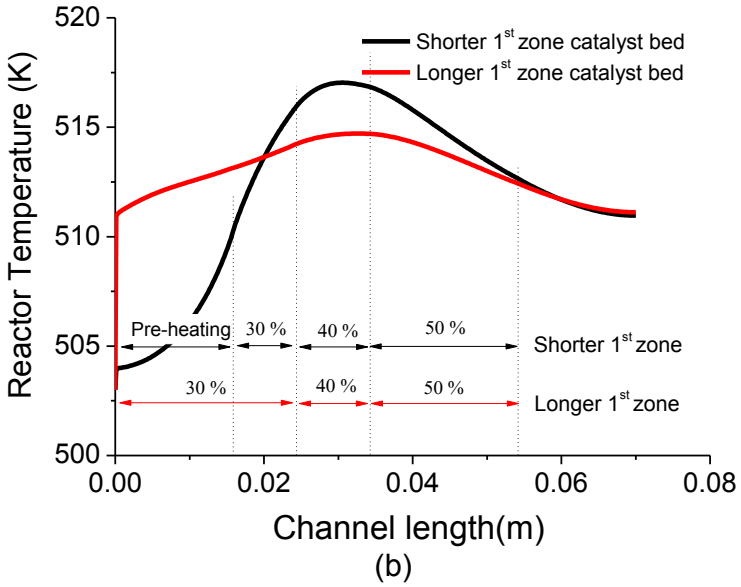

Figure 3.24. Temperature profile showing effect of different catalyst loading strategy in divided zones. (a) showing difference between 2 and 3 zone division, (b) showing effect of zone length.

Temperature profile in Figure 3.23 indicates slightly better result in terms of ΔT_{max} for strategy –I compared to strategy –II. Effect of different number of zones (between 2 zone division and 3 zone division) and different zone length is illustrated in Figure 3.24. It can be clearly seen that 3 zone division is better than 2 zone division in terms of ΔT_{max} and having longer 1^{st} zone length is better than having shorter 1^{st} zone.

3.3.3 Nano-fluid as coolant

Nanofluids are thermal fluids with nanoparticles added in it to increase the thermal conductivity of the thermal fluids. The thermophyscial properties can vary depending on the type of nanoparticle, base fluid, particle volume fraction and particle size. Nanofluids are usually used for heat transfer enhancement in microchannel heat sinks by Hung et al[51]. It was first proposed by Choi et al[52] while working at Argonne National Laboratory, USA as a means to raise thermal conductivity of coolant and allow improved heat transfer performance.

In the present study, alumina water nanofluid with property given in Table 3.8 is considered for comparison of simulation prediction with that of Melotherm Oil as coolant. As shown in the temperature contour on Figure 3.23, a small heat transfer enhancement (ΔT_{max} decrease of 3 ^{o}C) is able to achieve by using nanofluid (alumina water in this case) compared to using melotherm Oil. However, the relative price of the two coolant may offset the benefit in heat transfer enhancement. In that case, operating cost calculation can be conducted, which is not covered in the present work. On the other hand, thermal performance of other nanofluids like SiO2-H2O, CuO-H2O can also be investigated.

Table 3.8. Physical properties of candidate coolant medium.

Properties	Water (Base fluid)	Oil	Nanofluid (alumina water)	
			2.5% vol	5% vol
Density (kg/m3)	998.2	936	1072.5	1140.79
Heat capacity (J/kg-K)	4182	1967	3865.79	3590.55
Thermal conductivity (W/m-K)	0.613	0.0974	0.658	0.706
Viscosity (Ns/m2)	0.00088	0.001003	0.001066	0.001128

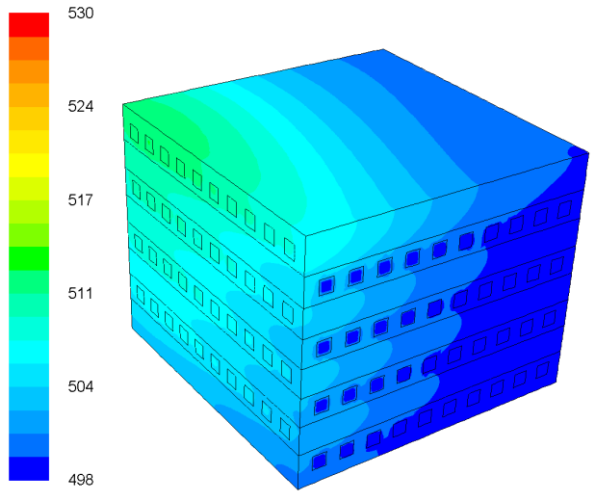

(a)

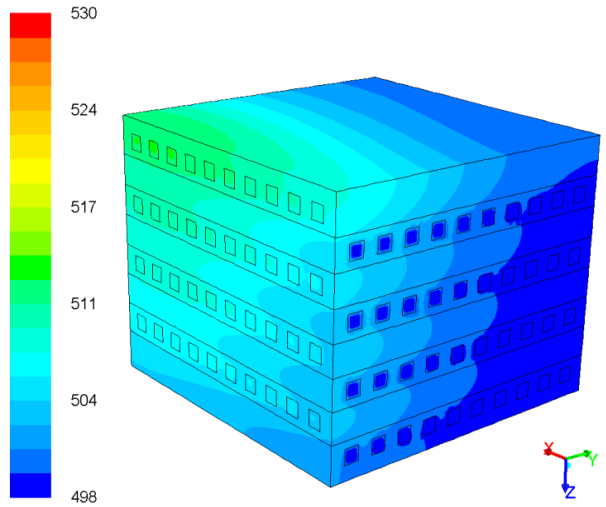

(b)

Figure 3.26. Reactor temperature contour showing enhancement in heat removal for (a) nanofluid as coolant (ΔT_{max} = 12 ºC) compared to (b) Oil as coolant (ΔT_{max} = 15 ºC).

3.4 Process intensification

Performance in terms of temperature control under intensified process condition (30, 000 hr^{-1} GHSV, catalyst loading 300 %) is tested for subcooled water and saturated water as coolant. This process condition is well above those used in commercial slurry and fixed bed reactor (Cao et al.[10]) indicating the feasibility for process intensification with microchannel teachnology, combined with cobalt based active catalyst produced by Oxford Catalysts[53] that can produce high CO conversion even with contact time as low as 0.029 s.

Figure 3.27 shows the predicted heat generation profile from single channel simulation at intensified condition. It may be mentioned here that catalyst loading above 100 % simply means catalyst activity above activity of the present Co-based catalyst of Velocys. As can be seen from the simulation predictions, heat generation rate scales up in equal proportion as the rate of reaction and hence coolants that active cooling means is needed. Therefore, cooling oil was not tested with the intensified condition as cooling oil was found to have much lower cooling capacity compared to other two coolants even at lower process condition (5, 000 hr^{-1} GHSV, catalyst loading 120 %).

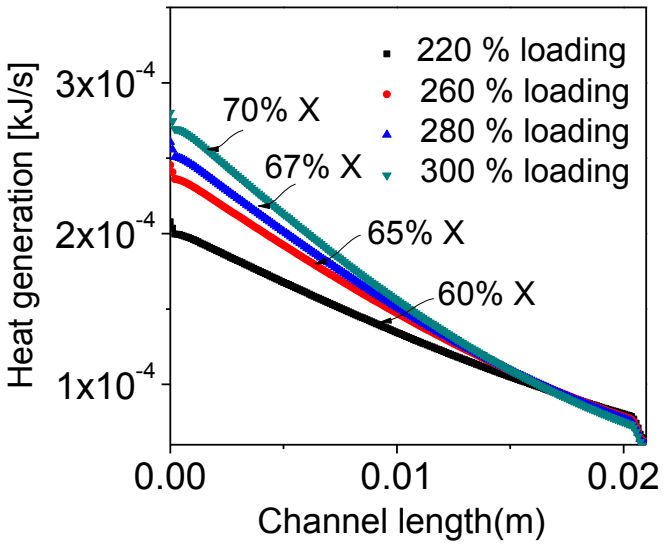

Figure 3.27. Heat generation profile from FT reaction simulation in single-channel-B for different catalyst loading [GHSV = 30000; H_2/CO = 2]. 220% catalyst loading corresponds to catalyst activity of 2.2 times the activity of the present catalyst.

As can be seen from Figure 3.28, at high value of coolant flow rate of 13.2 g/min per channel, cooling capacity for saturated water is much higher as compared to that of subcooled water. With saturated water, the mean FT temperature was 510 K, whereas in the case of subcooled water, it was 519 K. This tells us that at intensified process condition, subcooled water cannot sufficiently remove the generated heat from FT reaction in reaction channels, whereas saturated water through its wall boiling condition is able to sufficiently cool the reaction channels below a desired temperature of 513 K. Computed average heat flux through coolant channels was 39101 W/m^2 and 39095 W/m^2 for saturated water and for subcooled, respectively.

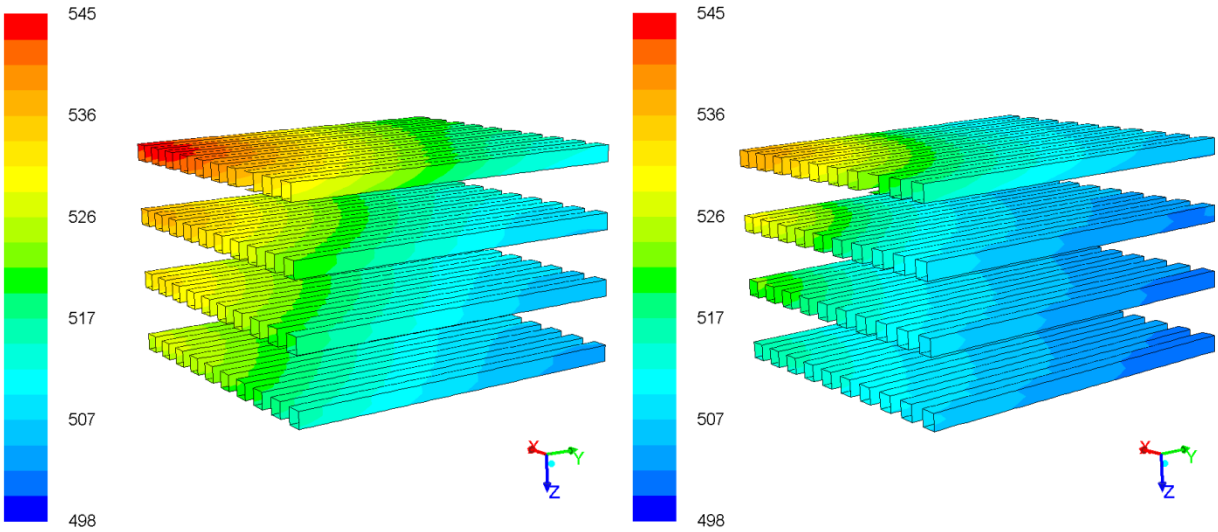

Figure 3.28. 3D Temperature contour (in Kelvin) on reaction channels for (a) subcooled water as coolant and (b) saturated as coolant (wall boiling condition) for intensified process condition (GHSV = 30000 hr^{-1}; Catalyst loading 300 %). Coolant flow rate = 13.2 g/min per channel. %); +ve X direction: coolant flow; +ve Y direction: syngas flow

Just 6 W/m^2 difference resulted to 9K indicating that heat flux is an important parameter in thermal performance of microchannel reactor.

This lead us to the reasoning that if effective thermal conductivity and heat transfer co-efficient on reaction channel side is high, the reactor may give better thermal control. In a catalyst filled reaction channel, effective thermal conductivity can be increased by using catalyst support having high thermal conductivity, for example $\beta-$SiC which has a thermal conductivity of 106 W/m-K (Zhu et al.[54]). However, results for heat transfer simulation with catalyst support having different conductivities is not discussed here. Also, from temperature contour of reactor block, it is clear that hot spot is located at the corner of top most reaction channel plane (e.g. channel plane at -ve most Z in Figure 3.28) where the reaction channel plane does not have two coolant channel planes on either of the adjacent sides. Therefore, it becomes an obvious reasoning that if a coolant channel plane is added on top of the reaction channel plane (located at -ve most Z), hot spot can be prevented significantly. Correctness of this idea will be checked and presented in one of the following section.

Simulation analysis with intensified process condition (Cao et al.[10]) showed effective conductivity of reaction channel to have strong effect on reactor thermal performance. Consequently, for such applications, to obtain high effective conductivity of reaction channel, catalyst support having high thermal conductivity, for example $\beta-$SiC which has a thermal conductivity of 106 W/m-K (Zhu et al.[54]) may be preferred.

3.5 Modified reactor block

With an attempt to prevent forming hot spot, as seen in temperature contour of base case reactor block, reactor geometry was modified by adding an additional coolant channel plane to make reactor block of 4 reaction channel planes and 5 coolant channel planes. As seen in Figure 3.29(a), temperature contour on modified reactor block considering same process condition (5000 hr^{-1} GHSV, catalyst loading 120 %) and saturated water as coolant showed significant reduction in the temperature of hot spot. Except for the syn-gas inlet region, where the reaction rate is highest and temperature peak is 505 K ($\Delta T_{max} = 7$ K), rest of the region along channel length has temperature between 498 K and 502 K. However, due to an additional coolant plane, the average exit vapor fraction in this case has also lowered, from 0.13 % in base case reactor block to 0.06 % in the modified reactor block. Similar significant improvement are expected with the cooling oil and subcooled water. In fact, as seen in Figure 3.29(b), with subcooled water as coolant, the peak temperature has decreased from 515 K to around 509 K ($\Delta T_{max} = 11$ K). Therefore, it can be concluded that modified reactor block gives better thermal performance than the base case reactor block. Additionally, as can be understood from the values of ΔT_{max} , when saturated water was used as coolant, even at exit vapor fraction less than 0.1%, the modified geometry predicted noticeably smaller temperature gradient (5 K less) than the single phase subcooled water. With cooling oil the difference is expected to be significant.

It may be commented that for laboratory scale single channel FT reaction, coolants with higher rank in cooling capacity like saturated water may not be

necessary and the generated heat can be sufficiently removed by lower rank coolant like heating oil- Marlotherm SH (Deshmukh et al.[655]). For laboratory scale operation, getting saturated water supply may either be not economical or difficult to get. Also, lower rank coolants may be able to cool the reaction channels sufficiently in case of high-temperature FT synthesis, even for multichannel FT reactor, as was explored by Gumuslu and Avci[12] in their simulation study. In low temperature FT synthesis, active cooling methods would generally be necessary to maintain reactor temperature between 493 and 523 K to maximize middle distillate among FT products. Song et al.[55], from their experimental work, proposed a correlation for chain-growth probability as a function of temperature and H_2/CO ratio. At the maintained FT channel temperature range in present study, 500 K - 510 K, the value of chain-growth probability was calculated to be between 0.77 and 0.82 for H_2/CO molar ratio of 2. This value falls under the desired growth-probability of FT synthesis. Finally, thermal runway can cause the reactor material to melt and get damaged partially or fully. Therefore, material that can withstand high thermal stress, like SUS 304 may be preferred for reactor block. Also, conditions for thermal critical heat flux and partial dry out in microchannel cooling with wall boiling condition may be studied in detail to get insights of the risky scenario.

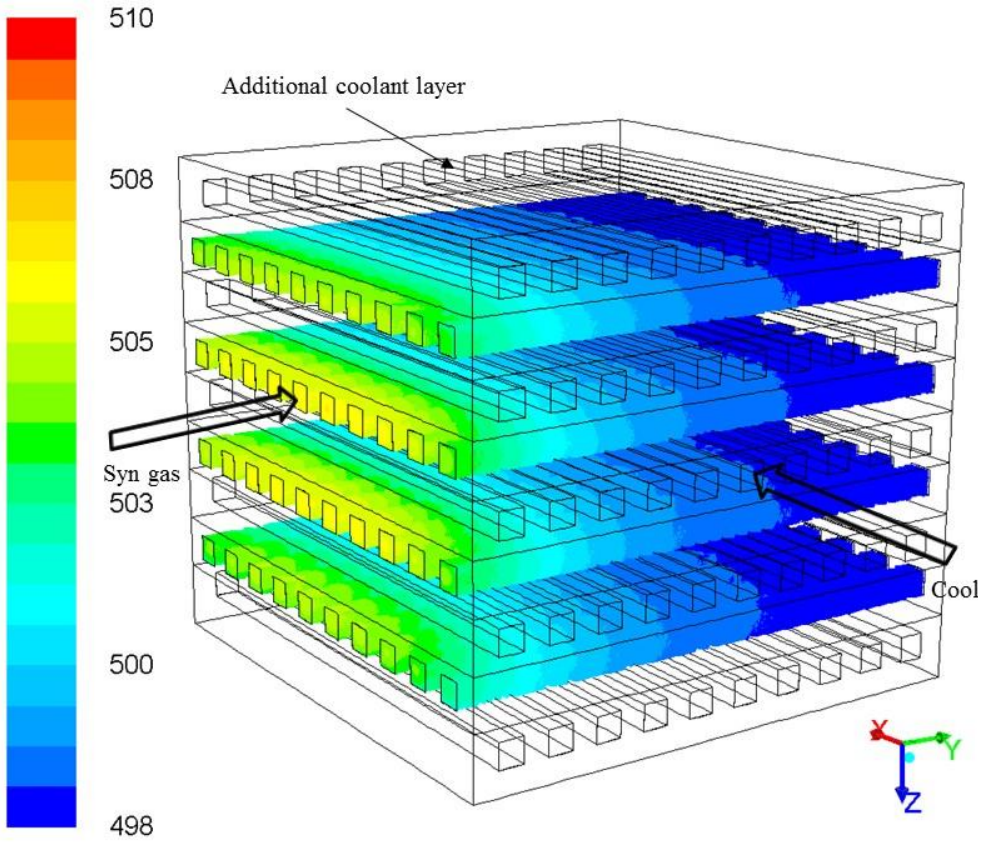

Figure 3.29 (a). Simulation result for geometry with an additional coolant layer. 3D Temperature [K] contour on reaction channels of microchannel reactor block for wall boiling coolant flow (GHSV = 5000 hr^{-1}; catalyst loading 120 %; saturated water flow rate = 5.4 g/min per channel). +ve X direction: coolant flow; +ve Y direction: syngas flow

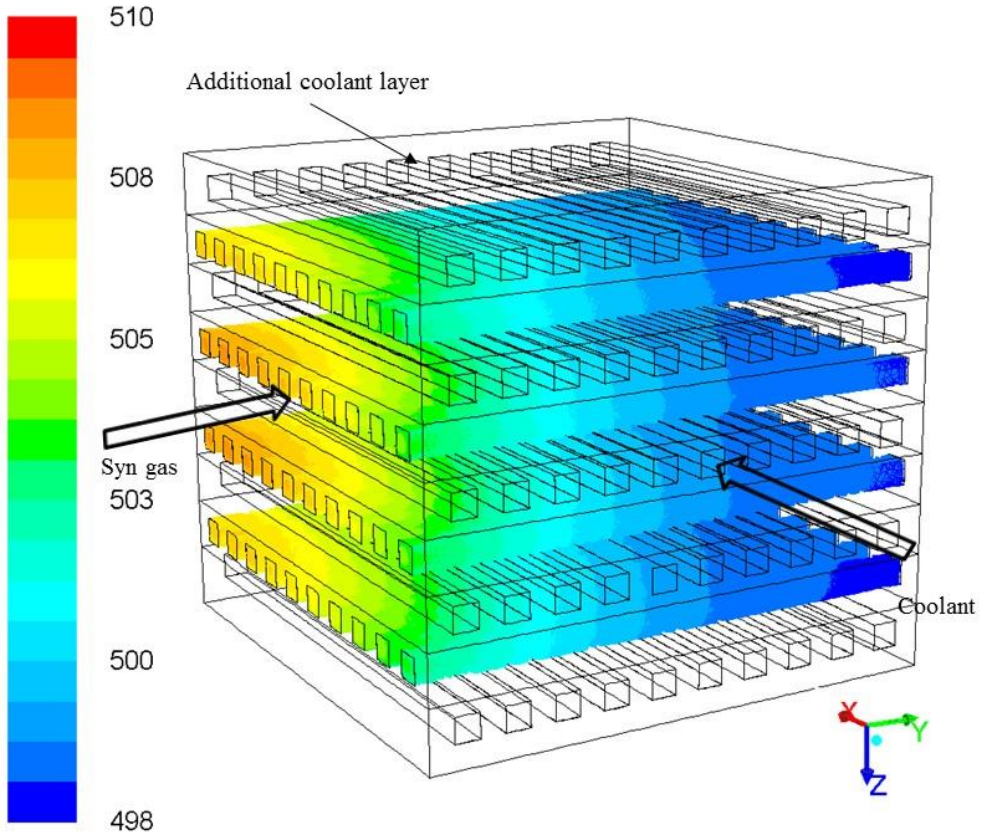

Figure 3.29(b). Simulation result for geometry with an additional coolant layer. 3D Temperature [K] contour on reaction channels of microchannel reactor block for subcooled water as coolant (GHSV = 5000 hr^{-1}; catalyst loading 120 %; subcooled water flow rate = 5.4 g/min per channel). +ve X direction: coolant flow; +ve Y direction: syngas flow

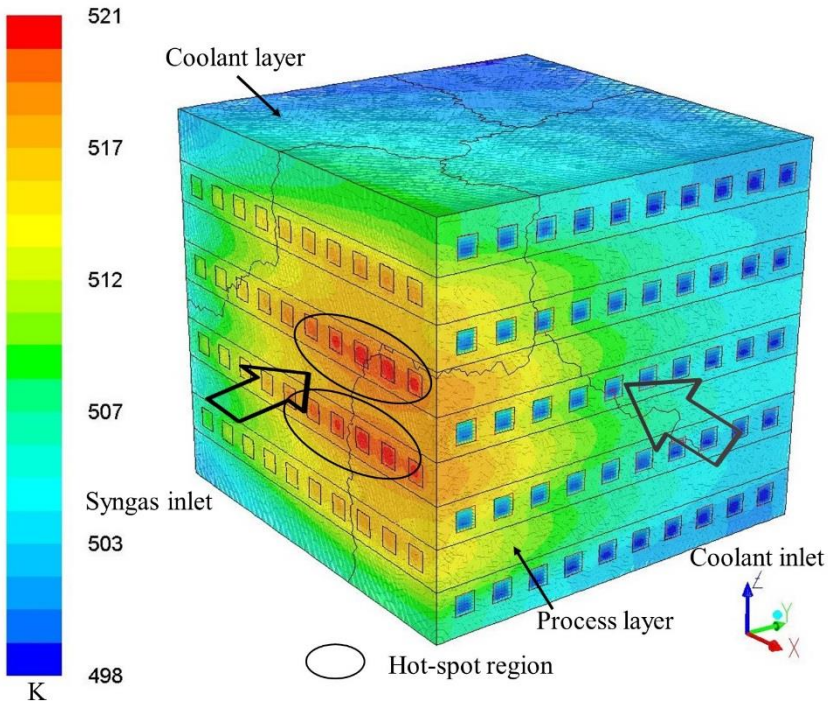

Figure 3.30. Temperature contour of modified reactor at intensified process condition (GHSV = 30000 hr-1 and catalyst activity 300 %). 300 % catalyst loading implies catalyst activity of 3 times the present catalyst activity, a situation of super active catalyst).

Temperature contour in Figure 3.30 indicates that with the modified microchannel reactor block, adequate heat removal and thermal control is possible even when reactor is operated with intensified process condition (GHSV = 30000 hr-1 and catalyst activity 300 %). 300 % catalyst loading implies catalyst activity of 3 times the present catalyst activity, a situation of super active catalyst). By increasing the coolant flow rate ΔT_{max} can be brought down to below difference of 23 ^{o}C, although not shown here.

3.6 Reactor configuration

Another important aspect of microchannel reactor operation is the flow configuration of syngas and coolant flows. As understood from the FT reaction characteristics in Section 3.2, reaction rates are higher near the inlet region compared to rest of the catalyst packed region (unless discrete catalyst loading strategy is applied), reactor may give better heat transfer performance if we configure the reactor in such a way that more heat in removed near the syngas inlet region. This would be possible if we configure the flow in concurrent mode.

Figure 3.31 shows the temperature contour from co-current configuration for same operating conditions (GHSV = 5000 hr^{-1}; catalyst loading 120 %; saturated water flow rate = 5.4 g/min per channel). Compared to cross flow configuration with ΔT_{max} of 12 ºC, described in previous section, concurrent configuration predicts ΔT_{max} of 6 ºC. This clearly indicates that concurrent configuration gives better heat transfer performance compared to cross flow configuration in microchannel reactor block operation.

Figure 3.32 shows similar predicted temperature contour at intensified operating conditions (GHSV = 30,000 hr^{-1}; catalyst loading 300 %) and when wall boiling condition was applied using saturated water as coolant. As can be seen in the figure, ΔT_{max} achieved was around 13 K is well within acceptable value. This mean an advantage of 10 K ΔT_{max} decrease in changing from cross-flow configuration to c-current flow configuration, see Figure 3.30 for comparison. This better outcome of concurrent configuration is also explained by the higher heat flux near the inlet region in case of concurrent configuration compared to cross flow configuration, as illustrated in Figure 3.33 by comparing heat flux profile along reaction channel

length for the two cases.

However, in actual design of a microchannel reactor block, if both coolant and syngas distributor face the same side of the reactor block, then positioning of the respective distributor would prove to be a major challenge . Therefore, coolant can be allowed to enter cross and flow in concurrent mode in the reaction region and exit cross the reaction channels. This way, syngas distributor and coolant distributor to the microchannel reactor block can be positioned on the different faces of the reactor.

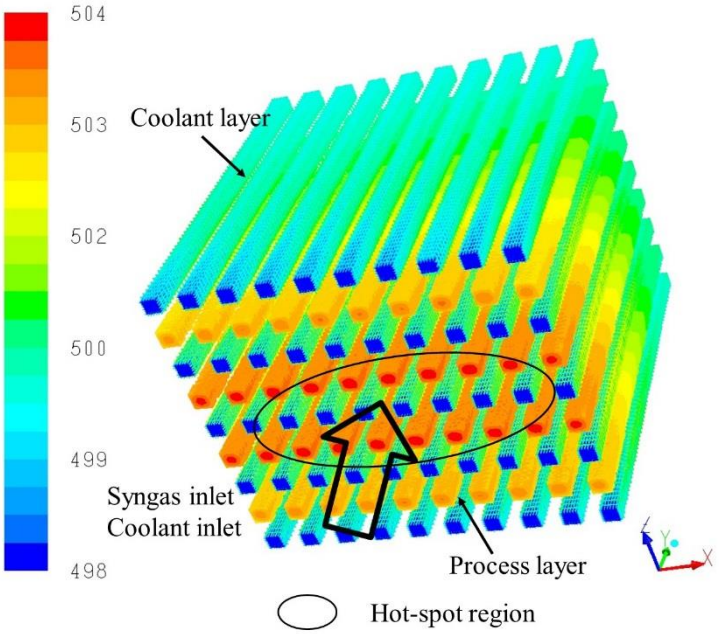

Figure 3.31 Temperature contour from co-current configuration for same operating conditions (GHSV = 5000 hr^{-1}; catalyst loading 120 %; saturated water flow rate = 5.4 g/min per channel). (Syngas and coolant in +Y-axis direction)

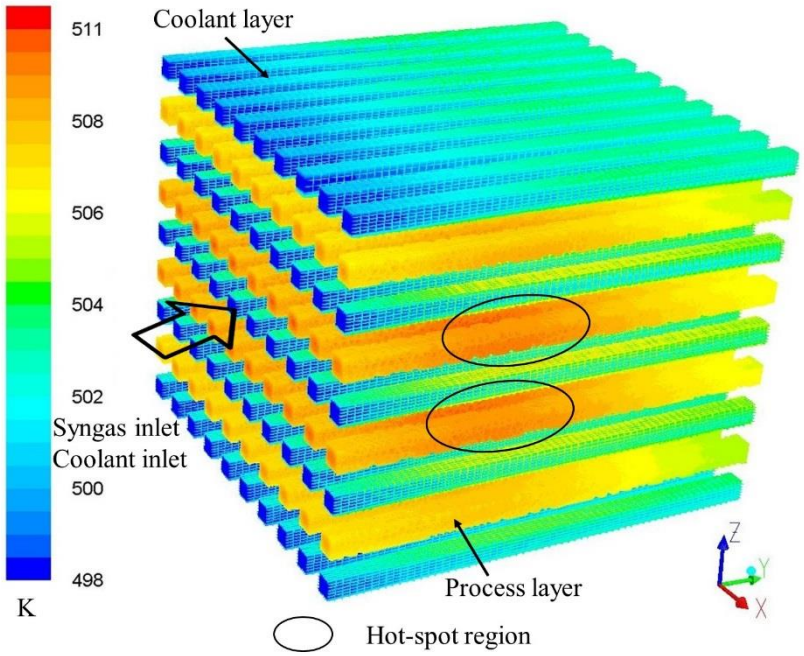

Figure 3.32 Temperature contour from co-current configuration for intensified operating conditions (GHSV = 30,000 hr^{-1}; catalyst loading 300 %; saturated water flow rate = 12 g/min per channel). (Syngas and coolant in +Y-axis direction)

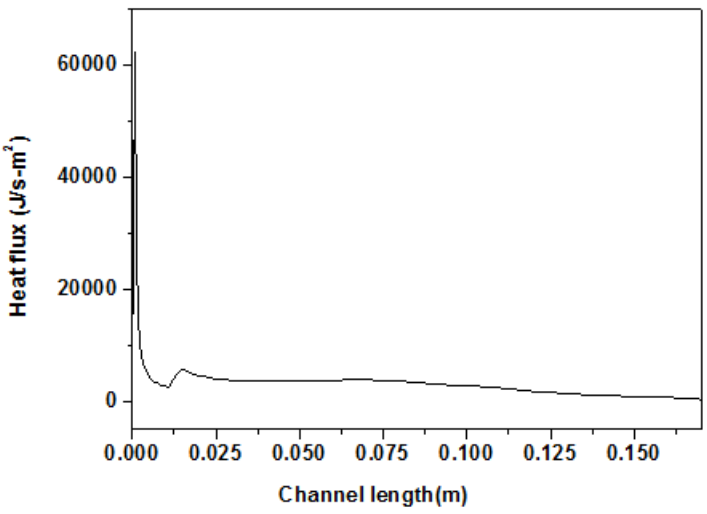

(a)

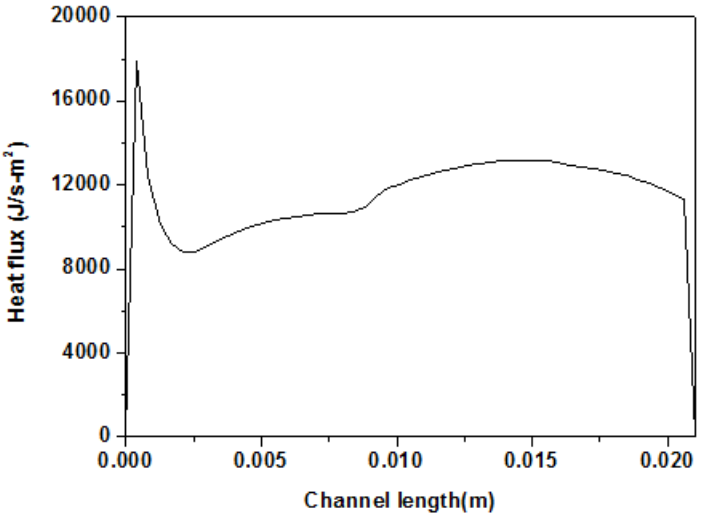

(b)

Figure 3.33. Heat flux profile along reaction channel length for (a) co-current configuration (b) for cross current configuration

3.7 Additional comments

A number of additional comments can be made with regard to detail study of microchannel reactor for FT synthesis. However in this work, for brevity, further comments are limited two important aspects – modeling conventional FT reactors and FT product distribution.

3.7.1 Modeling conventional FT reactors

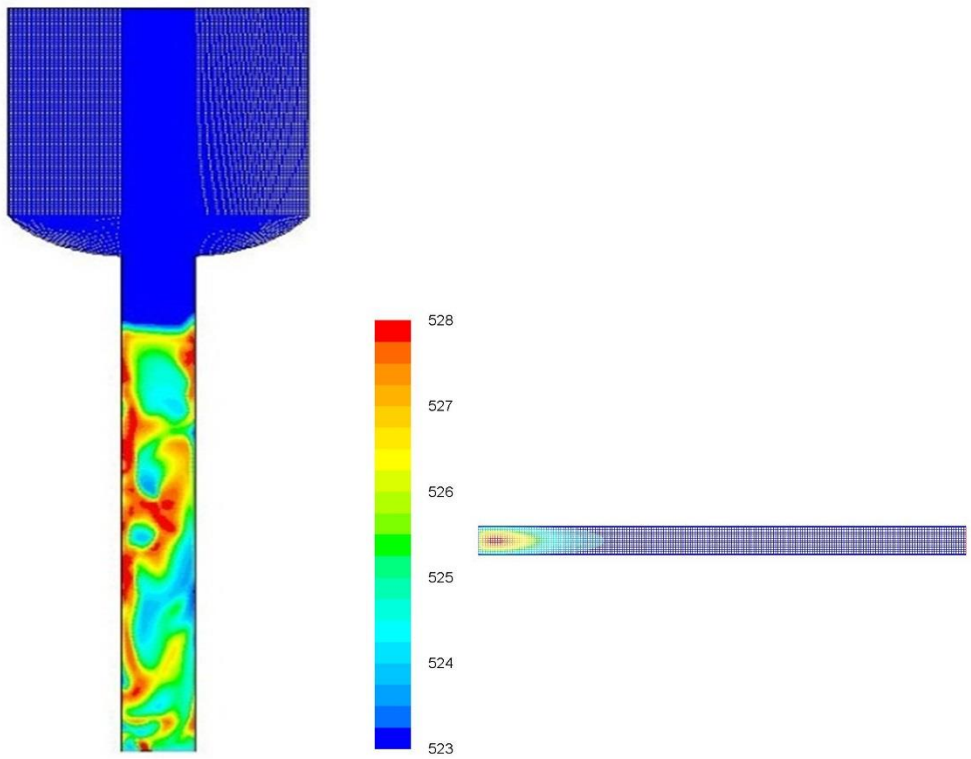

Figure 3.34. Typical flow profile FT synthesis in conventional reactors (a) fluidized bed reactor, (b) single pass of multitubular fixed bed reactor

Figure 3.34 illustrates simulated flow profile of syngas-FT product-catalyst system for typical FT synthesis in fluidized bed reactor and temperature profile for single pass model of fixed-bed multitubular reactor. By tradition at commercial scale operation, fluidized bed reactor is mainly used for gasoline production (high temperature FT synthesis) while slurry bubble column and multitubular fixed bed reactors are preferred for waxy distillate production (low temperature FT synthesis). This is because, waxy distillate would create problems in the fluidization. However multitubular fixed bed reactors are proving to be failure in term of thermal performance if active Co-based catalyst is used for the FT reaction. Both fluidized bed reactor type and slurry column reactor type, on the other hand, require internal cooling coil to remove the exothermic heat. Complete reactor modeling of conventional FT reactor would be far more complex than modeling microchannel FT reactor.

3.7.2 FT product distribution

Song et al.[55], from their experimental work, proposed a correlation for chain-growth probability as a function of temperature and H_2/CO ratio, as given below.

$$\alpha = \left(a \frac{y_{CO}}{y_{H_2} + y_{CO}} + b \right) (1 - 0.0039(T - 533)) \qquad 3.$$

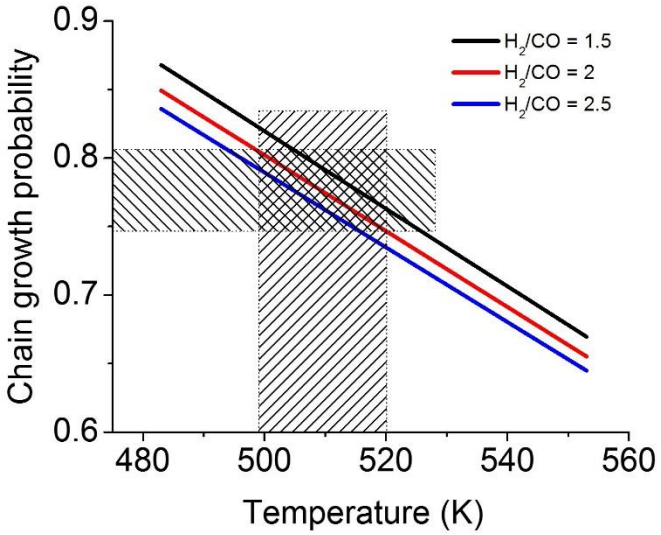

Figure 3.35. Chain growth probability as function of temperature.

At the maintained FT channel temperature range, 500 K - 520 K, the value of chain-growth probability was calculated to be between 0.74 to 0.82 for H_2/CO molar ratio as 2, as illustrated in Figure 3.35. This value falls under the desired growth-probability of FT synthesis. Finally, thermal runway can cause the reactor material to melt and get damaged partially or fully. Therefore, material having high thermal stress, like SUS 304 may be chosen for reactor block. Also, conditions for thermal critical heat flux and partial dry out in microchannel cooling with wall boiling condition may be studied in detail to get insights of the risky scenario.

3.8 Conclusion

Detail study of microchannel reactor operation for FT synthesis is carried out. First FT kinetics of low temperature and high temperature FT kinetics are evaluated to

find the more reliable and robust kinetic model. Reaction scheme and kinetic data of Velocys[16] is found to be more reliable than that of Marvast et al[35]. Effect of coolant channel and process channel geometry on heat removal efficiency is studied to evaluate different candidate design. On comparing the heat flux for design with 1.5 mm and 0.5 mm wall thickness, the later has 5.26 % increment over the former. Coolant channel oriented in such a way that surface area of the wall facing the process channel layer is higher, ensures higher heat flux. This is evident from the heat flux comparison between coolant channel orientation of 1 mm x 2 mm and 2 mm x 1 mm.2 mm x 1 mm orientation (more surface area in contact with the process channel layer) allows 11.1 % increase in the average heat flux as compared to 1 mm x 2 mm. Reducing the coolant channel height to 1 mm from 2 mm has an effect of 12.51 % increase in average heat flux (for coolant channel base width as 2 mm) and 71.23 % increase in average heat flux for (coolant channel base width as 1 mm). For the fixed mass flow rate of the coolant by varying velocities, 1 mm and 1.5 wall thickness showed higher heat flux as compared to 0.5 wall thickness. This is because the coolant velocities are higher in channels with wall thickness 1 mm and 1.5 mm than that of 0.5 mm thickness.

From the study of effect of temperature on reactor performance, it is found that for a desired reaction conversion and product selectivity, it is necessary to maintain reaction channel temperature below a particular value, say 523K in this case. Based on the predicted result, temperature of 517 K could be an optimum value. However, in general, as the intrinsic activity of the catalyst decline, reactor is operated at slightly higher temperature to achieve the same level of CO conversion. From studying effect of syngas ration and reactor operating pressure, syngas ratio of 2 and operating pressure of 20 – 22 bar predicts more desired product selectivity compared

to other set of values.

Wall boiling phenomena in the coolant side microchannel reactor is discussed in detail. Heat transfer simulations on multichannel block reactor predicted much higher cooling capacity of subcooled water compared to that of cooling oil, $\Delta T_{max} = 32$ K for subcooled water and 17 K for cooling oil at a process condition of GHSV 5000 $hr^{-1}$and catalyst loading 120 %. Wall boiling condition in saturated water provided heat transfer enhancement compared to that of subcooled water, $\Delta T_{max} = 12$ K for saturated water, with degree of enhancement depending on the fraction of saturated water vaporized. Therefore, it can be concluded that saturated water provides an effective means of removing heat from the exothermic FT reaction. However, saturated water flow rate above local dry out condition should be used for reactor safety.

A modified reactor block with improved thermal performance predicted noticeable heat transfer enhancement due to wall boiling even at very low exit vapor fraction. Accordingly modified reactor block is tested for intensified process condition (GHSV = 30,000 hr-1 and super active catalyst condition). Simulation predicts much improves heat transfer performance of the modified reactor as against the original reactor, decrease in ΔT_{max} from 47 K (without additional coolant layer on top) to 23 K (with additional coolant layer on top).

Method of catalyst bed zone division and loading different % of catalyst in different zone is evaluated. Study indicates noticeable advantage of the method when applied to 2 zones and 3 zones division cases, and longer 1st zone and shorter 1st zone cases. Between 2 zones and 3 zones division cases, the latter shows more uniform temperature profile (temperature difference less of 1 K) compared to the

former under same condition of CO conversion. And between longer and shorter 1st zone cases with both under 3 zone division, longer 1st zone case gave slight advantage in terms of uniform temperature profile. Also, the method can be optimized to optimum number of zone division, zone length and strategic loading % in each zone.

Further, evaluating heat transfer performance of cross flow and concurrent flow configuration of syngas and coolant flow, there is clear indication that concurrent configuration gives better heat transfer performance compared to cross flow configuration in microchannel reactor block operation. Decrease in ΔT_{max} from 23 K to 13 K was achieved in changing reactor flow configuration from cross-flow configuration to co-current flow configuration.

CHAPTER 4 : Microchannel Design Procedure Development

4.1 Introduction

A rigorous and systematic design procedure was adopted to achieve a design that can guarantee maximum productivity and safety of the highly exothermic FT reactor. Geometry details of single channels (both process and coolant channels), and multichannel reactor block comprises the main design variables. Feasible range of each design variables along with the range of each reactor operating parameter/condition are collected from literature to help in the design process.

4.2 Design procedure

The whole design activity and operation starting from deciding single channel dimensions to the end step of pilot plant demonstration is divided into four stages—single channel reactor design (Stage-I), multichannel block reactor design (Stage-II), design and operation optimization (Stage-III), and fabrication and pilot plant demonstration (Stage-IV). For the purpose of formulating a systematic design procedure and determining feasible values of reactor design variables, various types of knowledge from our previous works[21-28,56-59] were used. The systematic design procedure followed to achieve the final design specifications of the microchannel block reactor used in the present pilot scale experiment is shown in Figure 4.1. Table 4.1 and 4.2, details information on main reactor design variables, model parameters

and simulations conditions based on the results from our previous study and information collected from literature.

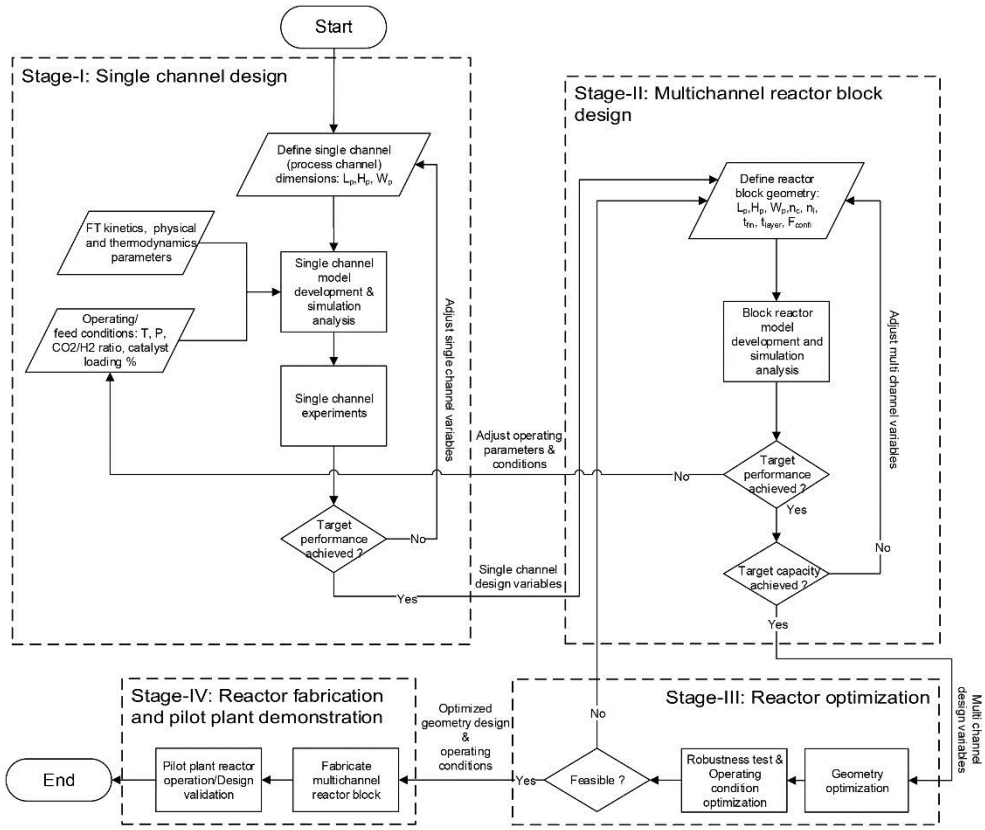

Figure. 4.1. Microchannel block (modular) reactor design procedure. Division of design procedure into 4 stages (stage – I to IV) comprising single channel design, multichannel reactor block design, geometry and operation optimization, and reactor fabrication and pilot plant demonstration.

In single channel design stage, single channel geometry variables --channel width (L_p), height (H_p) and length (W_p), are preliminary defined for FT synthesis

reactor model development and simulation analysis. Details of reaction kinetics, physical and thermodynamic parameters are defined at this stage. Catalyst loading %, reactor operating temperature and pressure, syn-gas feed and channel wall boundary conditions are also defined to develop rigorous simulation models of single channels in multiple platforms – ASPEN, MATLAB and CFD tool-ANYS FLUENT for different analysis. For instance, CFD models of exothermic FT reaction on the surface of spherical Co-based catalyst was developed by Lee et al[56] considering different single channel geometry (varying W_p and H_p) to study thermal effects of process channel geometry. The study found that varying H_p has more effect on heat removal capacity compared to varying W_p with higher heat removal capacity at lower H_p. For instance, decreasing the value of H_p from 4 mm to 2 mm, leads to increase in heat flux three fold while the value remain nearly the same for decrease in W_p from 5 mm to 2 mm. Accordingly, it was concluded that process channel geometry with smaller H_p (1 to 2 mm) and larger W_p (4 to 5 mm) would be an effective geometry from the point of heat transfer. Then, ASPEN model of detail FT reaction kinetics (Velocys Kinetics[16]) was studied to investigate the reaction profile and hence the FT product components profile along the channel length[25,26]. It was found that reaction rate was much faster (3 to 4 order higher) near the inlet region as compared to the middle region, which was expected. To further investigate single channel reactor, CFD models of FT reaction in a catalyst packed single channel was developed by Kshetrimayum et al[27] considering 1 mm × 1 mm × 21 mm and 1 mm × 3 mm × 16.7 mm sized channels and performance parameters (CO conversion, CH4 selectivity and three-dimensional temperature profile) of these single channel

models were evaluated through simulation study. Both 1 mm and 3 mm width channels gave CO conversion above 80 %, hence it was concluded that by widening the channel dimension to 2 to 3 times that of channel height in channel cross section dimensions, shortening the channel length is possible. Results from CFD simulation of single channel model also showed that most heat is generated near the inlet region of the reaction channel. Accordingly, it was proposed based on the results of simulation study combining CFD tool and MATLAB that discrete dilution method of catalyst loading be applied to distribute the heat generation evenly along the channel length[28]. Reactor performance was evaluated based on CO conversion, CH4 selectivity, C5+ selectivity and temperature profile along the channel length. Additional single channel models were also considered and process of simulation and performance evaluation was iterated until a channel geometry of H_p = 2 mm, W_p= 4 mm and L_p = 120 mm that meet performance criteria was chosen as a candidate process channel design. However, due to ease of fabrication, for single channel experiments, a channel of 100 mm length with circular cross section of 3 mm diameter was used. Single channel experiments were conducted for two main purpose, one to find out KOGAS catalyst performance of FT reaction and to develop FT kinetic models, and another to observe the thermal behavior of a single channel reactor. Accordingly, in the two experiments, the catalyst loading length was kept different, with only 6 mm for the first experiment and 25 mm for the second experiment. Details of the experiments and performance results are described in Park et al[57]. Bases on the performance of single channel reactor, design variables are updated to obtain the best candidate single channel design.

In the stage-II of the design procedure, single channel geometry obtained from

stage-I of the design activity is then used as a basis to extend the reactor design to multichannel block reactor design by defining multichannel geometry variables—coolant channel length (L_c), width (W_c) and height (H_c), number of channels in a microchannel layer (n_c), number of microchannel layers (n_l), channel wall or fin thickness (t_{fin}), channel layer support thickness (t_{layer}) flow-configurations (F_{conf}) etc. The multichannel block reactor design is then analyzed by developing rigorous multichannel FT synthesis simulation model and reactor performances were evaluated. For instance, a multichannel CFD model of 2 process channel layers interleaved between 3 coolant channel layers was developed to study effect of coolant channel geometry-- L_c, W_c and H_c, and channel wall or fin thickness, t_{fin} on the wall heat flux and reactor temperature . Process channel geometry in this case was kept constant at 3 mm × 3 mm. The study found that lower values of channel geometry set (L_c=, W_c= 0.6 mm, H_c=0.5 mm and t_{fin} = 0.646 mm) result to higher wall heat flux compared to larger values of channel geometry set (L_c=, W_c=2.2 mm, H_c= 2.0 mm and t_{fin} = 2.6 mm). In another CFD model of multichannel block reactor (21 mm × 21 mm × 17 mm) consisting of 4 process channel layers and 4 coolant channel layers, heat transfer simulation was conducted by Kshetrimayum et al[27] to evaluate the effect of different types of coolant and heat removal enhancement of wall boiling coolant. The same study also showed the process intensification of microchannel reactor by simulating more intensified condition of FT synthesis (GHSV of 30000 hr-1). Because, the goal of study with each multichannel models developed is different and where the effect of process channel geometry is not of interest, dimensions of process channel are made small to reduce computational load in CFD simulation. In a different approach to simulate multichannel block reactor in

a much reduced calculation time, unlike those of CFD models which usually take much longer calculation time, reactor decomposition and cell coupling method was applied to develop simulation model of large scale microchannel reactor block[24]. The multichannel model developed in this approach could handle as many as 5800 process channels, 7500 cooling channels, and 130 channel layers considering process channel geometry achieved in stage-I of design procedure. Effects of both geometry and operating variables such as catalyst loading ratio, coolant flow rate, and channel layout were examined. In a separate study by Park et al[57] using 3D model of decomposition and cell coupling approach, different reactor configurations of coolant side – cross-counter-cross, cross-cocurrent-cross and full cross current was evaluated. The study found that cross-cocurrent-cross configuration was the most effect configuration in terms of thermal control of reaction channels. Multiple block reactor designs were than evaluated by iterating the design process (adjusting the design variables) to find the most promising multichannel block reactor design.

The output design from multichannel design stage is then passed through rigorous optimization process to obtain a set of optimized geometry design variables as well as optimized operating conditions. Uniform flow distribution at the inlet of process channel and coolant channels sides are necessary to achieve reactor operation at its optimum flow conditions. While a uniform flow distribution is easily achievable at the syn-gas channel side, coolant being in liquid phase, flow distributor design needs to be optimized to achieve uniform flow distribution for the coolant side. In the first optimization task conducted, CFD and neural network technique were used by Jung et al[58] to optimize coolant flow guiding fin in a U-type coolant layer manifold (manifold for cross-cocurrent cross configuration) for a large-scale

microchannel block reactor. Robustness of the manifold design was shown by predicting uniform flow distribution over a wide range of flow conditions ($500 \leq$ ReGF ≤ 10800). And in another optimization work, multi-objective optimization using CFD and genetic algorithm was carried out by Na et al[28] to find the optimum discrete dilution method (number of catalyst packed discrete zones and respective % loadings). Minimum ΔT and maximum C5+ selectivity were chosen as objectives in the optimization process.

Finally, a rigorous multi-objective optimization was carried out by Jung et al[58] to optimize reactor channel geometry and over all block reactor dimensions by using multichannel FT reactor block model of reactor decomposition and cell-coupling approach and a surrogate model of the same FT reactor block model. Details (although not complete, due to confidentiality) of final multichannel block reactor design achieved based on the design procedure adopted is given in Fig 4. The single module of multichannel reactor block design consist of 528 process channels in total with W_p = 10 mm, H_p = 5 mm and L_p = 460 mm, and expected to produce FT product upto 0.5 BPD. By adding another module of the same design 1BPD capacity is expected to achieve. .Various cases of operating conditions were considered to find the best set of operating conditions for stable operation and maximum reactor performance.

The final design of multichannel block reactor achieved through stage-I, stage-II and stage-III of the design procedure was sent for fabrication at a third party fabrication facility (Innowill^{TM}). Details on the method and material used for fabrication are not given here for brevity. The fabricated reactor, shown in Figure 5 is then brought to KOGAS site for pilot plant experimentation/demonstration.

Table 4.1. Reactor geometry design variables and feasible design range, microchannel reactor block type FT reactor.

Design variables	Feasible design range	References
Process channel		
Length, L_p (mm)	20 – 600	1, 21, 56, 59
Width, W_p (mm)	0.5 -10	1, 21, 56, 59
Height, H_p (mm)	0.5 – 10	1, 21, 56,59
Coolant channel		
Length L_c (mm)	20 – 600	1, 6, 24, 56, 59
W_c (mm)	0.5 – 5	1, 6, 24, 56, 59
H_c (mm)	0.5 – 5	1, 6, 24, 56, 59
Fin thickness, t_{fin} (mm)	0.1 – 2	1, 26, 58
Layer support thickness, t_{layer} (mm)	1 – 3	25, 26, 27
Number of channels per layer, n_c	adjustable	25, 26, 27
Number of channel layers, n_l	adjustable	25, 26, 27
Flow configurations, F_{cong}	cross flow, contour flow, cross co-current-cross flow	1, 57

Table 4.2. Reactor model parameters and simulation conditions

Simulation parameters	Feasible operating range
FT reaction kinetics	Lumped, detail model
Catalyst	
Type/activity	Fe-based, Co-based
Support	Al_2O_3, SiO_2
Loading type	Filled, wall coating
Syn-gas conditions	
GHSV (hr^{-1})	2500 – 40,000
Syn-gas ratio	1.5 – 2.5
Inert gas dilution (%)	0 – 25
Inlet temperature (^oC)	200 – 260
Coolant conditions	
Coolant type	Single phase, Wall boiling (Two phase)
Inlet temperature (^oC)	190 - 220
Flow rate (L/min)	200-1500

4.3 Final design and reactor operation data (from KOGAS)

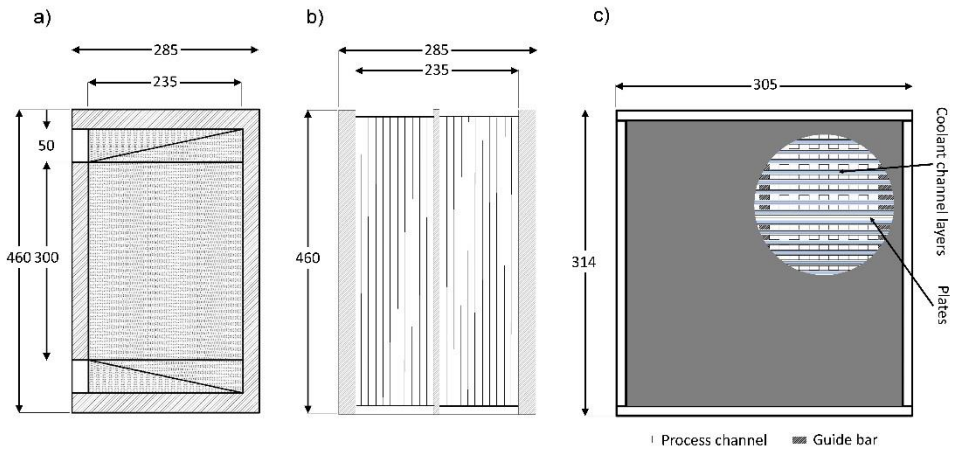

Figure 4.2. Final microchannel block (modular) reactor design. (a) Process channel side, (b) Coolant channel side, (c) Side view showing process channel and coolant channel layers along with guide bars and support plates.

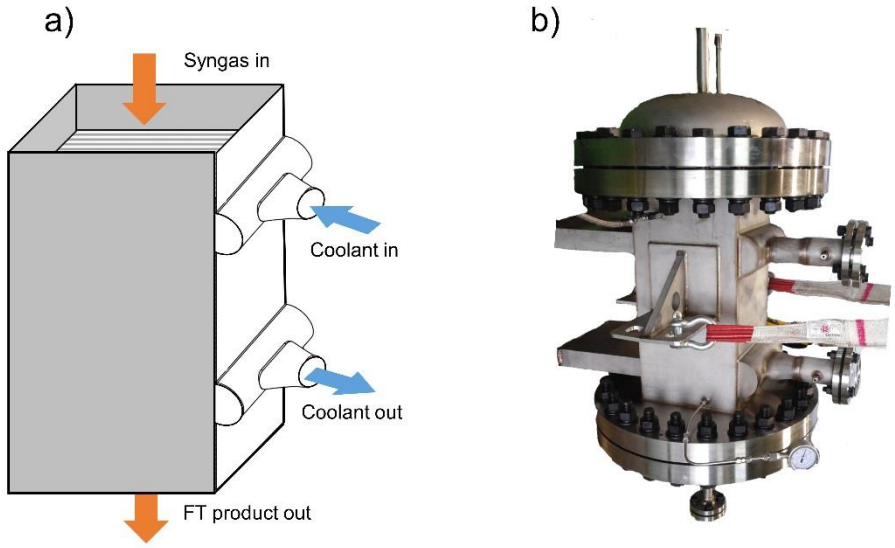

Figure 4.3. Final microchannel block (modular) reactor design. (a) configuration showing cross-cocurrent-cross flow of syn-gas and coolant, (b) fabricated multichannel reactor block.

The pilot plant operation started with initial checks of all the process units and control systems. Utility systems, raw materials, catalyst packing, catalyst reduction, compressor, pump, heat, level test, pressure safety valve, controller, drum, and refrigerator were checked in detail. Finally leak test for feed line, N_2 header to T-7, T-7 to CO_2 separation section, and CO_2 separation section to T-11 were performed. For reducing the catalyst packed in the microchannel FT reactor, the reactor catalyst bed was heated to 300 °C using H_2 flow. Thereafter, hydrogen was flown at a flow rate of 25 LPM for 57 hours. The reactor temperature was maintained at 220 ^oC for

34 hours, 230 °C for 83 hours, and 240 °C for 22 hours based on TC-3 to determine the effect of operating temperature on reactor performance. The specifications of syngas flow to the FT reactor were as follows-- average H_2:CO:N_2 ratio of syngas was 63.2:31.8:5.0. Retantate of M-2 (25 Nm^3/hr) was mixed with 1.32 Nm3/hr of N_2 supply, which makes up the GHSV of the inlet feed gas to about 2500 ml/gcat·hr. In the present pilot plant operation, this value of GHSV corresponds to synthetic wax production of 0.5 BPD. In case of the multitubular fixed bed FT reactor, hydrogen was flown at a flow rate of 30 LPM for 29 hours for reducing the catalyst. Other setting was same as that microchannel reactor operation.

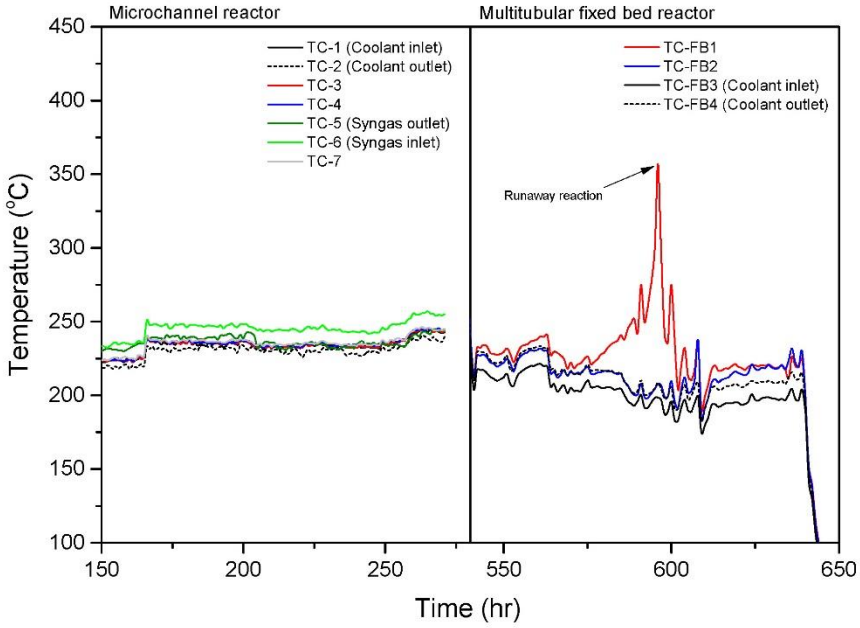

Figure 4.4. Reactor temperature of the microchannel FT reactor and multitubular fixed bed FT reactor as given by thermocouples installed inside the reactors [data from KOGAS].

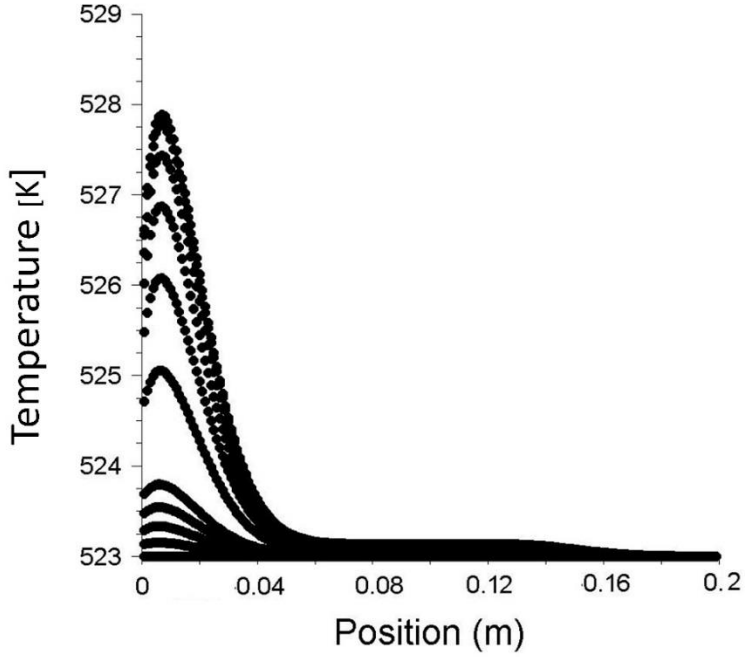

Figure 4.5. Predicted reactor temperature profile from single pass model of multitubular fixed bed FT reactor.

As illustrated in Figure 4.4, temperature data from thermocouples installed inside both 0.5BPD modular microchannel and packed bed type FT reactors operated in parallel showed stable temperature control for microchannel FT reactor for the entire plant operation up to 270 hr, while the multitubular fixed bed type FT reactor operation failed due to reaction runaway. The failure of multitbular fixed bed reactor in controlling reactor temperature is also supported from the prediction from simulated model of single pass tube model, illustrated in Figure 4.5 where sharp temperature rise is seen near the inlet region. A microchannel reactor under same

operating conditions predicted uniform temperature profile along the channel length, as described in section 3.2 of chapter 3.

From the modular microchannel FT reactor operation, although undesirably high value of CH_4 selectivity (50.13 %) was obtained from the plant operation, high CO conversion of 83%, illustrated in Figure 4.6, and stable temperature control at 220 ^oC, 230 ^oC and at 240 ^oC during the entire pilot plant operation (140 hr to 270 hr) demonstrated the appreciable performance novel microchannel FT reactor designed in due course of this thesis work. Reasons for undesirably high value of CH_4 selectivity are mostly reactor operation related rather than the design related. Accordingly, following practices are recommended to achieve appreciable CO conversion with low CH_4 selectivity: reducing the catalyst with syngas, increasing the reduction temperature above 300 ^oC, producing the catalyst with IWI method, and operating with moderate value (below 80 %) of CO conversion. Further, the compact GTL process described, the systematic modular microchannel reactor design procedure and pilot plant operation data presented in the this chapter may serve as a general guideline in similar future works on pilot scale reactor model development, design and operation.

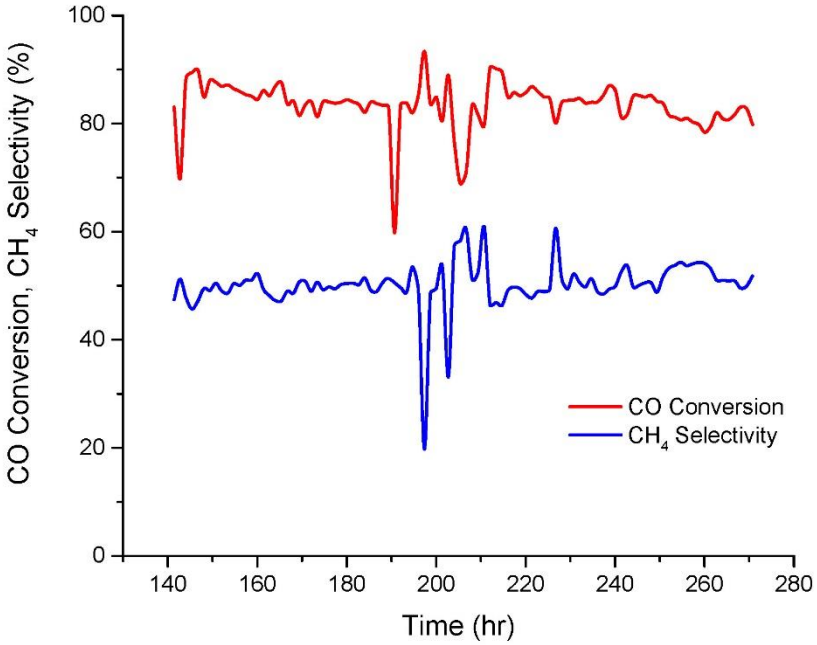

Figure 4.6. CO conversion and CH_4 selectivity of compact GTL pilot plant with microchannel FT reactor in the FT reaction section [data from KOGAS].

4.4 Conclusion

The whole reactor design process starting from single channel reactor design, multichannel block reactor design, design and operation optimization, and fabrication and pilot plant demonstration is described with aim to formulate a design procedure framework for potential use in future similar reactor design process. Feasible design and operating range are summarized. Few details on final design specifications are given through illustration. Pilot plant operation data from KOGAS in presented to serve as design validation in general.

CHAPTER 5 : Concluding Remarks

5.1 Conclusions

Modeling, simulation, and design procedure development of microchannel reactor for FT synthesis is addressed in this thesis mainly using CFD technique. CFD modeling and simulation of FT synthesis in a catalyst packed microchannel reactor considering both single channel and multichannel reactor models is presented. Simulation of Velocys' experiment (Deshmukh et al.[6],Tonkovich et al.[16]) with short single channel reactor validated our single channel model. At catalyst loading of 1060 kg/m^3 CO conversion of 60.02% was achieved with selectivity for CH_4 and C_{5+} (modeled as $C_{14}H_{30}$ here) as 8.38% and 87.41% respectively. When the catalyst loading was increased 1.2 times, CO conversion increased to 74.60 % while the selectivity for CH_4 and $C_{14}H_{30}$ increased to 11.18% and 85.26% respectively. Temperature effect on CO conversion and selectivity for CH_4 and C_{5+} revealed necessity for maintaining reaction channel temperature below 523 K, for low-temperature FT synthesis.

Heat transfer simulation in a complex microchannel reactor block can be conducted by decoupling reaction and heat transfer. Comparing a decoupled model with that of reaction and heat transfer coupled model shows less than 1 ^oC difference in temperature profile along the channel length. Thermal profile for the simulated microchannel reactor block is also qualitatively compared with temperature data of Velocys' pilot plant operation[6]. Overall, based on the validation of the single channel

reactor with Velocys single channel operation data[6] and qualitative comparison with multichannel reactor operation data, it can be understood that the various microchannel reactor models developed using CFD tools can be used to conduct detail study of FT synthesis.

Detail study of microchannel reactor operation for FT synthesis is carried out. First FT kinetics of low temperature and high temperature FT kinetics are evaluated to find the more reliable and robust kinetic model. Reaction scheme and kinetic data of Velocys[16] is found to be more reliable than that of Marvast et al[35].

Effect of coolant channel and process channel geometry on heat removal efficiency is studied to evaluate different candidate design. On comparing the heat flux for design with 1.5 mm and 0.5 mm wall thickness, the later has 5.26 % increment over the former. Coolant channel oriented in such a way that surface area of the wall facing the process channel layer is higher, ensures higher heat flux. This is evident from the heat flux comparison between coolant channel orientation of 1 mm x 2 mm and 2 mm x 1 mm.2 mm x 1 mm orientation (more surface area in contact with the process channel layer) allows 11.1 % increase in the average heat flux as compared to 1 mm x 2 mm. Reducing the coolant channel height to 1 mm from 2 mm has an effect of 12.51 % increase in average heat flux (for coolant channel base width as 2 mm) and 71.23 % increase in average heat flux for (coolant channel base width as 1 mm). For the fixed mass flow rate of the coolant by varying velocities, 1 mm and 1.5 wall thickness showed higher heat flux as compared to 0.5 wall thickness. This is because the coolant velocities are higher in channels with wall thickness 1 mm and 1.5 mm than that of 0.5 mm thickness.

From the study of effect of temperature on reactor performance, it is found that for a desired reaction conversion and product selectivity, it is necessary to maintain

reaction channel temperature below a particular value, say 523 K in this case. Based on the predicted result, temperature of 517 K could be an optimum value. However, in general, as the intrinsic activity of the catalyst decline, reactor is operated at slightly higher temperature to achieve the same level of CO conversion. From studying effect of syngas ratio and reactor operating pressure, syngas ratio of 2 and operating pressure of 20 – 22 bar predicts more desired product selectivity compared to other set of values.

Wall boiling phenomena in the coolant side microchannel reactor is discussed in detail. Heat transfer simulations on multichannel block reactor predicted much higher cooling capacity of subcooled water compared to that of cooling oil, $\Delta T_{max} = 32$ K for subcooled water and 17 K for cooling oil at a process condition of GHSV 5000 $hr^{-1}$and catalyst loading 120 %. Wall boiling condition in saturated water provided heat transfer enhancement compared to that of subcooled water, $\Delta T_{max} = 12$ K for saturated water, with degree of enhancement depending on the fraction of saturated water vaporized. Therefore, it can be concluded that saturated water provides an effective means of removing heat from the exothermic FT reaction. However, saturated water flow rate above local dry out condition should be used for reactor safety.

A modified reactor block with additional coolant layer on top is tested for intensified process condition (GHSV = 30,000 hr-1 and super active catalyst condition). Simulation predicts decrease in ΔT_{max} from 47 K (without additional coolant layer on top) to 23 K (with additional coolant layer on top).

Study indicates noticeable advantage of dividing the catalyst bed zone and applying strategic catalyst loading%. Between 2 zones and 3 zones division cases,

the latter shows more uniform temperature profile (temperature difference less of 1 K) compared to the former under same condition of CO conversion. And between longer and shorter 1st zone cases with both under 3 zone division, longer 1st zone case gave slight advantage in terms of uniform temperature profile. Also, the method can be optimized to optimum number of zone division, zone length and strategic loading % in each zone.

Further, evaluating heat transfer performance of cross flow and concurrent flow configuration of syngas and coolant flow, there is clear indication that concurrent configuration gives better heat transfer performance compared to cross flow configuration. Decrease in ΔT_{max} from 23 K to 13 K was achieved in changing reactor flow configuration from cross-flow configuration to co-current flow configuration in microchannel reactor block operation.

The whole reactor design process starting from single channel reactor design, multichannel block reactor design, design and operation optimization, and fabrication and pilot plant demonstration is described with aim to formulate a design procedure framework for potential use in future similar reactor design process. Feasible design and operating range are summarized. Few details on final design specifications are given through illustration. Pilot plant operation data from KOGAS in presented to serve as design validation.

The systematic CFD modeling and simulation analysis presented in this thesis adopted in our present study, can in general, be used to study microchannel reactor design and operation for other exothermic and/or endothermic reactions.

5.2 Future works

Some authors like Avci et al and Arzamendi et al described microchannel reactor with catalyst coated on the channel wall. However, catalyst packed microchannels are expected to give a number of advantages relative to the wall coated microchannel reactors, such as higher catalyst inventory, use of proven efficient Fischer –Tropsch catalyst, easier reactor loading and possible catalyst replacement. Coated microchannel reactors may require specially designed catalyst. Also, coating (deposition) on the reactor wall can be challenging. However simulation test for comparison of reactor performance between catalyst packed microchannel reactors and wall coated microchannel reactors was not conducted in this thesis work. This aspect of study might give additional insight to microchannel reactor characteristics.

As understood from Chapter 3, reactor operating variables like temperature, pressure, syngas ratio, syngas flow rate etc. affects the reactor performance and productivity. Additionally, same reactor may be desired to operate with conditions targeted to produce different product distribution at different times. For instance the same reactor originally designed for low temperature FT synthesis may be opted for higher temperature FT synthesis due to practical constraints of designing an altogether separate reactor. In that case, a set of optimum values will have to be sought for. Therefore, given a particular reactor design, seeking optimum set of operating variables for low temperature and high temperature Ft synthesis can be interesting.

Another interesting future work would be to convert CFD models of present microchannel reactor to Reduced Order Models (ROM) without any loss of generality, and include it in process flow sheet level optimization.

Nomenclature

Abbreviations

BTL – Biomass-to-liquid

CFD – Computational fluid dynamics

CTL – Coal-to-liquid

FT – Fischer–Tropsch

GTL – Gas to liquid

GHSV – Gas hourly space velocity

LPM – Liter per minute

IWI – Gas hourly space velocity

SIMPLE – Semi-implicit method for pressure-linked equations

SST – Shear stress transport

TC – Temperature control

Latin letters

$\vec{v}$ – Velocity vector (m/s)

v_j – Velocity component in x, y and z directions (m/s)

p – Pressure (bar)

S_i – Momentum source term in porous media for i-th (x, y or z) momentum equation

μ – Viscosity (kg/m-s)

D_{ij} – Inverse of permeability factor in porous media and entries in matrix D ($1/m^2$)

C_{ij} – Inverse of inertial resistance factor in porous media, entries in matrix C (1/m)

Y_i – Mass fraction of species '*i*'

J_i – Diffusive mass flux of species '*i*' (mol/m^2-s)

E_f – Energy for fluid part in porous media (J)

E_s – Energy for solid part in porous media (J)

k_{eff} – Effective thermal conductivity of porous media (W/m-K)

k_{wall} – Thermal conductivity of solid wall material (W/m-K)

k_f – Thermal conductivity of fluid phase (W/m-K)

k_s – Thermal conductivity of solid phase catalyst and catalyst support (W/m-K)

h_i – Enthalpy of specie '*i*' (J/mol)

S_f^h – Fluid enthalpy source term (J/mol_{CO})

Q_c – Convective heat flux (W/m^2)

Q_Q – Quenching heat flux (W/m^2)

Q_E – Evaporative heat flux (W/m^2)

q –Heat flux through wall solid (W/m^2)

k_n – Knudsen number

Ma – Mach number

Re – Reynolds number

T – Temperature (K)

ΔT_{max} – Temperature difference between the hottest spot and coldest spot in the

reactor

C_2, C_4 and C_{5+} – Hydrocarbon compounds

L_p– Process channel length (mm)

H_p– Process channel height (mm)

W_p– Process channel width (mm)

L_c– Coolant channel length (mm)

H_c– Coolant channel height (mm)

W_c– Coolant channel width (mm)

t_{fin}– Fin (wall between channels) thickness (mm)

t_{layer}– Thickness of support plate (mm)

n_c– Number of process channels per layer

n_l– Number of process channel layers

F_{confi}– Flow configuration between process and coolant channels

X_{CO} – CO conversion

Greek Letters

ρ – Fluid density (kg/m^3)

ρ_f – Density for fluid part in porous media (kg/m^3)

ρ_s – Density for solid part in porous media (kg/m^3)

γ – Specific heat ratio (c_p / c_p)

ε – Porosity inside reaction channel

Literature cited

(1) Arzamendi, G.; Diéguez, P.; Montes, M.; Odriozola, J.; Sousa-Aguiar, E. F.; Gandía, L., Computational fluid dynamics study of heat transfer in a microchannel reactor for low-temperature Fischer–Tropsch synthesis. *Chem. Eng. J.* **2010,** 160, 915-922.

(2) Franz, F.; Hans, T., Process for the production of paraffin-hydrocarbons with more than one carbon atom. US Patent 1746464, **1930**.

(3) Petroleum, B., BP statistical review of world energy. In London: British Petroleum: **2012**.

(4) White, B., Can gas-to-liquids technology get traction? Alaska Natural Gas Transportation Projects, *Office of the Federal Coordinator,* **2012**.

(5) Steynberg, A.; Dry, M.; Davis, B.; Breman, B., Fischer-Tropsch reactors. *Stud. Surf. Sci. Catal.* **2004,** 152, 64-195.

(6) Deshmukh, S. R.; Tonkovich, A. L. Y.; Jarosch, K. T.; Schrader, L.; Fitzgerald, S. P.; Kilanowski, D. R.; Lerou, J. J.; Mazanec, T. J., Scale-up of microchannel reactors for Fischer− Tropsch synthesis. *Ind. & Eng. Chem. Res.* **2010,** 49, 10883-10888.

(7) Chambrey, S.; Fongarland, P.; Karaca, H.; Piché, S.; Griboval-Constant, A.; Schweich, D.; Luck, F.; Savin, S.; Khodakov, A., Fischer–Tropsch synthesis in milli-fixed bed reactor: Comparison with centimetric fixed bed and slurry stirred tank reactors. *Catal. Today* **2011,** 171, 201-206.

(8) Karim, A.; Bravo, J.; Gorm, D.; Conant, T.; Datye, A., Comparison of wall-coated and packed-bed reactors for steam reforming of methanol. *Catal. Today* **2005,** 110, 86-91.

(9) Myrstad, R.; Eri, S.; Pfeifer, P.; Rytter, E.; Holmen, A., Fischer–Tropsch synthesis in a microstructured reactor. *Catal. Today* **2009,** 147, S301-S304.

(10) Cao, C.; Hu, J.; Li, S.; Wilcox, W.; Wang, Y., Intensified Fischer–Tropsch synthesis process with microchannel catalytic reactors. *Catal. Today* **2009,** 140, 149-156.

(11) Lipski, R., Smaller-scale GTL enters the mainstream. In Velocys: **2012**.

(12) Almeida, L. C.; Sanz, O.; D'olhaberriague, J.; Yunes, S.; Montes, M., Microchannel reactor for Fischer–Tropsch synthesis: Adaptation of a commercial unit for testing microchannel blocks. *Fuel*, **2013,** 110, 171-177.

(13) Holmen, A.; Venvik, H. J.; Myrstad, R.; Zhu, J.; Chen, D., Monolithic, microchannel and carbon nanofibers/carbon felt reactors for syngas conversion by Fischer-Tropsch synthesis. *Catal. Today* **2013,** 216, 150-157.

(14) Harris, R. A., Commercializing and deploying microchannel FT reactors for smaller scale GTL facilities. *AIChE Process Development Symposium Houston (USA)* **2015**.

(15) Krepper, E.; Rzehak, R., CFD for subcooled flow boiling: Simulation of DEBORA experiments. *Nucl. Eng. and Des.* **2011,** 241, 3851-3866.

(16) Tonkovich, A. L.; Yuschak, T.; Neagle, P. W.; Marco, J. L.; Marco, J. D.; Marchiando, M. A.; Keyes, L. W.; Deshmukh, S.; Luzenski, R. J., Laminated, Leak-

Resistant Chemical Processors; Methods of Making, and Methods of Operating. US Patent 0132290, **2011**.

(17) Gumuslu, G.; Avci, A. K., Parametric analysis of Fischer-tropsch synthesis in a catalytic microchannel reactor. *AIChE J.* **2012,** 58, 227-235.

(18) An, H.; Li, A.; Sasmito, A. P.; Kurnia, J. C.; Jangam, S. V.; Mujumdar, A. S., Computational fluid dynamics (CFD) analysis of micro-reactor performance: Effect of various configurations. *Chem. Eng. Sci.* **2012,** 75, 85-95.

(19) Shin, M.-S.; Park, N.; Park, M.-J.; Jun, K.-W.; Ha, K.-S., Computational fluid dynamics model of a modular multichannel reactor for Fischer–Tropsch synthesis: Maximum utilization of catalytic bed by microchannel heat exchangers. *Chem. Eng. J.* **2013,** 234, 23-32.

(20) Shin, M.-S.; Park, N.; Park, M.-J.; Cheon, J.-Y.; Kang, J. K.; Jun, K.-W.; Ha, K.-S., Modeling a channel-type reactor with a plate heat exchanger for cobalt-based Fischer–Tropsch synthesis. *Fuel. Process. Technol.* **2014,** 118, 235-243.

(21) Na, J., Jung, I., Kshetrimayum, K.S., Park, S., Park, C., Han, C., Computational Fluid Dynamics Study of Channel Geometric Effect for Fischer − Tropsch Microchannel Reactor. *Korean Chem. Eng. Res.* **2014,** 52, 826-833.

(22) Shin, D.-Y.; Ha, K.-S.; Park, M.-J.; Kwak, G.; Lee, Y.-J.; Jun, K.-W., CFD modeling of a modular reactor for the Fischer–Tropsch synthesis: Effectiveness of a micro-scale cross-current cooling channel. *Fuel* **2015,** 158, 826-834.

(23) Chabot, G.; Guilet, R.; Cognet, P.; Gourdon, C., A mathematical modeling of catalytic milli-fixed bed reactor for Fischer–Tropsch synthesis: Influence of tube

diameter on Fischer Tropsch selectivity and thermal behavior. *Chem. Eng. Sci*. **2015,** 127, 72-83.

(24) Park, S.; Jung, I.; Lee, U.; Na, J.; Kshetrimayum, K. S.; Lee, Y.; Lee, C.-J.; Han, C., Design and modeling of large-scale cross-current multichannel Fischer–Tropsch reactor using channel decomposition and cell-coupling method. *Chem. Eng. Sci.* **2015,** 134, 448-456.

(25) Kshetrimayum, K. S.; Seongho, P.; Ikhwan, J.; Jonggeol, N.; Chonghun, H., Simulation Study of Heat Transfer Enhancement due to Wall Boiling Condition in a Microchannel Reactor Block for Fischer-Tropsch Synthesis. In *Computer Aided Chem. Eng.*, **2015**; Vol. 37, pp 1355-1360.

(26) Kshetrimayum, K. S.; Park, C.; Jung, I.; Park, S.; Na, J.; Han, C.,CFD simulation of heat transfer in a microchannel reactor for fischer-tropsch synthesis process, *Process Development Division, AIChE Annual Meeting*, **2013**; pp 258-260.

(27) Kshetrimayum, K. S.; Jung, I.; Na, J.; Park, S.; Lee, Y.; Park, S.; Lee, C.-J.; Han, C., CFD Simulation of Microchannel Reactor Block for Fischer–Tropsch Synthesis: Effect of Coolant Type and Wall Boiling Condition on Reactor Temperature. *Ind. & Eng. Chem. Res.* **2016,** 55, (3), 543-554.

(28) Na, J.; Kshetrimayum, K. S.; Lee, U.; Han, C., Multi-objective optimization of microchannel reactor for Fischer-Tropsch synthesis using computational fluid dynamics and genetic algorithm. *Chem. Eng. Sci.,* **2017,** 313, 1521-1534.

(30) Visconti, C. G.; Tronconi, E.; Lietti, L.; Forzatti, P.; Rossini, S.; Zennaro, R., Detailed Kinetics of the Fischer–Tropsch Synthesis on Cobalt Catalysts Based on H-

Assisted CO Activation. *Top. Catal.* **2011,** 54, 786-800.

(31) Lu, F.; Zhang, H.; Ying, W.; Fang, D., The Reaction Kinetics of a Fischer-Tropsch Synthesis Over a Commercial Eggshell Co/SiO2Catalyst. *Petrol Sci. and Technol.* **2010,** 28, 1834-1845.

(32) Eliason, S.; Bartholomew, C., Reaction and deactivation kinetics for Fischer–Tropsch synthesis on unpromoted and potassium-promoted iron catalysts. *Appl. Catal. A- Gen.* **1999,** 186, 229-243.

(33) Iglesia, E.; Reyes, S. C.; Madon, R. J.; Soled, S. L., Selectivity Control and Catalyst Design in the Fischer-Tropsch. *Adv. Catal.* **1993,** 39, 221.

(34) Yates, I. C.; Satterfield, C. N., Intrinsic kinetics of the Fischer-Tropsch synthesis on a cobalt catalyst. *Energy Fuel.* **1991,** 5, 168-173.

(35) Marvast, M. A.; Sohrabi, M.; Zarrinpashne, S.; Baghmisheh, G., Fischer-Tropsch Synthesis: Modeling and Performance Study for Fe-HZSM5 Bifunctional Catalyst. *Chem. Eng. Technol.* **2005,** 28, 78-86.

(36) Bachelor, G., An introduction to fluid mechanics. *In Cambridge University Press*, Cambridge, UK: **1967**.

(37) Merk, H., The macroscopic equations for simultaneous heat and mass transfer in isotropic, continuous and closed systems. *Appl. Sci. Res.* **1959,** A8, 73-99

(38) Ishii, M., Thermo-fluid dynamic theory of two-phase flow. *NASA STI/Recon Tech. Report A* **1975,** 75, 29657.

(39) Drew, D. A.; Passman, S. L., Theory of multicomponent fluids. *Springer*

Science & Business Media: **2006**; Vol. 135.

(40) Yeoh, G. H.; Tu, J., Computational techniques for multiphase flows. *Elsevier:* **2009**.

(41) Kurul, N.; Podowski, M. Z. In Multidimensional effects in forced convection subcooled boiling, *Proceedings of the Ninth International Heat Transfer Conference*, **1990**; pp 19-24.

(42) Kurul, N.; Podowski, M., On the modeling of multidimensional effects in boiling channels, *ANS Proceeding of the 27th National Heat Transfer Conference*, **1991**.

(43) Perry, R. H.; Green, D. W.; O, M.J., Perry's chemical engineers' handbook. 7th ed., *Mc Graw-Hills Inc., New York,* **1999.**

(44) Fincher, S. N., Numerical Simulations of Boiling in Dielectric Fluid Immersion Cooling Scenarios of High Power Electronics. *Auburn University*, 2014.

(45) Ying, X.; Zhang, L.; Xu, H.; Ren, Y.; Xuan, J., An Experimental Study on a Microchannel Reactor for Fischer-tropsch Synthesis. *Energy Procedia* **2014,** 61, 1394-1397.

(46) D. Danziger, D. Popović, G. Schulz-Ekloff, Simulation of temperature peak attenuation by catalyst dilution in a tubular packed-bed reactor, *The Canadian J. of Chem. Eng.*, **1983**, Vol.61, 126-128.

(47) A. Caldwell, C. PH, Catalyst Dilution-A Means of Temperature Control in Packed Tubular Reactors, *British Chem. Eng.*, **1969**, Vol.14, 470-&.

(48) M.M.J. Quina, R.M. Quinta Ferreira, Thermal Runaway Conditions of a

Partially Diluted Catalytic Reactor, *Ind. & Eng. Chem. Res.*,**1999**, Vol.38, 4615-4623.

(49) M.M.J. Quina, R.M.Q. Ferreira, Start-up and wrong-way behavior in a tubular reactor: dilution effect of the catalytic bed, *Chem. Eng. Sci.*, **2000**,55, 3885-3897.

(50) S. Hwang, R. Smith, Heterogeneous catalytic reactor design with optimum temperature profile I: application of catalyst dilution and side-stream distribution, *Chem. Eng. Sci.*, **2004,** Vol.59, 4229-4243.

(51) T. C. Hungg, W. M. Yan, X.D. Wang, C. Y. Chang, Heat transfer enhancement in microchannel heat sinks using nanofluids, *International J. of Heat and Mass Transfer*, **2012**, Vol. 55, 2559-2570.

(52) S. U. S Choi, Enhancing thermal conductivity of fluids with nanoparticles, ASME FED231, **1995**, pp 99 - 103,

(53) Tonkovich, A. L. Y.; Litt, R. D.; Werner, T. M.; Yang, B., Integrated microchannel synthesis and separation. US Patent 8497308, **2012**.

(54) Zhu, X.; Lu, X.; Liu, X.; Hildebrandt, D.; Glasser, D., Heat transfer study with and without Fischer-Tropsch reaction in a fixed bed reactor with TiO 2, SiO 2, and SiC supported cobalt catalysts. *Chem. Eng. J.l* **2014,** 247, 75-84.

(55) Song, H.-S.; Ramkrishna, D.; Trinh, S.; Wright, H., Operating strategies for Fischer-Tropsch reactors: A model-directed study. *Korean J. Chem. Eng.* **2004,** 21, 308-317.

(56) Lee, Y.; Jung, I.; Na, J.; Park, S.; Kshetrimayum, K. S.; Han, C., Analysis on Thermal Effects of Process Channel Geometry for Microchannel Fischer-Tropsch Reactor Using Computational Fluid Dynamics. *Korean Chem. Eng. Res.* **2015,** 53,

(6), 818-823.

(57) Park, S.; Jung, I.; Lee, Y.; Kshetrimayum, K. S.; Na, J.; Park, S.; Shin, S.; Ha, D.; Lee, Y.; Chung, J.; Lee, C.-J.; Han, C., Design of microchannel Fischer–Tropsch reactor using cell-coupling method: Effect of flow configurations and distribution. *Chem. Eng. Sci.*, **2016,** Vol.143, 63-75.

(58) Jung, I.; Kshetrimayum, K. S.; Park, S.; Na, J.; Lee, Y.; An, J.; Park, S.; Lee, C.-J.; Han, C., Computational Fluid Dynamics Based Optimal Design of Guiding Channel Geometry in U-Type Coolant Layer Manifold of Large-Scale Microchannel Fischer–Tropsch Reactor. *Ind. & Eng. Chem. Res.*, **2016,** 55, (2), 505-515.

(59) Jung, I.; Na, J.; Park, S.; Jeon, J.; Mo, Y.-G.; Yi, J.-Y.; Chung, J.-T.; Han, C., Optimal design of a large scale Fischer-Tropsch microchannel reactor module using a cell-coupling method. *Fuel Process. Technol.*, **2017,** 159, 448-459

Abstract in Korean (요 약)

Gas-to-Liquid (GTL), coal-to-liquid (CTL) 그리고 biomass-to-liquid (BTL) 공정에서 피셔-트롭시 반응은 주요 과정에 속한다. GTL공정에서 탄화수소 연료를 생산하는 FT 반응에 필요한 syn-gas(이산화탄소와 수소의 화합물)를 생산하기 위해 천연가스를 feedstock으로 사용한다. CTL과 BTL에서 syngas는 연료와 바이오메스 기화로부터 생산된다. GTL은 불안정한 연료가격, offshore GTL에서 수반가스의 flaring로 인한 환경 규제들 그리고 이런 자원들을 화폐화 시키는 것에 대한 의문들로 인해 oil과 gas 산업에서 오늘날 주목을 받고 있다. GTL에서 산업화된 반응기로는 생산 조건과 운전 조건에 따라서 고온 FT (593-623 K)와 저온 FT (493-523 K)로 분류된다. 반응은 생산물 선택성과 촉매 비활성화가 온도에 매우 민감하면서 높은 발열 반응(반응열 = 165 KJ/mol 반응한CO)으로 특징지어진다. 이는 높은 수득률을 얻기 위해서는 적절한 열 제거와 온도 제어가 필수적임을 의미한다.

상업화 GTL 플랜트에서의 저온 FT 반응은 전통적인 fixed bed와 slurry bubble column 반응기를 사용한다. 그러나, fixed bed 반응기는 높은 압력강하와 확산 한계 그리고 불충분한 열 제거 용량 때문에 한계가 있다. 그리고 slurry bubble column의 경우에는 액상 생성물과 촉매와의 분리가 주요 문제점이다. 오늘날에, 연구자들 사이에서 마이크로채널 반응기

가 주목받고 있다. 이 반응기는 확산 거리를 줄여줄 수 있고, 열 전달 저항 및 물질 전달 저항을 줄여줄 수 있기 때문에 FT 반응에 적합한 기술로 여겨지고 있다. 열 전달 거리와 물질 전달 거리를 줄여주는 것은 공정을 집적화 할 수 있게 만들어 주며 이는 매우 활성도가 높은 FT 촉매에 적합하다. 그러므로, offshore와 원격 생산 시설 등에 이러한 소형, 모듈 전환 기술이 필요하다. 그리고, 마이크로채널 반응기 블록들은 매우 집적화되있고 운반이 쉬우며 안전한 기술이기 때문에 활용 시에 안전하다. syngas를 생산하는데 사용되는 생활 쓰레기 혹은 바이오메스 같은 작은 스케일의 에너지원에도 마이크로채널 반응기 기술을 적용할 수 있다. 그러나 FT 반응의 높은 발열과 짧은 체류량은 열 제거를 위한 saturated water와 같은 효율적인 냉각 물질을 필요로 한다.

피셔-트롭시 반응을 위해 마이크로 채널 블록에서는 반응 채널과 냉각 채널이 십자 모양으로 흐르게 배열되었다. 몇 년 전 이래로, 비싸고 어려운 실험을 대체하기 위해서 마이크로 반응기 혹은 마이크로채널 반응기 모사하는 전산유체역학(CFD) 기술이 트랜드가 되었다. 마이크로채널 블록에서 열전달을 CFD로 모사하는 것은 반응기 온도에서 냉각 채널 속의 wall boiling 조건이 미치는 영향을 보여주었다. 첫째로, 여러 운전 조건을 고려할 때 채널 길이에 따라서 열 생성 프로파일을 얻기 위해서 촉매가 가득찬 싱글채널에서의 반응이 모사되었다(GHSV 5000 hr^{-1}; 30,000 hr^{-}

[1]; chrao 로딩 혹은 활성도 60 % - 300 %, 여기서 100 % 로딩은 1060 kg/m^{3}이고 Oxford Catalyst Ltd 에서 개발한 코발트 베이스 촉매이며 촉매 활성도는 100으로 여겨진다.) 싱글채널 반응 모델은 실험에서의 싱글 채널 반응 모델을 모사하고 이 모델 예측 값을 실제 실험 데이터와 비교함으로써 입증되었다. 열 생성 프로파일을 열 전달 모사를 위하여 멀티 채널 블록으로 시간 당 일정하게 넣어주었다. 냉각 오일 (Merlotherm SH^{TM}), subcooled water와 saturated water (반응 운전 조건에서 포화된)이 냉각 물질로 선택되었다. 이 연구는 냉각 오일의 경우에 최소한 saturated water과 채널 벽 사이에 가장 열전달을 잘하는 것을 밝혔다. 한 가지 경우에서 가장 온도가 높은 부분과 낮은 부분의 차이는 냉각 오일, subcooled water그리고 saturated water 각각에 따라서 32K, 17K, 그리고 12K였다. 채널 당 3 – 6g/min으로 흐르는 saturated water는 벽으로 8900 W/m^2-K 를 넘는 높은 열 유량을 보낸다. 특정 운전 조건에서는 (GHSV 30,000 hr^{-1}; 촉매 로딩 300 %), 평균 FT 온도는 saturated water에 대해서 510K 그리고 subcooled water에 대해서 519K 이다.

반응기 열 전달 효율 측면에서 채널의 구조를 고려하면서 냉각 채널과 반응 채널의 여러 후보군을 평가하였다. 냉각 채널 층을 추가한 반응기 블록은 매우 낮은 vapor fraction의 배출과 wall boiling이 일어나는 조건에서 두드러질 만한 열 교환 성능의 향상을 보여준다. 특정 운전 조건

(GHSV = 30,000 hr-1 그리고 활성도 높은 촉매 조건)에서 변형된 반응 블록에서 실행한 결과에 따르면 온도, 반응 전환율 그리고 생산 선택성간의 강한 상관관계를 보여준다. 저온 FT반응의 경우에 523K아래에서 주요 반응이 일어난다. 예측 결과에 따르면 517K가 최적 값이다. 그러나, 일반적으로 촉매의 활성도 감소에 따라서, 같은 CO 전환율을 얻기 위해서 반응기는 좀더 높은 온도에서 운전된다. Syngas 비율과 반응 운전 압력의 효과에 대한 연구에 따르면, syngas비율은 2, 그리고 운전 압력은 20 – 22bar가 다른 값에 비하여 적절한 생성물 선택성을 보여준다.

촉매층 존의 분리와 각각의 존에 다른 %의 로딩 방법에 대해서 평가하였다. 연구를 통해서 이 방법의 이점을 알 수 있었다. 또한, 이 방법론을 통해서 최적의 존 배분, 존의 길이와 각각의 존에 대해서 전략적인 로딩 비율을 이끌어 냈다. 또한, syngas와 냉각 흐름의 교차 흐름과 같은 방향으로 흐르는 경우에 대해서 열 전달 성능을 평가해봤을 때 같은 방향으로 흐를 경우에 교차 흐름보다 마이크로채널 반응기 블록 운전에 더 효율적이라는 결과가 도출되었다. 미래의 마이크로채널 반응기 모사와 디자인 공정을 위한 규격화된 디자인 절차 또한 제안하였다.

학번: 2011-30282

성명: 크리스나다스